(4)

FINAL REPORT

(February 15, 1985 – February 14, 1990)

entitled

RESEARCH ON MERCURY CADMIUM TELLURIDE

prepared for the

Defense Advanced Research Projects Agency

SFR Contract No.: N00014-85-K-0151

and administered by the

Office of Naval Research

I.B. Bhat

S.K. Ghandhi

Principal Investigators

Electrical, Computer and Systems Engineering Department

Rensselaer Polytechnic Institute

Troy, New York 12180

Unclassified

SECURITY CLASSIFICATION OF THIS PAGE

REPORT DOCUMENTATION PAGE

1a. REPORT SECURITY CLASSIFICATION Unclassified	**1b. RESTRICTIVE MARKINGS** None
2a. SECURITY CLASSIFICATION AUTHORITY None	**3. DISTRIBUTION/AVAILABILITY OF REPORT** Approved for public release; distribution unlimited
2b. DECLASSIFICATION/DOWNGRADING SCHEDULE None	
4. PERFORMING ORGANIZATION REPORT NUMBER(S) N00014-85-K-0151-1	**5. MONITORING ORGANIZATION REPORT NUMBER(S)**
6a. NAME OF PERFORMING ORGANIZATION Rensselaer Polytechnic Inst. — **6b. OFFICE SYMBOL** *(If applicable)*: 3A707	**7a. NAME OF MONITORING ORGANIZATION** Office of Naval Research
6c. ADDRESS *(City, State and ZIP Code)* 110 8th Street Troy, New York 12180-3590	**7b. ADDRESS** *(City, State and ZIP Code)* Resident Representative 715 Broadway, Fifth Floor New York, NY 10003-6896
8a. NAME OF FUNDING/SPONSORING ORGANIZATION Defense Advanced Research Projects Agency — **8b. OFFICE SYMBOL** *(If applicable)*	**9. PROCUREMENT INSTRUMENT IDENTIFICATION NUMBER** N00014-85-K-0151-1
8c. ADDRESS *(City, State and ZIP Code)* 1400 Wilson Boulevard Arlington, VA 22209	**10. SOURCE OF FUNDING NOS.** PROGRAM ELEMENT NO.: 61101E — PROJECT NO.: YD14006 — TASK NO.: n/a — WORK UNIT NO.: 03
11. TITLE *(Include Security Classification)* Research on Mercury Cadmium Telluride	
12. PERSONAL AUTHOR(S) Sorab K. Ghandhi and Ishwara B. Bhat	
13a. TYPE OF REPORT Final	**13b. TIME COVERED** FROM 2/15/85 TO 2/14/90 — **14. DATE OF REPORT** *(Yr., Mo., Day)*: July 9, 1990 — **15. PAGE COUNT**
16. SUPPLEMENTARY NOTATION Approved for public release; distribution unlimited	
17. COSATI CODES FIELD / GROUP / SUB. GR.	**18. SUBJECT TERMS** *(Continue on reverse if necessary and identify by block number)* CdTe, ZnSe, HgCdTe, MCT, Epitaxy, MOCVD, OMVPE

19. ABSTRACT *(Continue on reverse if necessary and identify by block number)*

This report summarizes work done over a five-year period on a program entitled, "Research on Mercury Cadmium Telluride. Using the alloy growth OMVPE process, we have obtained compositional uniformity of ±0.005 over a 2" GaAs slice. p-type doping to $10^{17}/cm^3$ and n-type doping to $4 \times 10^{18}/cm^3$ have been achieved using As and In respectively. Annealing studies have shown that the background concentration of undoped HgCdTe is around $5 \times 10^{14}/cm^3$. Passivation techniques, using anodic sulfidization, have been developed for HgCdTe. Both p-n diodes and field effect transistors have been demonstrated on material grown during the course of this program. A diffusion length of 120 microns has been measured in material with x = 0.3.

The work was supported by the Defense Advanced Research Projects Agency (Contract monitor: Dr. J. Murphy), and administered through the Office of Naval Research (Dr. M. Yoder).

20. DISTRIBUTION/AVAILABILITY OF ABSTRACT UNCLASSIFIED/UNLIMITED ☒ SAME AS RPT. ☐ DTIC USERS ☐	**21. ABSTRACT SECURITY CLASSIFICATION** Unclassified
22a. NAME OF RESPONSIBLE INDIVIDUAL Sorab K. Ghandhi	**22b. TELEPHONE NUMBER** *(Include Area Code)*: (518) 276-6085 — **22c. OFFICE SYMBOL**

DD FORM 1473, 83 APR — EDITION OF 1 JAN 73 IS OBSOLETE.

Unclassified

SECURITY CLASSIFICATION OF THIS PAGE

APPROVED FOR PUBLIC RELEASE: DISTRIBUTION UNLIMITED

FINAL REPORT

(February 15, 1985 – February 14, 1990)

entitled

RESEARCH ON MERCURY CADMIUM TELLURIDE

prepared for the

Defense Advanced Research Projects Agency

SFR Contract No.: N00014-85-K-0151

and administered by the

Office of Naval Research

I.B. Bhat

S.K. Ghandhi

Principal Investigators

Electrical, Computer and Systems Engineering Department

Rensselaer Polytechnic Institute

Troy, New York 12180

SK-90.23

July 9, 1990

CONTRIBUTORS

DR. H. EHSANI (PART TIME)

C. HANKE (MASTERS STUDENT)

V. NATARAJAN (DOCTORAL STUDENT)

V. PARTHASARATHY (DOCTORAL STUDENT)

DR. K. PATEL (PART TIME)

C. PATEROUS (SENIOR)

M. SHERWIN (SENIOR)

N.R. TASKAR (DOCTORAL STUDENT)

D. TERRY (DOCTORAL STUDENT)

J. BARTHEL (TECH. - PART TIME)

TABLE OF CONTENTS

APPENDIX B – Indium Doping of n-Type HgCdTe Layers Grown by Organometallic Vapor Phase Epitaxy

APPENDIX C – Annealing and Electrical Properties of HgCdTe Grown by OMVPE

APPENDIX D – The Influence of Accumulation Layers on the Hall Effect in n-Type HgCdTe

FOREWORD

This report summarized work entitled, "Research on Mercury Cadmium Telluride". This work was carried out at Rensselaer Polytechnic Institute over the time frame February 15, 1985 to February 14, 1990 on behalf of the Defense Advanced Research Projects Agency. It was monitored by Drs. R. Reynolds and J. Murphy of DARPA and administered by Dr. M. Yoder of the Office of Naval Research.

Additional funding was provided by a Fellowship from the IBM Corporation and a Grant from the Raytheon Corporation. These funds were used to support one student (N.R.T.) in addition to general support of our research program.

Work on this program has involved the help of many students, over and above those directly funded by it. In addition, they have provided a generous sharing of knowledge gained on past projects. This last item, while freely given, is an important advantage of running a solid state Materials and Characterization effort which has been ongoing for the last 20 years. Their support is gratefully acknowledged.

Finally, many of the accomplishments of this program would not have been made without the support, technical guidance and enthusiasm provided by our contract monitors. They have allowed us to direct our efforts along productive channels as they unfolded during the course of this program, and to terminate tasks as they came to a fruitful conclusion. We greatly appreciate their continuing interest in our program.

I.B. Bhat

S.K. Ghandhi

SUMMARY

The goal of this program was to conduct research on the growth of HgCdTe and related compounds. The following are the main accomplishments of this effort.

- $Hg_{1-x}Cd_xTe$ has been grown on CdTe substrates by the alloy method, and fully characterized.
  - The Conventional Alloy Growth Method has been used.
  - $x = 0.2 \pm 0.002$ over 1 cm $\times$1 cm has been achieved.
  - Fully annealed background carrier concentration $\simeq 5 \times 10^{14}/cm^3$.
  - Minority carrier lifetime 45 nsec (microwave transient method).
- $Hg_{1-x}Cd_xTe$ has been grown on GaAs substrates with a CdTe buffer layer.
  - The Conventional Alloy Growth Method has been used.
  - $x = 0.2 \pm 0.005$ over a 2" dia. substrate has been achieved.
  - Hillock density $500/cm^2$.
- Extrinsic p-type doping of HgCdTe has been accomplished.
  - Arsine gas used as the dopant source.
  - Doping to $10^{17}/cm^3$ with a 77K hole mobility of 500 cm^2/Vsec (for $x = 0.2$).
  - Stable after annealing at 270°C for 15 hours.
- Extrinsic n-type doping of HgCdTe has been accomplished.
  - Trimethylindium and triethylindium used as dopant sources.
  - Doping to $4 \times 10^{18}/cm^3$ with a 77K electron mobility of 6×10^3 cm^2/Vsec (for $x = 0.23$).
- n^+-p diodes have been made on HgCdTe using vacancy doping.
  - Diffusion length of 120 μm for diodes with a 5 μm cutoff wavelength.
- Surface passivation of HgCdTe has been accomplished with anodic sulfidization.
  - Enhancement mode FET devices have been demonstrated in this material.
- HgTe and HgCdTe have been grown at low temperatures ($\simeq$ 240°C).

- Methylallyltelluride has been used as the tellurium source.
- X-ray FWHM values as low as 29 arc sec have been obtained.

- CdTe has been grown and doped both p- and n-type.
  - p doping to $10^{17}/cm^3$.
  - n doping to $10^{18}/cm^3$.
- Extrinsic doped p-n diodes have been fabricated from CdTe and tested.
  - Performance is comparable or superior to that of GaAs diodes.
  - n = 1.04 for forward voltages in excess of 0.4V.
  - $I_o = 1.3 \times 10^{-12}$ A/cm^2.
  - Reverse leakage of 10 pA (diode of 0.7 mm $\times$ 0.7 mm area).
  - Light emission has been measured from these diodes at 77K.
- ZnSe has been grown on GaAs.
  - Photoluminescence of GaAs is seen to improve by a factor of 100-200 with this overgrowth.
  - Effect is reproducible on both p- and n-GaAs.
  - Evidence of pseudomorphic growth of ZnSe, with a clean ZnSe-GaAs interface.

A number of papers, resulting from this effort, have been published or submitted for publication in the refereed journals. Published papers are listed in Section 3. Those which have been submitted are provided as Appendices. Additional papers are in preparation.

1. INTRODUCTION

The goal of this program is to conduct research on Mercury Cadmium Telluride and related compounds. Its emphasis is on the growth and characterization of thin films of these materials by means of Organometallic Vapor Phase Epitaxy. This report outlines tasks proposed and the accomplishments during our program.

2. WORK ACCOMPLISHED DURING REPORTING PERIOD

2.1 Reactor Development

In order to get off to a rapid start, an existing epitaxial reactor (System I) was adapted to meet the special research needs of this program, during the early months of our effort. Specifically, a new mass flow controller channel was installed for the cadmium source, and a new graphite susceptor was designed and incorporated into the reactor. In addition, many of the existing lines were removed and replaced with new plumbing.

This machine is a relatively small one, with a 2" ID reaction chamber. Although very simple in design, its main advantage is that it can be rapidly reconfigured to meet the needs of a specific research problem. Many of our developments during the course of this program were first demonstrated on this system.

A new reactor, capable of large area slices, was designed and components ordered for it. Construction of this system (System V) was carried out during Year I and the machine brought into operation during Year II, about 10 months ahead of schedule. This system is an all welded unit, with VCR fittings and mass flow controllers on all its channels. Operation at pressure from 1 atm to 0.1 atm is possible, under closed loop control. Both manual and full computer control have been incorporated into this machine. An extremely flexible software program was written and tested on dry runs with the system. This program not only runs the reactor, but keeps a complete log of reactor conditions while it is in operation.

The reaction chamber design is a unique one, in that it eliminates all heated lines for transport of mercury into the system. Moreover, the mercury source is not in the main reactor chamber, so that it does not get contaminated by the flow of organometallic reactants over it. This combination of features allows for good control of the Hg vapor pressure during growth, and still maintains a low level of impurities in the growing layer.

This new design was constructed with a stationary susceptor system as a cost saving feature. (The loading mechanism for this system was fabricated at a cost of $5,500, as compared to $70,000 for a system with a rotating susceptor.) During Year III, we demonstrated on this machine that we could exceed the DARPA goal of $x = 0.2 \pm 0.005$ over a 1 cm $\times$ 1 cm slice. Measurements, made by Dr. C. Castro at Texas Instruments, confirmed a uniformity of $x = 0.2 \pm 0.002$ over a 1 cm $\times$ 1 cm layer grown on CdTeSe substrates [1, 2].

In System V, the entire reaction chamber, including the loading and unloading mechanism, was built as a separate module, so that it could be replaced with a more sophisticated one if future requirements necessitated such an upgrade. Successful operation of the reactor during Year III heightened our awareness of its shortcomings, so that we instituted this upgrade at the request of DARPA. This was carried out along the following lines:

- A reaction chamber unit, with provisions for a rotating susceptor, was designed. Its construction was well beyond our capabilities, so it was farmed out to CVD Equipment, Inc. This unit was delivered and installed at the beginning of Year IV.
- The reaction chamber was reconfigured. Some computer modelling was necessary for this purpose.
- The gas handling on a number of the alkyl channels was redesigned to allow for stable operation over long periods of time.

- The Hg chamber and its heating were modified to improve reproducibility.

All of these improvements were made with the view towards obtaining ±0.005 uniformity over a 2" diameter substrate. Using this rotating heater, HgCdTe layers were grown with a ±0.001 compositional uniformity over a 1" diameter during Year IV. The goal of $x = 0.2 \pm 0.005$ variation over a 2" diameter GaAs slice was achieved during the final year of our program.

During Year IV, a new machine (System VII) was designed, incorporating many advanced features. The machine was constructed during the final year of this program. It has been designed as an extremely flexible unit, with high speed valves, pressure balancing, and full computer control. Two completely separate channels are provided, to allow growth by conventional as well as by atomic layer epitaxy.

The machine was originally developed to be used for HgCdTe. However, we have altered some aspects of the design in order to respond more closely with the recent DARPA shift in emphasis towards wide gap materials such as ZnSe and ZnTe. The pressure balancing feature, combined with computer control, will allow the growth of superlattices as well as ternary alloys in this system.

System construction was carried out to the point where all of the input and exit plumbing are in place. Time and cost constraints have prevented the fabrication of an advanced reactor chamber. Consequently, a simple reaction chamber, made for another reactor, has been installed on this system. The susceptor for this chamber is r.f. heated; again, because of the availability of an existing unit.

2.2 Growth and Doping of Cadmium Telluride

During Year I, a considerable amount of our research effort was placed on the growth of CdTe for two reasons. First, it is relatively easy to grow on a high quality, lattice matched substrate such as InSb. Thus, it is a starting point for the understand-

ing and development of processes for HgCdTe. Next, it serves as a useful intermediate layer in the growth of HgCdTe on GaAs. Our studies have addressed problems on both of these areas.

Considerable effort has been spent on growing CdTe on InSb [3-5], to which it is closely lattice matched (0.02%). The resulting material is therefore of excellent crystal quality, and can be used to study the basic properties of this semiconductor.

Studies have been made to investigate the effect of varying processing conditions [6] on the growth of the resulting CdTe material. These have shown that material quality is strongly dependent on whether growth is initiated on a Cd-stabilized substrate or on one which is Te-stabilized. One result of this study is our ability to grow extremely pure CdTe, with a photoluminescence (PL) full width half maximum (FWHM) of 2.1 meV at 12K, in undoped material. This value is the lowest reported for epitaxial CdTe grown by OMVPE. The PL spectrum of these layers is dominated by emissions from the radiative recombinations of the free and bound excitons, which are very well resolved. A level at 1.596 eV is associated with the recombination of free excitons. Additional levels at 1.593 eV and at 1.591 eV are also observed, and have been associated with an exciton bound to a neutral donor and to a neutral acceptor respectively. The well resolved narrow exciton band and low value of the FWHM indicate that layers are of high quality.

During Year II, this work was augmented by a detailed double crystal x-ray diffraction analysis of strain in layers as a function of the growth conditions. In this study both symmetric (004) and asymmetric (115) reflections were used to determine tetragonal distortion and strain in the grown layers, for a series of different growth conditions. Our work showed that, with suitable process conditions, it is possible to grow CdTe with a full width half maximum of 20 arc seconds [5, 7]. This is the lowest value ever reported for OMVPE grown layers. Moreover, coherent epitaxy can be achieved for growth at 350°C.

An interesting result of our work was the observation of tilt between the epi-layer and the substrate, if growth is carried out under Te-stabilized conditions. A misorientation of 235 arc seconds was observed in these films. (Misorientation as large as 48 arc minutes has been observed by other workers in the area.) We believe that this is probably due to the presence of an interfacial layer of In_2Te_3 formed during the growth of Te-stabilized films.

2.2.1 Growth Mechanisms

During Year I, a detailed study was made to determine the reaction mechanisms for the growth of CdTe [8]. This study involved growth on a variety of substrates (CdTe, InSb, GaAs and Al_2O_3) in addition to an extensive study of the results of other workers. In this work, we had shown that it is possible to grow CdTe from elemental cadmium and DETe at temperatures as low as 230°C. Thus, there is no a priori reason to postulate the formation of a DMCd-DETe adduct to accomplish this low temperature growth. In addition, our experiments indicate that CdTe growth begins by the heterogeneous decomposition of DMCd to cadmium, which is chemisorbed on the surface. This process is the rate limiter in the growth of CdTe, and also in the growth of other cadmium compounds (CdS, CdSe) from alkyl source materials.

2.2.2 p-Type Doping of CdTe

p-doping in CdTe requires the incorporation of the impurity (arsenic in our case) into Te sites, where it behaves as a singly ionized acceptor. Unfortunately, this is accompanied by the incorporation of some of the impurity into Cd sites as well, where it behaves as a triple donor. Thus, high p-doping is very difficult to achieve, since the material becomes rapidly compensated.

In our work during Year II, we were able to dope CdTe p-type, to 2×10^{17} cm^{-3}, with a uniformity of better than $\pm 20\%$ over a 1.5 cm $\times$ 1.5 cm area [9, 10]. This doping

concentration is about a decade higher than that reported by other techniques such as MBE. Moreover, large area uniformity is readily achieved, without the need for complex photo or laser excitation techniques for this purpose.

CdTe growth was carried out in an atmospheric pressure reactor using diethyltelluride (DETe) and dimethylcadmium (DMCd) as the Te and Cd sources, respectively, at a growth temperature of 350°C, with DMCd to DETe partial pressure ratios of approximately 2. Arsine in hydrogen was used as the As source. Substrates used were (100)2° $\rightarrow$ (110) oriented undoped CdTe, and also semi-insulating GaAs wafers of the same orientation. Buffer layers of 2.5 μm thick undoped CdTe was grown on semi-insulating GaAs ($> 10^8 \Omega$ cm), prior to the growth of the 4.5 μm thick doped CdTe layers. Doping showed a linear relationship up to a concentration level of $2 \times 10^{17}/\text{cm}^3$, indicating good control of the doping. As the arsine flow is increased further, the hole concentration begins to saturate.

The layers were characterized by photoluminescence measurements at 12K and by Hall measurements as a function of temperature. A 300K mobility of 80 cm^2/Vs was measured for p-CdTe layers doped in the 3×10^{15} to 3×10^{16} cm^{-3} range. The ionization energy of the arsenic acceptor was determined to be 62 $\pm$ 4 meV, by means of variable temperature Hall and resistivity measurements. It was also shown that the electronic activity of the As incorporated is a function of the dimethylcadmium to diethyltelluride partial pressure ratio in the gas phase. This is to be expected since the Te-vacancy concentration can be altered by this means.

A number of experiments were devised to obtain some insight into the mechanism by which arsenic doping is so readily achieved in CdTe by OMVPE. In contrast, we note that this has only been achieved by laser excitation in MBE. One critical experiment which we have conducted was an attempt to dope CdTe using elemental arsenic which has been pre-cracked. Here, we could not achieve a hole concentration in excess of 1 $\times$

$10^{15}/cm^3$, regardless of the partial pressure of the As species (As_2 and As_4).

The situation for arsenic incorporation from arsine is quite different; in fact, care must be taken to prevent excessive arsenic incorporation. Decomposition studies of this hydride [K. Tamaru, J. Phys. Chem., 59, 777, 1955] have established that the rate limiter is the removal of the first hydrogen atom, with subsequent hydrogen release being more rapid. Studies of AsH_3 decomposition over CdTe have not been made; however, results with AsH_3 over GaAs indicate that significant decomposition occurs at temperatures as low as 172°C, by a surface catalyzed reaction. One model for dopant incorporation, therefore, is that AsH_3 breaks down to AsH_3 and is chemisorbed on the CdTe surface, where further loss of the remaining two hydrogens results in its decomposition to monatomic As. This Column 5 atom incorporates into Te (Column 6) sites which are electronically favored over Cd (Column 2) sites. As a consequence, the As incorporation can be altered by changing DMTe overpressure during growth. Thus, increasing this overpressure reduces the Te-vacancy concentration, resulting in a fall in the p-doping concentration. We have demonstrated that this is indeed the case, with an inverse dependence as predicted.

The situation with As_2 is probably quite different, since its incorporation as a p-dopant would necessitate the substitution of one As atom into a Te-site, followed by the breaking of the As-As bond. The bond strength of As-As is extremely large (92 kcal/mole) so that this is not readily achieved at growth temperatures. As a result, it is entirely possible for the second As to be incorporated into a neighboring Cd site, where it would behave as a triple donor, and compensate the CdTe. We conclude, therefore, that it is necessary to provide atomic arsenic to the CdTe in order to promote is ready incorporation into the CdTe lattice. The use of the hydride AsH_3 allows this to be done in a convenient manner. A variety of arsenic alkyls can also be successful for this doping process, provided their eventual decomposition is surface catalyzed to As-H. Tertiary-

butylarsenic is a likely candidate for this reason; on the other hand, trimethylarsenic would probably be a poor choice since it does not decompose to As-H.

An alternative model we have considered is that AsH_3 and DMCd form an adduct in the gas phase, and that this adduct is directly incorporated as a complex during the growth of CdTe. This model would also explain the doping behavior of As in CdTe. Certainly, mass spectrometric studies will be required before definitive conclusions can be reached concerning these models.

2.2.3 n-Type Doping of CdTe

In our work during Year II, we demonstrated [10] that CdTe can be readily doped to $2 \times 10^{17}/cm^3$ with indium, using trimethylindium as the dopant source. Further work along these lines was conducted in Year V, using trimethylindium. A maximum doping level of $2 \times 10^{18}/cm^3$ was obtained with this source. n-type layers, doped to 8×10^{15} cm^{-3}, had a 300K Hall mobility value of 900 cm^2/Vs and a 30K Hall mobility of 3500 cm^2/Vs. This is comparable to values obtained for the best bulk CdTe with the same doping level.

In these layers, indium is incorporated into Cd sites where it behaves as a donor, so that all samples are n-type. By varying the Te/Cd ratio during growth, it is possible to alter the Cd vacancy concentration and hence the indium incorporation. High values of Hall mobility indicate that this material has a low degree of compensation.

Schottky diodes were made from these samples, using Au as the metal, and were investigated by Deep Level Transient Spectroscopy [11, 12]. A total of five trap levels were detected, with four being presented in all of the samples. A study of the concentration of these traps as a function of Te pressure has allowed three of these to be identified, as the Cd vacancy, the Te vacancy and the Cd interstitial, at $E_c - 0.74$ eV, $E_c - 1.15$ eV and $E_c - 0.65$ eV respectively. An additional trap level at $E_c - 0.36$ eV was also ob-

served, but its nature was not identified. This is probably an indium-related complex since it has been observed in bulk material which is indium doped as well. The fifth trap level was only observed in one sample, and is probably a contaminant.

2.2.4 CdTe Devices

During Year IV, further work was done in developing techniques for p- and n-doping of CdTe using AsH_3 and $(C_2H_5)_3In$ as the acceptor and donor dopant sources respectively. With both dopants, concentration levels up to 3×10^{17} cm^{-3} have been obtained.

Extrinsic doped junction diodes have been fabricated by the successive growth of p- and n-layers on InSb substrates. The diode structure consisted of a 3 μm thick n-type layer followed by a 3 μm thick p-type layer, grown on an InSb substrate. Ohmic contact to the p-type layer was made by electroless deposition of gold. The diode size was 0.7 mm $\times$ 0.7 mm [13, 14].

The I-V characteristic of diodes of this type show a breakdown voltage of 10V. Room temperature capacitance-voltage (C-V) measurements on this diode show an effective doping concentration of 1×10^{15} cm^{-3} in the n-layer and a built-in voltage of 1.2V. The p-doping concentration measured to be 1×10^{17} cm^{-3}. These values for the doping give a theoretical value of 1.2V for the built-in voltage. Forward and reverse ln(I)-V measurements made on this diode show an ideality factor of 1.04 at a forward bias above 0.4V, and a saturation current density of 1.3×10^{-12} A/cm^2. The reverse leakage current was 10 pA. These values indicate that diodes of excellent quality can be made by extrinsic doping of CdTe layers. Light emission has also been measured from forward biased extrinsic doped CdTe diodes made in our laboratory.

2.2.5 Growth of CdTe on GaAs

We have also studied the growth of CdTe on alternative substrates with a view towards evaluating its suitability as an intermediate layer for the eventual growth of

HgCdTe. This research was stimulated by our observation that bulk CdTe substrates are generally twinned in character, so that there is a need for an alternative substrate.

Although InSb is an excellent potential candidate, we chose GaAs an an alternative substrate material because of its wider energy gap (E_g = 1.51 eV at 77K). This material is transparent to 10.6 μm radiation, so that semi-insulating GaAs can be used for detectors which can be back-lit. A large lattice mismatch ($\simeq$14%) is present between GaAs and CdTe (the lattice constant of GaAs is 5.653$\AA$ at 27°C as compared to 6.482$\AA$ for CdTe). Nevertheless, epitaxial growth of high quality (100) CdTe layers on (100) GaAs were demonstrated by us during Year I [15].

Electron channeling studies were undertaken to investigate the crystalline quality and orientation of the grown layer. This technique is preferable to x-ray diffraction for thin epitaxial layers, since it has a depth resolution of under 500$\AA$, whereas that of x-ray diffraction ranges from 5 to 10 μm. Typically, the grown layer in our experiments was about 2.5 μm thick. The electron channeling pattern for a 2.5 μm CdTe layer grown at 350°C showed that the pattern is replicated with almost the same line sharpness, indicating the excellent crystal quality of the CdTe. Finally, the grown layer is seen to be of (100) orientation; i.e., it follows the substrate orientation. The orientation of the layers grown at other temperatures was also confirmed to be (100) by observing Laue back-reflection photographs, which also showed fourfold symmetry.

We have also shown that it is possible to grow (111) CdTe on (100) GaAs by minor changes to the cleaning procedure, and by raising the growth temperature. There is no advantage to pursuing this approach, however, since the OMVPE growth of (100) HgCdTe is considerably easier than for material of (111) orientation. The elastic strain associated with the lattice mismatch in (100) CdTe/(100) GaAs heterostructures was investigated by performing photoluminescence measurements as a function of CdTe layer thickness. Estimates of strains, stresses and lattice constants were obtained from

shifts near band edge photoluminescence features [16]. Biaxial compressive strains were present in the CdTe layers, and their magnitudes were found to be larger than those expected from equilibrium models and from transmission electron microscopy results.

During Year II, transmission electron microscope studies were made of CdTe-GaAs to determine the defect structure in this greatly mismatched (14.6%) system [17]. Here, two significant results were obtained. First, the CdTe-GaAs interface was found to be completely free of oxides or other interface layers, and comparable to that obtained with MBE. This is an important result, since it shows that chemical cleaning in a flowing gas medium is a viable alternative to thermal cleaning in an ultra-high vacuum environment. Second, we found the expected array of misfit dislocations, about 31$\AA$ apart. These were accompanied by glide plane dislocations, with a dramatic fall-off in density after a thickness of about 1.1 μm. Although the precise nature of this fall-off has not been determined, we believe that the increasing compressive strain in the CdTe layer with thickness reaches a point where dislocations are bent parallel to the substrate, and propagate in the [110] directions in this plane.

The significance of this result is that relatively thin layers of CdTe result in HgCdTe material of reasonable quality. Our work showed that the mobility of HgCdTe layers, grown on a 2 μm thick CdTe buffer layer, was comparable to that of bulk material. In practice, however, this buffer should be made at least 4-6 μm thick in order to achieve good minority carrier properties, such as lifetime, in the HgCdTe material.

2.3 Growth of Zinc Selenide

Our effort on II-VI compounds was expanded in Year III to explore the growth of ZnSe. This wide gap (2.7 eV) semiconductor is of technological importance because of its possible use in the blue-green spectrum. n-type doping of ZnSe is readily achievable, with Column III dopants such as aluminum. The possibility of achieving p-type doping

has opened the door for the development of junction devices in this material.

An important characteristic of ZnSe is that it is closely lattice matched to GaAs. As a result, pseudomorphic layers can be grown on GaAs to a thickness of about 1500Å. Below this thickness we can expect an interface which is relatively defect free, with an absence of dislocations. Thus, it should be possible to greatly reduce the surface recombination velocity (SRV) of the GaAs on which such layers are grown. This represents a second important use for ZnSe layers. In fact, if inversion of the GaAs could be achieved by this means, it would open the door to a true MOS technology for GaAs.

ZnSe was grown on GaAs by the reaction of dimethylzinc (DMZ) and dimethylselenide (DMSe) at a temperature of 400°C and a system pressure of 200 Torr. For these runs, the partial pressure of DMZ was 0.6 Torr, while that of DMSe was 1.0 Torr. Layers from 800-1800Å were grown, with a growth rate of about 0.17 μm/hr. Thus, some of these layers were thinner than the critical value for pseudomorphic growth ($\simeq$ 1200Å), whereas others were thicker.

The ZnSe layers were grown on both n^+GaAs and semi-insulating GaAs substrates, on which was previously grown an epitaxial layer of GaAs by a conventional OMVPE process. Both n- and p-type GaAs layers were used, with a doping concentration of about 2.5-3 $\times 10^{15}$ cm^{-3}.

Photoluminescence studies were made of the GaAs using a system comprising of an Ar-ion laser, a 3/4 meter spectrometer, and a photomultiplier with a liquid nitrogen cooled S-1 photocathode. PL data was taken on the GaAs, and also on the GaAs with a ZnSe cap layer. In all cases, the PL response on the ZnSe capped layers was from 100-200 times larger than that on the bare GaAs, for cap layers of 800-1100Å in thickness [18]. The shape of the PL spectrum was, however, unchanged. On the other hand, there was no improvement when 1800Å layers (which are thicker than the critical value), were used. Moreover, the results described here were quite reproducible. Removal of the ZnSe

layer immediately eliminated the PL improvement, which was recovered by regrowth of the ZnSe cap layer. The ratio $PL_{ZnSe/GaAs}/PL_{GaAs}$ is taken to be indicative of good interfacial properties of the ZnSe/GaAs heterojunctions. This ratio was found to be as high as 190 at 300K. Similar experiments, using p-p^+ GaAs, resulted in a PL improvement of 150 at 300K. The laser chopping frequency was varied between 90 Hz to 4000 Hz, with no change in these improvement factors.

The PL intensity from a sample is proportional to the total number of excess carriers generated. The excess charge associated with these carriers can be calculated by solving the continuity equation with appropriate boundary conditions. We have used this approach to solve for an epitaxial layer with front and back surface recombination velocity (SRV) taken into account. By this means, the estimated front SRV is approximately 1-2 $\times 10^3$ cm/s. In the case of the p/p^+ GaAs, (Case 3 in Table I), the observed improvement ratio was 145, comparable to the n/n^+ case. Assuming a back SRV of 2×10^3 cm/s, we estimate the front SRV to be 1.5×10^3 cm/s. This result implies that the observed intensity improvement caused by the ZnSe layer is not related to some surface field alone, but results from improved interfacial properties.

2.4 Growth of HgCdTe

This was the central thrust of our research, and all of the work described in Sections 2.1 and 2.2 was carried out with this in mind [19-22]. Additionally, the effort described in Section 2.5 was aimed at the characterization of this material.

$Hg_{1-x}Cd_xTe$, with $x = 0.2$ was the main focus of this program. Higher values of x (0.2 to 0.3) were often grown, however, because of the relative ease with which they could be characterized. This section outlines our work over the five-year period.

There are two aspects to this work. The first is the growth of HgCdTe with composition uniformity on lattice matched substrates. The second is the growth of this mate-

rial on mismatched substrates. In both cases, a high degree of compositional uniformity is required. We have worked on both of these tasks.

Growth of HgCdTe on lattice matched substrates is of importance in order to conduct scientific studies of this material, and to optimize the OMVPE growth process. These studies can only be made if the material is of high quality. Initially, we used CdTe substrates for this purpose. Here, the lattice mismatch (0.3%) between $Hg_{1-x}Cd_xTe$ with $x = 0.2$ and CdTe will generate dislocations at the interface which propagate into the epilayer. Alternative substrates, such as $Cd_{1-w}Zn_wTe$ ($w \simeq 0.04$) or $CdTe_{1-y}Se_y$ ($y \simeq 0.04$), have been proposed, which are lattice matched to $Hg_{0.08}Cd_{0.2}Te$. The addition of either Se or Zn into CdTe also increases its hardness and reduces the dislocation density of bulk grown substrates, so that these are inherently better starting materials than CdTe.

The use of Se is advantageous over Zn since it has a distribution coefficient of about 0.97, compared to 1.31 for Zn. As a result, compositional control of the substrate is maintained over larger boule lengths, so that CdTeSe is potentially a less expensive substrate material than CdTeZn. For this reason, we have chosen CdTeSe substrates for our research. Some work was, however, done with CdTeZn substrates as well since these are more readily available. Moreover, some of the purity issues of CdTeSe have not been resolved at the present time.

HgCdTe was grown on 1 cm $\times$ 1 cm substrates, by the process we have outlined earlier, using diisopropyltelluride as the tellurium source. Growth was carried out at an estimated substrate temperature of 370°C, with a growth rate of about 3.5 μm/hr.

Fourier transform infrared (FTIR) transmission spectroscopy was used to study the compositional uniformity across the wafer. Initial measurements were made for us by Texas Instruments (courtesy of Dr. Carlos Castro), with subsequent data taken on our newly acquired FTIR system. Measurements show that layers have edge to edge compo-

sitional uniformity (Cd fraction) of ± 0.002 (standard deviation = 0.0014) over a 1 cm $\times$ 1 cm area. The thickness uniformity of the layer is also excellent, better than ± 0.7 μm for 12-μm thick layers. Many layers have been grown with a composition of $x \simeq 0.2$, and the uniformity was found to be reproducible from run to run. Layers were grown on both CdTe and CdTeSe substrates [1, 2].

We believe that this is the first time such compositional uniformity has been demonstrated over this large area, using conventional alloy growth techniques by OMVPE. Layers of comparable uniformity have been grown using an interdiffused multilayer process (IMP), where alternate layers of CdTe and HgTe are grown under optimized growth conditions for each binary compound, and homogenized at the growth temperature with an annealing step. The crystallinity of interdiffused HgCdTe has been shown to be poorer than that of alloy grown HgCdTe, as determined by double crystal x-ray diffraction. This has been attributed to defects generated due to the lattice mismatch between HgTe and CdTe, and to incomplete interdiffusion. Moreover, extrinsic doping of layers grown by the IMP process is difficult because of the widely differing doping efficiencies of CdTe and HgTe.

Double crystal diffraction measurements, made on these layers, confirm the advantage of using CdTeSe substrates over CdTe. Typically, FWHM values of 47 ± 2 arc sec. were obtained on CdTeSe, as compared to 151 ± 15 arc sec. when CdTe substrates were used. This improvement comes about because of two reasons. First, the CdTeSe substrates had FWHM values of $\approx$14 arc sec., whereas CdTe substrates had values of about 32 arc sec. Thus, in addition to CdTeSe being a better lattice match to HgCdTe, its crystal quality is superior to that of CdTe. We believe, however, that the significant improvement in the quality of HgCdTe layers grown on CdTeSe substrates is primarily due to its better lattice match to the substrate.

2.4.1 Growth of HgCdTe on GaAs Substrates

An important question that arises when HgCdTe is grown on a foreign substrate is the doping of the layer from the substrate, either by interdiffusion or by vapor phase transport. With GaAs, Ga is an n-type dopant in both CdTe and HgCdTe, so that doping by Ga from the GaAs substrate can be a potential problem. To investigate this possibility, we have performed SIMS studies of several CdTe layers grown at 350°C on GaAs [23-25]. These measurements were done using oxygen ion bombardment and positive secondary ion spectrometry by Charles Evans and Associates. Here, we have found that, within about 1000Å, the Ga concentration falls to below the background level and remains constant at this value. SIMS measurements were also made on CdTe layers grown at 350°C and held at 415°C for 75 min. under DMCd overpressure. This was done in order to see the effect of keeping the above CdTe layer at a time and temperature associated with HgCdTe growth. The interdiffusion distance was found to be very small, the Ga concentration falling to below 1×10^{15} within about 0.5 μm. Hence, we can conclude that the Ga diffusion into HgCdTe layers can be ignored if the CdTe buffer layer is at least 0.5 μm thick. In practice, 4-6 μm thick layers are usually grown.

We have grown (111) CdTe at 375°C on (100) GaAs substrates after a five minute deoxidation step at 580°C. When these samples were heat treated at 415°C for one hour, however, significant Ga diffusion was observed. Whether this diffusion is due to the high temperature heat treatment step before the growth or because of the growth of the CdTe is carried out at higher temperature (375°C vs 350°C) is not clear at the present time. One possibility is that the high temperature heat treatment leaves a Ga rich surface which acts as a diffusion source during the 415°C anneal step.

HgCdTe layers have been grown on these CdTe buffer layers with $x \simeq 0.2$, and with a series of buffers of variable thickness. In all cases, the electron mobility of the HgCdTe layers steadily improved with increasing buffer layer thickness, until a buffer thickness

of 2.5 μm. Typically, a 77K mobility of 3×10^5 cm^2/Vsec was obtained in these layers. Buffer layers, 1000$\AA$ thick, resulted in mobility values around 10,000 cm^2/Vsec [24]. The direct growth of HgCdTe on GaAs was also tried. However, this was discontinued after a few runs, because of the poor layer quality resulting from this approach.

Growth of HgCdTe on GaAs was extended during Year III to the growth of wider gap material with $x = 0.27$, which is of interest for detectors in the 3-5 μm range [26]. Results here were very similar to those obtained for $x = 0.2$. As before, the thickness of the buffer layer had a pronounced effect on the mobility of the HgCdTe layers. Thus, the mobility value rises until the buffer thickness is 2 μm. The trend in mobility is similar to the results obtained for $x = 0.2$ layers described earlier.

The electron concentration of the HgCdTe was studied as a function of the buffer layer thickness. A linear fall-off in carrier concentration was observed with increasing buffer thickness. This fall in carrier concentration is to be expected if we consider the strain induced migration of Hg interstitials during growth. This causes a strong n-type behavior in the layer, probably because the mercury diffusion occurs via charged defects. The lower limit to this value is set by the residual impurities in the starting chemicals and by the annealing process conditions. We found a value of 2×10^{16}/cm^3 to be the lowest for buffer layers in excess of 1.9 μm thickness.

Our results indicate that bulk mobility can be approached as buffer layer thickness exceeds 1.9 μm. However, since this limitation is defect induced, it will be necessary to grow considerably thicker buffer layers in order to obtain HgCdTe films with lifetimes comparable to those on CdTe substrates. In practice buffer layers of 4-6 μm are used, so that these effects are essentially negligible.

2.4.2 Growth of Large Area HgCdTe

Growth of large area HgCdTe has been confined to 2" dia. GaAs slices, on which a

CdTe buffer is grown prior to the growth of the HgCdTe. Here, our work has shown that we can grow this material with a compositional uniformity of $x = 0.2 \pm 0.005$ over this diameter, using a rotating pedestal susceptor.

There are two additional issues which are problem areas for HgCdTe/CdTe/GaAs. The first of these is the overall growth morphology which is extremely featured. The second is the formation of macro defects or hillocks. A number of approaches have been used to attack these problems. Although they have been greatly reduced, the problems are not solved at the present time.

Ridged features are greatly reduced if the HgCdTe layer is grown at reduced temperatures. Our work with methylallyltelluride, a more easily pyrolyzable substitute for DIPTe, has greatly helped in this regard. This work is outlined in the next section. In addition, growth on misoriented substrates greatly reduces this morphology problem. We have experimented with different misorientations, and find that there is a significant improvement as we go from 0° to 8°, but much less with further misorientation. We currently use (100) GaAs which is 8° misoriented towards the (110), and this gives satisfactory results.

Macro defects or hillocks are Cd-rich in character. Their incidence is reduced by growth of the CdTe layer (not the HgCdTe layer) at elevated temperatures. In our initial experiments, the hillock density was in the range of 4000 to 5000 cm^{-2}. Hillocks became more pronounced and bigger in size as the buffer layer thickness was increased. The elongated hillocks were aligned towards the (110) direction, irrespective of the sample orientation on the susceptor, indicating that they might be related to the misorientation plane of the samples.

As mentioned, growth of the CdTe at elevated temperatures reduces the hillock density but tends to result in (111) CdTe layers. This tendency can be effectively blocked by the growth of an intervening ZnTe layer. Using this approach, we have reduced the

hillock density by a factor of 10, i.e., to 400-500/cm^2.

We have conducted many experiments along these lines in order to determine the reasons for this improvement, so that it may be optimized. As yet, however, no completely satisfactory solution has been reached. One theory for the effectiveness of the ZnTe layer is that it promotes two-dimensional growth on the GaAs. Yet, another is that it represents an intermediate mismatch value ($\simeq$7% to GaAs and $\simeq$7% to CdTe) between GaAs and CdTe. Double crystal x-ray measurements, made on CdTe layers growth with the ZnTe layer show that their strain (biaxial compressive) is reduced to about 50% of the value obtained with direct growth of CdTe:GaAs.

Our work in this area was limited by the termination of the program, and is certainly far from complete. Nevertheless, we believe that a satisfactory solution of the hillock problem will be essential to the fabrication of focal plane array devices on GaAs substrates.

2.4.3 Low Temperature Growth of HgCdTe

The epitaxial growth of HgCdTe is difficult since this semiconductor is very susceptible to thermally induced defects at the growth temperature. Thus, significant improvements can be realized if growth is carried out at reduced temperature. Many approaches, using laser, UV and plasma excitation have been proposed for this purpose. We believe that the approach of using Te alkyls, which are more readily cracked, is the most promising one. Historically, diethyltelluride (DETe) was used for the OMVPE of HgCdTe, at a growth temperature of 415°C, to achieve a reasonable growth rate (around 3-4 μm/h). More recently, the use of diisopropyltelluride (DIPTe) has allowed the growth temperature to be reduced to around 370°C, while maintaining this growth rate. Other Te precursors such as ditertiarybutyltelluride and diallyltelluride have been used to grow HgTe or CdTe at low temperatures (250-350°C). A disadvantage of these

chemicals is their low vapor, which necessitates the use of heated bubblers and lines to transport a sufficient amount of Te to the reactor.

A number of tellurium sources are available for the growth of HgCdTe at the present time. During Years IV and V we have investigated the growth of HgCdTe using methylallyltelluride (MATe) as the tellurium alkyl. This source has the advantage of relatively high vapor pressure (6.2 Torr at 20°C) so that it can be transported readily to the reaction zone.

The epitaxial growth of HgTe and HgCdTe was carried out at reduced pressure (380 Torr) in a vertical reactor using MATe, DMCd, and Hg as the Te, Cd, and Hg sources respectively. Both HgTe and HgCdTe layers were grown in the temperature range from 250-320°C, with growth rates comparable to those obtained at 50°C higher temperatures using DIPTe [27, 28].

The morphology of HgTe layers grown at all temperatures was featureless, with a notable absence of ridges which are usually observed when DIPTe or DETe are used as the Te source chemicals. Growth at higher temperatures using MATe resulted in layers with similar step features to those obtained using DIPTe. This confirms that the improved morphology of layers grown by MATe is mainly due to the lower growth temperature. The addition of DMCd to the growth environment, to produce HgCdTe, resulted in further improvement to the morphology.

The crystal quality of HgTe epilayers was investigated by double crystal x-ray diffraction, and tilt was observed between the epilayer and the substrate. This tilt was measured to be an additional 60-150 arc sec away from the surface normal. Epilayer tilt of this type has been observed in other lattice mismatched systems, but is generally not seen when HgTe layers are grown at higher temperatures using DIPTe or DETe. This is because growth at higher temperatures results in significant interdiffusion between the HgTe epilayer and the CdTe substrate, causing a gradual change of the lattice constant,

so that no tilt is observed.

Double crystal x-ray diffraction data was taken on thin (1.7 μm) HgTe layers grown on a CdZnTe substrates, which is a reasonably close lattice match to HgTe. Here, we found that both the epilayer and the substrate have nearly identical x-ray full width half maximum (FWHM) values (29 and 28 arc sec, respectively), indicating the excellent quality of the epilayer that can be obtained by the low-temperature growth process. The lattice mismatch between the substrate and the layer is estimated to be below 0.07%, assuming that the epilayer is in bilateral tension. The layer followed the exact orientation of the substrate.

HgCdTe layers were also grown with MATe at 320°C. FTIR transmission data showed sharp interference fringes, even for thin (1.3 μm) layers, indicative of an absence of interdiffusion effects. Electrical measurements showed that the layers behaved n-type with a carrier concentration at low temperatures of 2×10^{15} cm^3 and a mobility value of 40,000 cm^2/Vs at 40K (for $x = 0.23$). The n-type behavior of this layer is attributable to a number of factors. First, the use of a low growth temperature results in a low concentration of Hg vacancies, which are acceptors. Next, the mismatch to the CdTe substrate results in defects that are active and probably n-type. This effect would be reduced for lattice matched substrates. Finally, we note that the value of mobility is not as high as that obtained when DIPTe was used, probably because the layer is heavily compensated. We attribute this to the fact that MATe is a relatively newly developed Te source, and that it will be available in higher purity with the passage of time. As a result, work with this chemical was not further pursued during this program.

2.4.3 p-Type Doping of HgCdTe

As grown HgCdTe is generally p-type due to the presence of native defects such as mercury vacancies, provided that the residual (donor) impurities in the starting chem-

icals are in very low concentration. In order to obtain layers with stable and controllable doping, it is necessary to introduce external impurities. Both group V elements, which are incorporated on the Te sublattice, and the group I elements, which incorporate on the metal sublattice, act as p-type dopants. Group V elements are preferred because they are much slower diffusion acceptors and hence can be used to form stable device structures. However, doping of HgCdTe by group V elements such as Sb, As and P has not been very successful by many growth methods. In our work, we have successfully doped HgCdTe p-type, using arsine gas as the dopant source [29, 30]. Layers were grown as described earlier. In addition, arsine gas was introduced during the direct alloy growth process.

Arsenic-doped layers were grown with p-doping levels from 3.5×10^{15} to 10^{17} cm^{-3}. No evidence of surface inversion was observed in these doped layers, except for lower doped samples, and at temperatures below 30K. The low temperature mobility values remained constant at ~500 cm^{-2}/Vs down to 20K and showed negligible change (<5%) when the magnetic field was increased from 2.1 to 4.5 kG, indicating the absence of any surface inversion. The high value of hole mobility observed here indicates that most of the As is electrically active in the layer.

In order to determine the acceptor ionization energy and the acceptor doping concentration, the low temperature Hall coefficient curve was fitted to the theoretical model assuming a fully ionized donor N_d and a single acceptor N_a at E_a above the valence band. The activation energies obtained from this fit were compared to values for the Column II acceptor. In general, the ionization energy for the mercury acceptor was found to be a factor of 2 higher than that for the arsenic, for comparable doping levels.

Isothermal annealing was carried out in order to annihilate the excess mercury vacancies. The annealing was performed for 15 hours at 270°C, in a sealed quartz ampoule in which a small amount of Hg was placed. For these experiments, uncapped, doped

HgCdTe layers were grown side by side, in the same run. The as grown layer had a p-type carrier concentration of 3.7×10^{16} cm^{-3}. The second layer, annealed in a Hg-rich ambient as described above, had a measured carrier concentration of 4.3×10^{16} cm^{-3}. The small increase observed here as most probably due to the nonuniformity in the doping of the adjacent layers. However, increased activation of As cannot be ruled out.

SIMS measurements on these layers, provided by Dr. G. Scilla of IBM, confirmed the presence of arsenic in these layers. In addition, the SIMS count was seen to be linearly related to the arsenic concentration, well into the saturation region. This unusual result indicates that saturation of the p-concentration with increasing AsH_3 is not due to the incorporation of As into neutral or compensating sites. Rather, the surface coverage of the arsenic limits with increasing AsH_3 flow. The high mobility of these layers, well into the saturation region (400 $cm^2/Vsec$ for a doping of $1 \times 10^{17}/cm^3$) is a direct consequence of these observations.

As-doping was also found to increase, approximately linearly with Hg overpressure, by up to a factor of 4. This strongly suggests that the arsenic is in Te-sites, and that HgCdTe material, doped in this manner, is uncompensated [31]. Details of this work are provided in Appendix A.

We have also made a number of arsenic doping experiments with both CdTe and HgTe, in order to understand the physics of dopant incorporation, towards the end of Year V of this program. Our results are of a very preliminary nature, but indicate that the doping efficiency for CdTe is approximately 200 times that for HgTe, for our set of growth parameters. Reasons for this large difference are not understood at the present time.

2.4.4 n-Type Doping of HgCdTe

n-type doping is readily accomplished in HgCdTe. Here, both Group III elements,

incorporated on a metal sublattice, and Group VII elements on the Te sublattice, behave as n-type dopants. Group VII dopants are undesirable in OMVPE growth because of possible reaction with alkyls. Of the Group III dopants, In is preferred over others since it is a slower diffusing species, by a factor of more than 10. In our work [32], we have used triethylindium, trimethylindium (TMIn) and elemental indium as dopant sources, with qualitatively similar results. The work to be described now was carried out using TMIn as the dopant source.

HgCdTe layers were grown as described previously, with the hydrogen flow through the dopant bubbler (held at 20°C) used to provide a partial pressure of TMIn over the range 3×10^{-7} to 1.5×10^{-5} atm. Controlled n-type doping, with a linear variation of electron concentration with flow through the TMIn bubbler, was achieved using this approach.

Hall measurements were made with magnetic field strength values from 0.5 to 6 kG during the course of this study. In all cases, the Hall coefficient showed classical extrinsic n-type behavior over the entire 300 to 10K temperature regime, and was independent of the magnetic field strength. In two experiments, the carrier concentration was estimated to be 5×10^{16} cm^{-3} for the layer with $x = 0.28$ and 3×10^{16} cm^{-3} for the layer with $x = 0.23$. The low temperature mobility values, of 3.3×10^4 and 7.3×10^4 cm^2/Vs for cadmium compositions of 28% and 23% respectively, are consistent with these carrier concentration values.

The linear dependence of the donor concentration on the dopant flux, combined with the high values for mobility, implies an electrical activation of almost 100% for the indium incorporated in the layers, until a doping level of 4×10^{18} cm^{-3} is reached. At higher values of the dopant flux, however, it is possible that indium gets increasingly incorporated in electrically inactive form as In_2Te_3, as has been reported for In doping of bulk HgCdTe in the melt.

The wave number corresponding to an absorption coefficient $\alpha = 500$ cm^{-1} was measured in these samples at room temperature, and the optical energy gap E_g determined from its value. E_g remained constant, at ~200 meV, for doping concentrations up to 1×10^{17} cm^{-3}. However, E_g increased to 350 meV for an electron concentration of 3×10^{18} cm^{-3}. This change in E_g can be interpreted as an increase in x from 0.23 to 0.3. Similar shifts in the composition were reported for the interdiffused multilayer process, where a change in x from 0.27 to 0.4 was observed when the TMIn partial pressure was increased from 10^{-6} atm. to 1.3×10^{-5} atm. It is possible that x changes with doping concentration due to relative changes in the effective growth rates of the HgTe and CdTe components of these layers. Alternatively, the increase in E_g can be accounted for the by the Burstein-Moss shift with doping concentration, that has been observed in bulk HgCdTe.

In order to resolve this issue, EDAX measurements of a number of layers were made for us by Dr. H. Schaake of Texas Instruments, to obtain a direct measure of the Cd fraction. These measurements confirm that the shift in optical bandgap can be closely predicted by the Burstein-Moss shift. Thus, within the accuracy of our measurement method, there is no change in the HgCdTe composition with n-type doping. Details of this work are provided in Appendix B.

2.5 Characterization

Characterization is an important component of any program of materials research, since it provides the necessary information which can be used to modify the growth process. During the course of this program, as our growth techniques became more routine, we developed a greater need to improve our characterization methods, and increased our effort on this phase of the program. Currently, a number of characterization tools have been acquired/developed for our work. Some of these are now detailed.

Fourier Transform IR Spectroscopy is a valuable tool for the measurement of layer thickness and composition; this tool was acquired during the early phase of our program. Our instrument, a Mattson Cygnus 100, is computer controlled so that measurements can be made at as many as 100 points over a 1 cm $\times$ 1 cm sample. Both composition and layer thickness can be determined with this instrument.

Layer thickness of HgCdTe films grown on CdTe/GaAs are complicated by the fact that three different refractive indices must be considered. A computer program has been written to analyze the complex fringe structure which is obtained under these conditions.

Double crystal x-ray diffraction, using (004) reflections, was acquired in order to measure layer quality. We have also developed methods for taking low angle measurements, using (115) reflections. This is useful for very thin layers, and also for corroborating strain measurements of HgCdTe films. Computer codes have been written to simulate rocking curves in the presence of strain, and allow a detailed analysis to be made of the x-ray data.

Hall effect measurements give a quick idea of both crystal quality and background concentration. For n-type samples, measurements at a few points from 10-300K can provide enough data for sample evaluation. p-type samples, on the other hand, require a detailed plot over this temperature range. Moreover, anomalous results often arise, especially in lightly doped, low x layers which are subject to surface inversion.

During this program we completely automated our Hall effect system so that it is now under full computer control. This has greatly improved our data acquisition capability. In addition, a number of computer programs have been written for p-HgCdTe, since the results of the Hall measurements can best be evaluated by fitting the data to a two layer model, with an n-type surface inversion layer.

2.5.1 Annealing Studies

Our first task on this five-year effort was the development of HgCdTe with a high degree of compositional uniformity. This has been achieved on a routine basis; as a result, the emphasis during Years IV and V has shifted to establishing material purity. An extensive series of annealing experiments have been carried out with this end goal.

Typically, our as-grown layers, which are p-type with carrier concentrations around 3-4 $\times 10^{16}/cm^3$ due to mercury vacancies, become light p-type with carrier concentrations around 1-2 $\times 10^{15}/cm^3$ after Hg saturated annealings at temperatures in the range of 200-300°C. These conditions are usually sufficient for the complete annealing of bulk $Hg_{1-x}Cd_xTe$ to n-type, but are inadequate for thin epilayers, grown by OMVPE as well as by LPE and MBE.

During our work, we have developed a new annealing technique which allows successful conversion of these layers to n-type [33]. We have found that the as-grown layers are converted to n-type, with carrier concentration of approximately $5 \times 10^{14}/cm^3$, by a higher temperature anneal around 270-290°C, followed by a low temperature anneal at 220°C.

All layers grown for our annealing studies were capped with a 0.5-1.0 μm thick layers of undoped CdTe which was grown in the same reactor run. This cap serves two purposes. First, it prevents an unintentional annealing of the HgCdTe layers during cool down after the layer growth. Second, it inhibits the formation of an inversion layer on the HgCdTe surface, which can affect the Hall characterization of as-grown p-type layers. Cap layers were removed just prior to the annealing by means of a short etch consisting of 1% Br in methanol. The epilayer thickness was determined from the interference fringes in the sub-bandgap regime of the IR transmittance curve. The bandgap of the layer was taken to be the energy at which the absorption coefficient of the material is 500 cm^{-1}, and then used to determine the alloy composition.

After cap removal, samples were rinsed in methanol, dried with nitrogen, and loaded in an aqua regia cleaned quartz ampoule with mercury of 99.99999% purity. The ampoule was evacuated to 10^{-7} Torr using a turbo-molecular pump equipped with a liquid nitrogen trap, and sealed using an oxy-hydrogen flame. All annealings were carried out with the sample kept 2°C warmer than the Hg reservoir, to avoid Hg from condensing on them. This prevented any surface deterioration during the anneal and sample surfaces showed no sign of damage. The annealed samples were characterized by van der Pauw techniques without any further surface treatment.

A number of samples showed anomalous behavior. This comes about because of an n-type surface accumulation layer on the p-epilayer. The fact that there is indeed a p-type layer with surface inversion was verified by sulfidizing these samples in an anodic bath. This anodic sulfide results in a low concentration of fixed positive charges and reduces the inversion layer to the point where p-type behavior is restored. Eventually, parameter extraction is performed by computer simulation Details of this work are provided in Appendix C.

The presence of an electron accumulation layer on the surface of n-type $Hg_{1-x}Cd_xTe$ causes the measured Hall mobility and carrier concentration to be significantly different from the actual bulk values. This discrepancy is not readily apparent in the temperature dependence of the Hall coefficient, R_H, since the data does not show any obviously anomalous behavior. However, it is observed in the magnetic field dependence of the R_H.

In one set of experiments, the B-field dependence of R_H, in the 0-5 kG range, was analyzed to extract the actual concentration and mobility of the bulk and surface carriers in $Hg_{1-x}Cd_xTe$ layers grown by organometallic vapor phase epitaxy. The bulk parameters thus calculated were verified by passivating the surface of these layers using an anodic sulfide to reduce the concentration of surface electrons. Here, interpretation of

Hall data which ignores the effect of surface electrons resulted in a measured carrier concentration of $8 \times 10^{14}/cm^3$ and a mobility at 30K of 188,000 $cm^2/Vsec$. The presence of the surface electrons in this sample became evident when the R_H was found to vary with the B-field. Computer analysis was undertaken for this sample, based on a model which includes both surface and bulk carriers. Now, the bulk carrier concentration was calculated to be $5 \times 10^{14}/cm^3$ with a mobility of 269,000 $cm^2/Vsec$ at 30K. The surface carrier concentration was calculated to be $5.2 \times 10^{11}/cm^2$ with a mobility of 25,000 $cm^2/Vsec$ at 30K.

To verify that the bulk parameters extracted by this technique are indeed the true values, and that the B-field dependence of the R_H was indeed caused by the effect of surface electrons, the layer was surface passivated using anodic sulfide and the Hall measurements were repeated. The variation in R_H with the B-field was again fitted using the two carrier model, with a bulk carrier concentration of $5 \times 10^{14}/cm^3$ and a mobility of 269,000 $cm^2/Vsec$, along with a surface carrier concentration of $1.1 \times 10^{11}/cm^2$ with a mobility of 28,000 $cm^2/Vsec$. Note that the bulk carrier parameters were the same as before; however, the surface carrier concentration is now a factor of 4-5 lower due to the sulfidization.

Details of this work are provided in Appendix D.

2.5.2 Lifetime Measurements

This is the single area in which we have the greatest need for materials characterization, and simultaneously the greatest weakness. Two approaches have been developed during the course of this program. The first of these involves the fabrication of photoconductor devices, from which the lifetime can be extracted by taking steady state photo-response measurements. Although simple in principle, this approach is fraught with experimental difficulties, so that only a few devices are useful for characterization

purposes.

A mask set was made to allow the fabrication of 16 devices simultaneously in view of the low yield of this process Both photolithography and sample delineation techniques have been developed for this purpose. Mounting of the chip to a cold finger in a dewar, and connection of the devices to the outside world, is the next step. Techniques for doing this have also been developed. Finally, a calibrated IR source, and the associated equipment (choppers, lock- in amplifiers, and monochromators) have been assembled in order to take these measurements. Using this approach, we can make spectral response measurements of our material, from which the minority carrier lifetime can be obtained.

We have explored a number of surface coatings for this purposed of making device measurements. Of these, our greatest success has been the use of a sulfidization methods for passivating the HgCdTe surface. This method is a modification of the one proposed by Nemirovsky et al. We have found it especially suitable for p-type layers and are using it for lightly doped HgCdTe. The sulfidized layer, which is essentially CdS, is not suitable by itself as the insulator of an MOS structure. Consequently, it is covered with an evaporated ZnS cap prior to the evaporation of gold dots for making the MOS structure.

The second approach is an extremely powerful one, which we have investigated during Year IV and V. This approach, developed by Prof. J.M. Borrego at Rensselaer, consists of measuring the microwave reflectance of a sample under transient illumination. In this system, a Gunn diode is used to generate 150 mW of power at ~36 GHz. This power is delivered via a hybrid tee to the sample, which is placed on a conductive shorting plane, ~1 mm away from the tip of the antenna. The area irradiated by this antenna is approximately 1 mm × 1 mm. The reflected signal from the sample is collected by the antenna and detected by a crystal detector. The reflected power is prevented from affecting the load seen by the oscillator, by means of an isolator. Thus the oscillator output power remains stable. The sample is also illuminated locally by an AlGaAs laser,

with a spot area of 0.1 mm × 0.1 mm. The fall time of this laser is 3 nsec. This limits the lowest lifetime which can be measured by the system.

The induced photoconductivity modulates the microwave power reflected at the samples and this serves as the probe for the excess carrier decay. The reflected microwave signal is detected by a fast responding crystal detector, the output of which is a voltage proportional to the incident microwave power at the detector. The output signal of the detector is proportional to the excess carrier density. The change in reflected microwave power for higher dopings and low lifetimes is small and hence amplification of the signal is required. To obtain a faithful reproduction of the photoconductivity transient a large bandwidth (0.1 to 1300 MHz) a.c. amplifier is used. The transients are viewed on a Tektronix 2432A digital oscilloscope. The bandwidth of the scope is 300 MHz for repetitive signals. The signal to noise ratio is improved by averaging as many as 256 acquisitions using this scope. The time constant of the decay of the transient reflected microwave power can be shown to be the effective lifetime of carriers in the semiconductor.

Our early work with the system shows that it is an extremely powerful tool for lifetime measurements, since it is nondestructive, and can be used rapidly to probe small regions of a large area sample. Moreover, it can be used for studying the behavior of different surface passivations, as well as for making basic studies of the recombination process.

The system, in its present form, was not designed for use with HgCdTe, and many changes will be required in order to optimize it for this purpose. At the present time it is only capable of being operated at room temperature, so that its adaptation to HgCdTe will necessitate its installation in a cryostat. Additionally, its frequency of operation, 35.5 GHz, is not optimum for this semiconductor. Changes here, if made, would have to be of a major nature.

3. UNSOLVED PROBLEMS

Over the last five years, there has been much progress in the epitaxial growth of HgCdTe for focal plane array applications. This report has outlined our contribution to this area. It is appropriate, therefore, that we conclude with a list of some of the problem areas which still have to be addressed.

- Composition Uniformity: This problem has been solved for 2" dia., single slice growth. Clearly, extensions to 3" dia. are necessary since most available GaAs substrates are now of this diameter (with 4" coming on stream). In addition, multiple slice reactors are not successful at the present time.

There is a serious need for computer simulation in this area. The problem is not in the development of codes, however. Rather, it is in an understanding of the reaction chemistry, which is not forthcoming at the present time. This is necessary before any code can be used with success, regardless of its sophistication.

- Run-To-Run Repeatability: This, we believe is a solvable, engineering problem. The use of an automatic Hg level in the reservoir, with a load lock system, is necessary to obtain this feature.
- Morphology and Hillocks: These problems have not been solved at the present time. We have outlined our progress in this report, but much more effort will be required before they can be eliminated.
- Low Temperature Growth: The use of new alkyls, such as MATe, is very promising. However, improvements will be required in their purity in order to be useful. Once an alkyl is identified (and MATe may not be the ideal choice), then techniques will have to be developed to obtain both p- and n-doping at these reduced growth temperatures.
- p- and n-Doping: We believe that these issues are essentially understood, for the dopants and tellurium source (DIPTe) we have selected. However, alternative

dopants (e.g., As vs. P vs. Sb) should be explored to determine their advantages and disadvantages. Moreover, there are many choices for dopant sources, based on toxicity, vapor pressure, and controllability. Although toxic, arsine gas is an excellent source of arsenic, because of its ready availability in a wide range of dilutions. Tertiarybutylarsenic is a less toxic source and will probably be a suitable alternative. The choice of TMIn, however, places undue burden on the chiller and the mass flow controller, because of its relatively high vapor pressure. Thus, TEIn would be a better (but not necessarily the best) choice for these reasons.

- Characterization: Minority carrier lifetime measurements are the most difficult to make; yet, they are the most important for determining the quality of the starting material. Here, a noninvasive technique, such as time domain microwave reflectance spectrometry, has a great advantage over others in that it provides rapid materials evaluation and can be used for making improvements to the growth process.
- Structural Evaluation: We have used double crystal x-ray diffraction for this purpose. Techniques for evaluating precipitate density and dislocations (such as selective etching and TEM) will be necessary to effect further improvements in the grown material.

The above list is by no means complete. However, in the course of our work, these are the items which we have identified as problems in the way of successful application of HgCdTe technology for focal plane array devices.

4. PUBLICATIONS

As an academic institution, we believe it is our responsibility to disseminate information to the technical community on a timely basis. The following is a list of publications which resulted from work on this program. In addition, a number of papers have been presented at professional conferences.

1. S.K. Ghandhi, I.B.Bhat and H. Fardi, "Organometallic Epitaxy of HgCdTe on CdTeSe Substrates with High Compositional Uniformity", Appl. Phys. Lett., 52, 392 (1988).
2. I. B. Bhat, H. Fardi, S.K. Ghandhi and C.J. Johnson, 'Highly Uniform, Large Area HgCdTe Layers on CdTe and CdTeSe Substrates", J. Vac. Sci. Tech., A6(4), 2800 (1988).
3. N.R. Taskar, I.B. Bhat and S.K. Ghandhi, "The Growth and Characteristics of CdTe on InSb by MOVPE", J. Crys. Growth, 77, 488 (1986).
4. N.R. Taskar, I.B. Bhat, J.M. Borrego and S.K. Ghandhi, "OMVPE Growth of CdTe on InSb Substrates", J. Electron. Mater., 15, 3, 165 (1986).
5. I.B. Bhat, N.R. Taskar, J.E. Ayers, K. Patel and S.K. Ghandhi, "CdTe Films Grown on InSb Substrates by Organometallic Epitaxy", Materials Res. Soc., 20, 471 (1986).
6. S.K. Ghandhi, N.R. Taskar and I.B. Bhat, "The Effect of Process Conditions on the Quality of CdTe Grown on InSb by Organometallic Epitaxy", Appl. Phys. Lett., 49, 1290 (1986).
7. I.B. Bhat, N.R. Taskar, J.E. Ayers, K. Patel and S.K. Ghandhi, "X-Ray Diffraction Studies of CdTe Grown on InSb by Organometallic Epitaxy", J. Crys. Growth, 88, 23 (1988).
8. I.B. Bhat and S.K. Ghandhi, "On the Mechanism of Growth for the OMVPE of CdTe", J. Electrochem. Soc., 134, 195 (1987).
9. S.K. Ghandhi, N.R. Taskar and I.B. Bhat, "Arsenic-doped p-CdTe Layers Grown by Organometallic Vapor Phase Epitaxy", Appl. Phys. Lett., 50(14), 900 (1987).
10. N.R. Taskar, V. Natarajan, I.B. Bhat and S.K. Ghandhi, "Extrinsic Doped n- and p-Type CdTe Layers Grown by Organometallic Vapor Phase Epitaxy", J. Crys. Growth, 86, 228 (1988).

11. W.I. Lee, N.R. Taskar, I.B. Bhat, J.M. Borrego and S.K. Ghandhi, "DLTS Studies of n-Type CdTe Grown by Organometallic Vapor Phase Epitaxy", Proc. 19th IEEE Photovoltaic Specialists Conf., 785 (1987).

12. W.I. Lee, N.R. Taskar, I.B. Bhat, S.K. Ghandhi and J.M. Borrego, "DLTS Studies of n-CdTe Grown by Organometallic Vapor Phase Epitaxy", Solar Cells, 24, 279 (1988).

13. I. Bhat. L. Sundaram, N. Taskar, J.M. Borrego and S.K. Ghandhi, "CdTe-InSb Heterostructures Grown by OMVPE: Preparation and Electrical Properties", Solid State Electron., 29, 257 (1986).

14. H.G. Bhimnathwala, N.R. Taskar, W.I. Lee, I. Bhat, S.K. Ghandhi and J.M. Borrego, "Photovoltaic Properties of CdTe Layers Grown by OMVPE", Proc. 19th IEEE Photovoltaic Specialists Conf., 1476 (1987).

15. S.K. Ghandhi, N. Taskar, I. Bhat, "Growth of CdTe on GaAs by Organometallic Vapor Phase Heteroepitaxy", Appl. Phys. Lett., 47(7), 742, (1985).

16. D.J. Olego, J. Petruzello, S.K. Ghandhi, N.R. Taskar and I.B. Bhat, "Elastic Strains in CdTe-GaAs Heterostructures Grown by Metalorganic Chemical Vapor Deposition", Appl. Phys. Lett., 50(14), 127 (1987).

17. J. Petruzello, D. Olego, S.K. Ghandhi, N.R. Taskar and I.B. Bhat, "Transmission Electron Microscopy of (001) CdTe on (001) GaAs Grown by Metal-Organic Chemical Vapor Deposition", Appl. Phys. Lett., 50, 1423 (1987).

18. S.K. Ghandhi, S. Tyagi and R. Venkatasubramanian, "Improved Photoluminescence of GaAs in ZnSe/GaAs Heterojunctions Grown by Organometallic Epitaxy", Appl. Phys. Lett., 53, 1308 (1988).

19. I.B. Bhat and S.K. Ghandhi, "The Growth of Mercury Cadmium Telluride by Organometallic Epitaxy", J. Crys. Growth, 75, 241 (1986).

20. S.K. Ghandhi, "The Organometallic Epitaxy of HgCdTe for Far Infrared Applica-

tions", Mater. Res. Soc., 102, 65 (1987).

21. P.M. Raccah et al., S.K. Ghandhi and I. Bhat, "Study of MCT Epilayers Grown by Metalorganic Vapor Phase Epitaxy", J. Appl. Phys., 57(6), 2014, (1985).
22. S.K. Ghandhi, "Recent Progress in the OMVPE Growth of HgCdTe", Materials Res. Soc. (accepted) (1989).
23. S.K. Ghandhi, I.B. Bhat and N.R. Taskar, "Growth and Properties of $Hg_{1-x}Cd_xTe$ on GaAs Substrates by OMVPE", J. Appl. Phys., 59(6), March (1986).
24. I. Bhat, N. Taskar, S.K. Ghandhi, "The Organometallic Heteroepitaxy of HgCdTe on GaAs Substrates", J. Vac. Sci. Tech., A4(4), 2230 (1986).
25. I.B. Bhat, N.R. Taskar, K. Patel, J.E. Ayers and S.K. Ghandhi, "Characteristics of OMVPE-grown CdTe and HgCdTe on GaAs", Proc. SPIE, 796, 194 (1987).
26. V. Natarajan, N. Taskar, I.B. Bhat and S.K. Ghandhi, 'Growth and Properties of $Hg_{1-x}Cd_xTe$ on GaAs with $x = 0.27$", J. Electron. Mater., 17, 493 (1988).
27. S.K. Ghandhi, I.B. Bhat, H. Ehsani, D. Nucciarone and G. Miller, "Low Temperature Growth of HgTe and HgCdTe Using Methylallyltelluride", Appl. Phys. Lett., 55(2), 137 (1989).
28. I.B. Bhat, H. Ehsani and S.K. Ghandhi, "Low Temperature Growth of HgTe and HgCdTe Using Methylallyltelluride", J. Vac. Sci. Tech., A8(2), 1054 (1990).
29. S.K. Ghandhi, N.R. Taskar, I.B. Bhat, K.K. Parat, D. Terry and H. Ehsani, 'Extrinsic p-Doped HgCdTe Grown by Organometallic Epitaxy", Appl. Phys. Lett., 53, 1641 (1988).
30. N.R. Taskar, I.B. Bhat, K.K. Parat, D. Terry, H. Ehsani and S.K. Ghandhi, "The Organometallic Epitaxy of Extrinsic p-Doped HgCdTe", J. Vac. Sci. Tech., A7(2), Mar/Apr (1989).
31. N.R. Taskar, I.B. Bhat, K.K. Parat and S.K. Ghandhi, "The Mercury Pressure Dependence of Arsenic Doping in HgCdTe, Grown by Organometallic Epitaxy", J.

Crys. Growth, (accepted) 1990.

32. S.K. Ghandhi, N.R. Taskar, K.K. Parat and I.B. Bhat, "Indium Doping of n-Type HgCdTe Layers Grown by Organometallic Vapor Phase Epitaxy", Appl. Phys. Lett., (accepted) 1990.
33. K.K. Parat, N.R. Taskar, I.B. Bhat and S.K. Ghandhi, "Annealing and Electrical Properties of HgCdTe Grown by OMVPE", J. Crys. Growth, (accepted) 1990.
34. K.K. Parat, N.R. Taskar, I.B. Bhat and S.K.Ghandhi, "The Effect of Surface Layers in n-Type Epitaxial HgCdTe", Materials Res. Soc. (accepted) (1989).
35. K.K. Parat, N.R. Taskar, I.B. Bhat and S.K. Ghandhi, "The Influence of Accumulation Layers on the Hall Effect in n-Type HgCdTe", J. Crys. Growth (submitted).

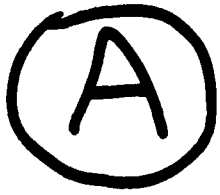

THE MERCURY PRESSURE DEPENDENCE OF ARSENIC DOPING IN HgCdTe, GROWN BY ORGANOMETALLIC EPITAXY

N.R. TASKAR

I.B. BHAT

K.K. PARAT

S.K. GHANDHI

ELECTRICAL, COMPUTER AND SYSTEMS ENGINEERING DEPARTMENT

RENSSELAER POLYTECHNIC INSTITUTE

TROY, NEW YORK 12180

AND

G.J. SCILLA

IBM THOMAS J. WATSON RESEARCH CENTER

YORKTOWN HEIGHTS, NEW YORK 10598

Submitted to Journal of Crystal Growth

Point of Contact:

S.K. Ghandhi

Telephone: 518-276-6085

FAX: 518-276-6261

SK-89.38

April 18, 1990

ABSTRACT

The effect of Hg partial pressure on arsenic doping of HgCdTe is studied. It is found that control of Hg partial pressure is very important in obtaining reproducible doping, and use of high Hg pressure is the key to obtain heavily doped layers. Typically, a factor of 4 increase in the partial pressure of Hg is found to increase the acceptor concentration by this same magnitude. In addition, arsine doping results in almost uncompensated layers, even though high concentration of Hg vacancies are present. A mechanism is proposed by which As is incorporated as a Cd-As complex, so that it substitutes preferentially on Te sites.

INTRODUCTION

The fabrication of stable p-n junctions in mercury cadmium telluride requires a p-type dopant that will be slow diffusing during subsequent device processing. HgCdTe layers grown by organometallic vapor phase epitaxy (OMVPE) are generally p-type [1] due to the presence of Hg vacancies, but these are fast diffusers. Hence, it is necessary to use external impurities to obtain stable p-type layers. Both Column I and Column V elements can be used as the p-type dopants, but Column V dopants are preferred because they have low thermal diffusivity [2, 3]. Group V elements, when substituted into Te sites, will behave p-type, but will be donor-like if incorporated on Hg sites. Hence, it is of concern that group V elements may substitute Hg sites to a significant concentration, and compensate the Te-substituted acceptors. In fact, arsenic (as well as other Column V species) doping has been unsuccessful in the liquid phase epitaxy of HgCdTe grown from a Te-rich melt, because some arsenic incorporates in Hg sites, resulting in heavily compensated layers [4]. In molecular beam epitaxy, doping using solid sources of As and Sb, has not resulted in p-type layers [5]. However, we have shown that it is possible to dope HgCdTe using arsine [6], even though it growth by OMVPE occurs under Hg-deficient conditions with a high concentration of Hg vacancies (mid 10^{15} - mid 10^{16}), as compared to Te vacancies. In this paper, we present a study of the effect of Hg pressure on the doping and propose a mechanism to explain the arsine doping process in HgCdTe, grown by OMVPE.

EXPERIMENTAL:

HgCdTe layers were grown at 370°C in an atmospheric pressure, horizontal reactor using diisopropyltelluride, dimethylcadmium (DMCd) and elemental mercury. Substrates were 2° misoriented (100) $CdZn_{0.04}Te_{0.96}$, which is closely lattice matched to the epilayer. The thickness of $Hg_{1-x}Cd_xTe$ layers reported here was $\sim$ 7μm, and the alloy composition x was in the range 0.27-0.31. A cap of CdTe layer, approximately 1 μm

thick, was grown on the HgCdTe as a passivant layer. A 500 ppm mixture of arsine in hydrogen was used for doping purposes.

Hall measurements were made over the temperature range 10-300K, with a magnetic field from 0.5-6.0 kG. Measurement at low temperature and at different magnetic fields was necessary to make sure that a surface inversion layer is not present. In those cases where a surface inversion layer was present, especially in low doped annealed layers without a cap, a two-layer model was used to curve fit the experimental points to obtain the true hole concentration [7, 8].

Secondary Ion Mass Spectrometry (SIMS) was employed for determining depth distribution profiles. A CAMECA 4f instrument was used in this study. Primary $^{32}O_2^+$ ions accelerated to 8.5 KeV were used for sputtering the samples, and positive secondary ions were monitored. Depth calibration was carried out by determining sputtering rates from crater depth measurements, made on a Tencor Instruments Alpha Step 200.

RESULTS AND DISCUSSION:

Figure 1 shows the acceptor concentration measured as a function of arsine flow, for arsenic-doped layers grown lattice matched on CdZnTe substrates. The measured doping concentration is seen to increase from 8×10^{15} cm^{-3} to 9×10^{16} as the arsine flow was increased from 10 to 250 sccm. The mobility of these films was in the range 400-600 cm^2/Vs range at low temperature. As the arsine flow was increased, the layer became HgTe rich, necessitating adjustment of the dimethylcadmium flow to obtain the same composition. Increasing the arsine flow beyond 250 sccm did not increase the doping concentration. Also shown is the result reproduced from Ref. 6 where GaAs substrates with 2 μm thick CdTe buffer layers were used as the substrate. Consistently, a factor of 2 to 4 higher doping level is achieved when lattice matched CdZnTe is used as the substrate. We believe HgCdTe grown on GaAs is more defected and As segregation in its defect sites is the main reason for this difference.

Arsenic in HgCdTe was found to be very stable, after low temperature isothermal annealing in a Hg-rich ambient. Figure 2 shows the Hall coefficient as a function of temperature for two samples, grown side by side, during the same run. Sample (O) was an as grown layer and sample (▲) was annealed under Hg overpressure at 270°C for 16 hours, followed by 220°C for 10 hours. Both samples show almost identical behavior, which suggests that arsenic is stable under this heat treatment process.

Secondary Ion Mass Spectrometric (SIMS) measurements were made in order to establish the presence of As in the layer. Figure 3 shows a typical SIMS profile of a HgCdTe layer grown with 50 sccm of arsine flow. The measured carrier concentration is 4.5 $\times 10^{16}$ cm^{-3}, and shows clearly the presence of incorporated arsenic.

In order to study the site occupation of As in HgCdTe, layers were grown under two different Hg partial pressures (P_{Hg}), 0.03 and 0.008 atm. For each value of Hg partial pressure, an undoped and two arsine doped layers were grown. The arsenic flow rate for these two layers was 25 and 125 sccm, corresponding to arsine partial pressures of 1.2 $\times 10^{-5}$ atm. and 6.0 $\times 10^{-5}$ atm. respectively.

The results on undoped layers were used to obtain the background donor concentration N_D, after annealing in an Hg environment. From this study, and from measurements on a number of previous undoped layers, the background donor concentration was estimated to be about 3 $\times 10^{15}$ cm^{-3}. The exact value of N_D is not very significant, because the p-type concentration with arsine doping is in the 10^{16} to 10^{17} cm^{-3} range. However, it is important to note that the background donor concentration is in the low 10^{15} cm^{-3} range.

All the As doped layers were analyzed after a two-step isothermal anneal (270° for 16 hours, followed by 220° for 10 hours) under Hg-rich conditions, so that eventually the net acceptor concentration due to As could be determined. We have confirmed that this two-step anneal results in n-type layers, so that essentially all the Hg vacancies are anni-

hilated. van der Pauw measurements were made on these layers and the results are summarized in Table 1. Here, the total acceptor concentration N_A is obtained by assuming the donor concentration to be about 3 $\times 10^{15}$ cm^{-3}, the same as that measured in the undoped sample. Moreover, we assume that the incorporation of any residual donor impurities is not affected by the arsine flow or by a change in Hg pressure. Figure 4 shows that the total acceptor concentration increased roughly in proportion to P_{Hg}. For the samples grown with 125 sccm arsine flow, a factor of 4 increase in P_{Hg} resulted in an increase in N_A by a factor of 4, and similar results hold for samples grown with 25 sccm arsine, considering the uncertainty in the measurement of low doped samples. This suggests that there is negligible compensation in the As doped samples. This can be shown as follows.

We first assume that [9] $V_{Te} \alpha P_{Hg}$, and that $V_{Hg} \alpha 1/P_{Hg}$, where V_{Te} and V_{Hg} denotes concentrations of Te and Hg vacancies respectively. If arsenic incorporates only into vacant tellurium sites, then a 4 fold increase in P_{Hg} will result in a 4 fold increase in total p-doping in the layer, as we have seen here. On the other hand, if As incorporates into both Te and Hg sites, then a 4 fold increase in P_{Hg} will result in more than a 4 fold increase in total p-doping in the layer. This is because the compensating As in Hg sites is reduced by 4 fold when P_{Hg} is increased.

One conclusion we draw from this study is that As does not get incorporated into Hg sites, even though a high concentration of Hg vacancies is present during growth. We propose that the incorporation mechanism for As involves the co-adsorption of DMCd and AsH_3 on the growing surface. Here, the decomposition of DMCd to Cd occurs rapidly [10], followed by the formation of a Cd-As complex. When incorporated into HgCdTe in this form, As is preferentially located on Te sites. Based on this mechanism, the As doping level should depend on the x value, with a high doping concentration in CdTe and almost no doping concentration in HgTe. Indeed, we have seen that 4 sccm

of arsine is sufficient to dope CdTe p-type to the 5 $\times 10^{16}$ cm^{-3} level, whereas 125 sccm arsine is necessary in order to obtain the same doping level in HgCdTe with $x = 0.3$.

As shown in Fig. 1, a saturation effect in the doping level is seen when arsine flow is increased beyond 50 sccm. For a fixed Hg partial pressure, this doping level is determined by the concentration of Te-vacancies. Since the V_{Te} concentration can be varied by changing the Hg pressure, we were able to dope HgCdTe to as high as 7×10^{17} cm^{-3}, by increasing the Hg pressure during growth. At higher arsine flow, the layer shifts to HgTe rich, presumably due to the pre-reaction of dimethylcadmium with arsine. This depletes dimethylcadmium available for growth.

CONCLUSION:

The effect of Hg pressure on As doping of HgCdTe was studied. It was shown that a high partial pressure of Hg is important to obtain heavily doped layers. In addition, arsine doping results in almost uncompensated layers, even though a high concentration of Hg vacancies is present. We propose that this is due to a mechanism by which As gets incorporated, probably in the form of a Cd-As complex, resulting from the co-adsorption of DMCd and AsH_3. Saturation effects in the doping concentration can be explained using the above mechanism. The presence of As is established using SIMS studies. Annealing for many hours at low temperature shows that As is a stable p-type dopant in HgCdTe.

ACKNOWLEDGEMENTS

The authors would like to thank J. Barthel for technical assistance on this program and P. Magilligan for manuscript preparation. CdZnTe substrate material was kindly supplied by C.J. Johnson and S. McDevitt of II-VI, Inc., Saxonburg, PA. This work was sponsored by the Defense Advanced Research Projects Agency (Contract No. N-00014-85-K-0151), administered through the Office of Naval Research, Arlington, VA, and by a

grant from the Raytheon Corporation. This support is greatly appreciated.

REFERENCES

1. S.K. Ghandhi, I.B. Bhat and H. Fardi, Appl. Phys. Lett., 52, (1988) 392.
2. E.S. Johnson and J.L. Schmit, J. Electron Mater., 6, (1977) 25.
3. M. Brown and A.F.W. Willoughby, J. Crys. Growth, 59, (1982) 27.
4. H.R. Vydyanath, J.A. Ellsworth and C.M. Devaney, J. Electron. Mater., 16, (1987) 13.
5. P.S. Wijewarnasuriya, I.K. Sou, Y.J. Kim, K.K. Mahavadi, S. Sivananthan, Appl. Phys. Lett., 51, (1987) 2025.
6. N.R. Taskar, I.B. Bhat, K.K. Parat, D. Terry, H. Ensani and S.K. Ghandhi, J. Vac. Sci. Technol., A7, (1989) 281.
7. L.F. Lou and W.H. Frye, J. Appl. Phys., 56, (1984) 2253.
8. A. Zemel, A. Sher, and D. Eger, J. Appl. Phys., 62, (1987) 1861.
9. H.R. Vydyanath, J. Electrochem. Soc., 128, (1981) 2610.
10. I.B. Bhat, N.R. Taskar and S.K. Ghandhi, J. Electrochem. Soc., 134, (1987) 195.

LIST OF FIGURES

TABLE 1

Arsine Flow sccm.	P_{Hg}	Net Acceptor Concentration, N_A-N_D (cm^{-3})	Total Acceptor Concentration, N_A (cm^{-3})
25	0.03	1.5×10^{16}	1.6×10^{16}
25	0.008	nearly intrinsic	3×10^{15}
125	0.03	6×10^{16}	6.3×10^{16}
125	0.008	1.3×10^{16}	1.6×10^{16}

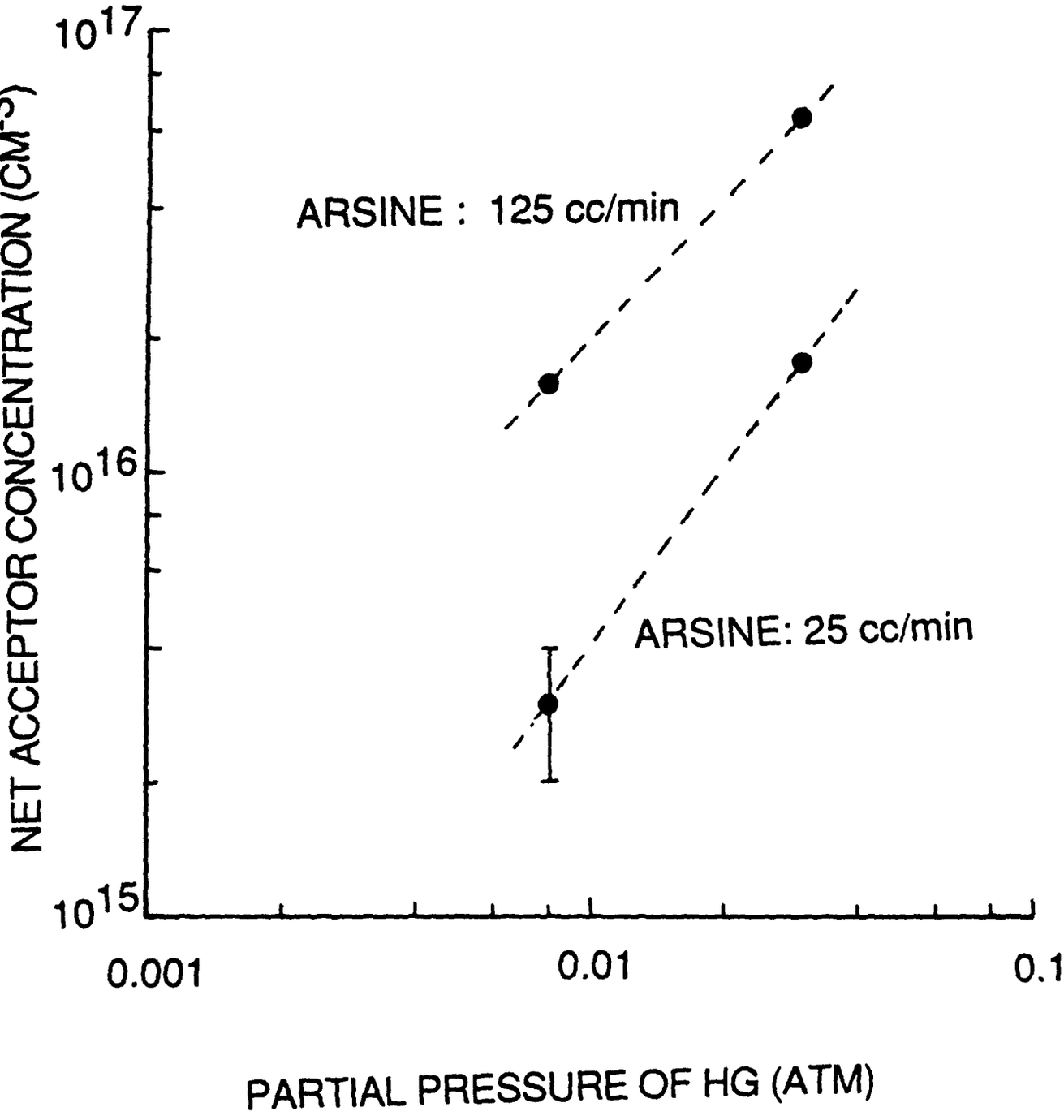
10^{17}
10^{16}
10^{15}
NET ACCEPTOR CONCENTRATION (CM^{-3})
ARSINE : 125 cc/min
ARSINE: 25 cc/min
0.001
0.01
0.1
PARTIAL PRESSURE OF HG (ATM)

PROCESSED DATA

IBM WATSON RESEARCH CENTER--CAMECA 4f

24 May 89 02

FILE: 49144G

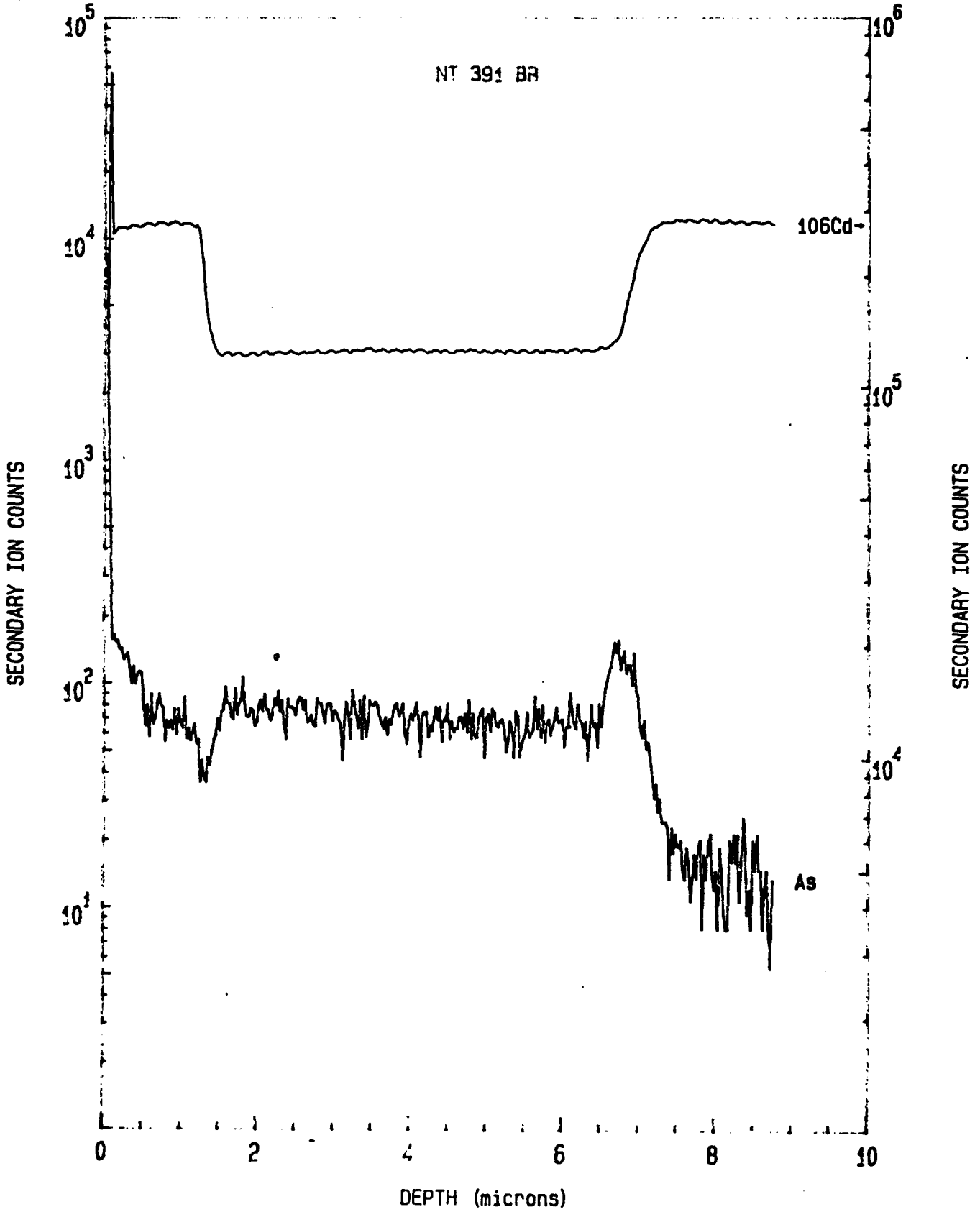

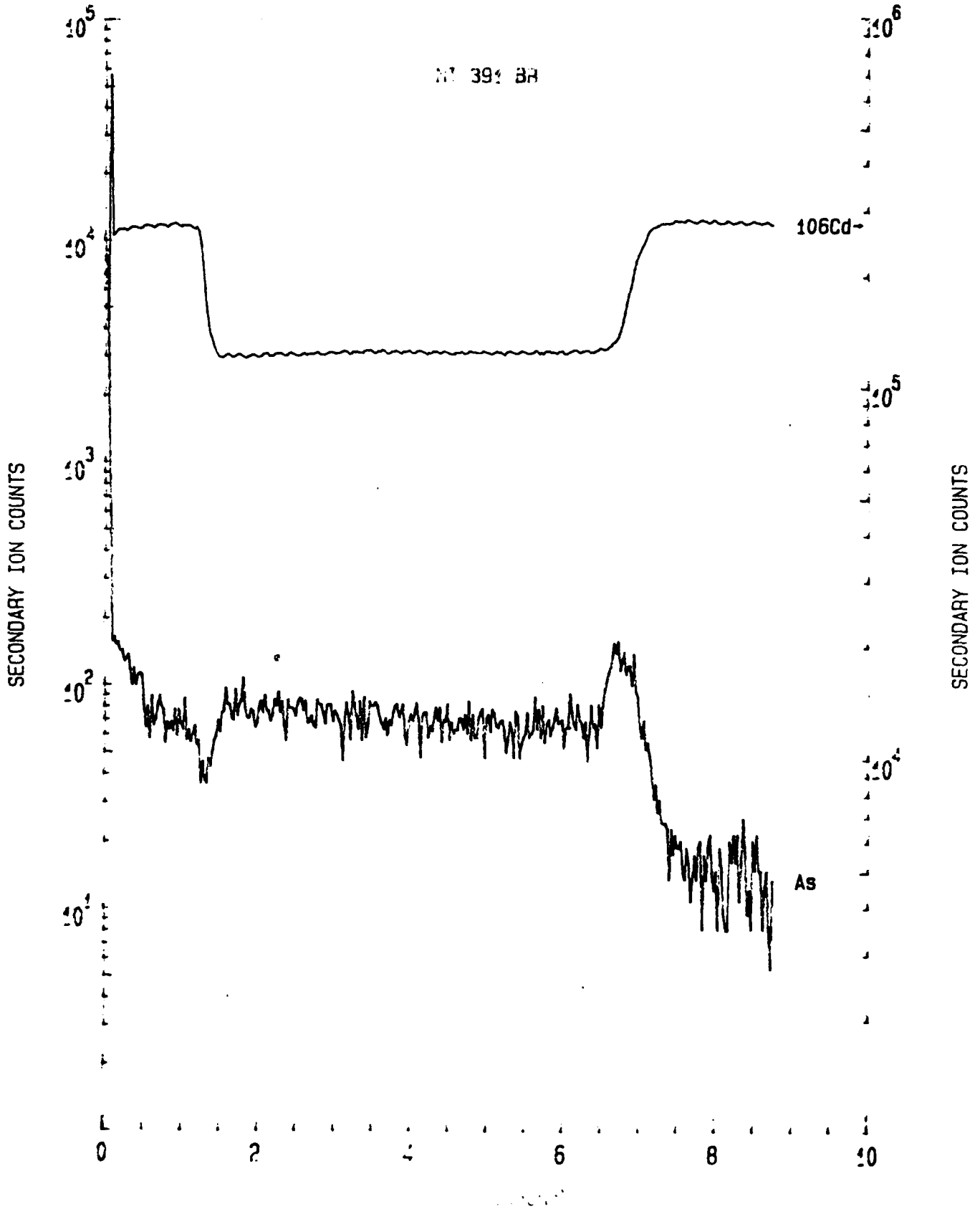
PROCESSED DATA
24 May 89 02
IBM WATSON RESEARCH CENTER--CAMECA 4f
FILE: 49144G
NI 391 BR
106Cd
As
SECONDARY ION COUNTS
SECONDARY ION COUNTS
10^5
10^4
10^3
10^2
10^1
10^6
10^5
10^4
0
2
4
6
8
10

B

INDIUM DOPING OF N-TYPE HgCdTe LAYERS GROWN BY ORGANOMETALLIC VAPOR PHASE EPITAXY

S.K. GHANDHI

N.R. TASKAR

K.K. PARAT

I.B. BHAT

ELECTRICAL, COMPUTER AND SYSTEMS ENGINEERING DEPARTMENT

RENSSELAER POLYTECHNIC INSTITUTE

TROY, NEW YORK 12180

Submitted to Applied Physics Letters

Contact:

S.K. Ghandhi

Telephone: 518-276-6085

FAX: 518-276-6261

SK-89.57

December 20, 1989

ABSTRACT

N-type doping of mercury cadmium telluride was achieved using trimethylindium as the dopant source. The layers, grown by the alloy growth technique, were doped to $\sim 5 \times 10^{18}$ cm^{-3}. The donor concentration in these layers was found to exhibit a linear dependence on the dopant partial pressure over the carrier concentration range from 5×10^{16} to 3×10^{18} cm^{-3}.

Reasonably high electron mobility values were observed in these indium doped layers. Typically, layers with a Cd fraction $x = 0.23$, doped to 3.5×10^{16} cm^{-3}, exhibited a mobility value of 7.5×10^{4} cm^2/Vs at 40K. High electron mobility values, measured over the entire doping regime, suggest a high electrical activity of indium in these layers.

The optically measured band edge in these indium doped layers was observed to shift to higher energy with increased doping. The band edge energy values measured in 1×10^{17} and 3×10^{18} cm^{-3} doped layers correspond to $x = 0.23$ and $x = 0.3$, respectively. This increase can be due to an increase in Cd fraction, or to a Burstein-Moss shift of the bandedge with doping.

Mercury cadmium telluride layers, grown by organometallic vapor phase epitaxy (OMVPE), have shown considerable promise for use in far infrared detector applications in recent years[1-3]. Layers with uniformity in composition and thickness that are required for present day device structures can be grown by this method[4,5]. In order to obtain device structures with n- and p-type controllable doping, that are stable under thermal processing, it is necessary to introduce external impurities and not rely upon electronically active defects, which are relatively mobile during subsequent processing.

Both group III elements, incorporated on the metal sublattice, and group VII elements on the Te sublattice[6], behave as n-type dopants. Group VII dopants have been used in bulk and vapor phase epitaxy layers[7,8]. However, the strong chemical reaction between the halides and the organometallic precursors makes their use in OMVPE extremely difficult. The electrical activity of group III elements has been conclusively established in several growth techniques such as bulk and liquid phase epitaxy[8,9]. Of these elements, In is preferred over others since it is a slower diffusing species[10], by a factor of more than 10.

Indium doping of HgCdTe layers, grown by the interdiffused multilayer process (IMP) has been reported previously[11]. However, the doping uniformity through these layers depends on the relative incorporation efficiencies of In in CdTe and HgTe, and has not been established. The doping characteristic in these layers showed a very abrupt increase from 3×10^{16} to 3×10^{18} cm^{-3}, with changes in the partial pressure of the In species. This makes it difficult to control in the intermediate range using this approach.

In this paper we report, for the first time, on the doping characteristics of indium in $Hg_{1-x}Cd_xTe$ grown by the direct alloy technique, which does not involve the interdiffusion of sequential layers of HgTe and CdTe. Controllable indium doping was achieved at a growth temperature of 370°C by using a trimethylindium (TMIn) source in the bubbler mode.

$Hg_{1-x}Cd_xTe$ layers were grown in an atmospheric pressure, horizontal reactor using elemental mercury, dimethylcadmium (DMCd), and diisopropyltelluride (DIPTe). The alloy growth method was used in which Hg, Cd and Te sources are introduced simultaneously into the reactor. TMIn was used as the dopant source.

Substrates were (100) 2° → (110) oriented semi-insulating GaAs. They were cleaned in hot organic solvents, followed by a 10 minute etch in H_2SO_4:H_2O_2:H_2O (10:1:1), resulting in a removal of about 15 μm of material. Next, a 2.5 μm thick CdTe buffer layer was grown at 350°C, using partial pressures of 1×10^{-4} atm. and 2×10^{-4} atm. for DMCd and DIPTe respectively. Previous studies have established that this thickness is sufficient to accommodate the 14.6% lattice mismatch between GaAs and CdTe, so that subsequent HgCdTe layers are comparable in quality to those grown on bulk CdTe[12]. The HgCdTe layers were grown at 370°C and were typically 6 μm thick. This was followed by the growth of a 1 μm thick CdTe cap.

Typical values of the reactant partial pressures were $P_{Hg} = 0.03$ atm., $P_{DMCd} = 9 \times 10^{-5}$ atm. and $P_{DIPTe} = 5 \times 10^{-4}$ atm. during the growth of the HgCdTe layers. For the doped layers, the TMIn bubbler was maintained at -10°C and was operated in the conventional bubbler mode. The H_2 flow through the bubbler was varied from 2 cm^3/min to 100 cm^3/min, corresponding to a partial pressure range of 3×10^{-7} to 1.5×10^{-5} atm. respectively. To obtain lightly doped layers, the bubbler was cooled to -20°C.

Ohmic contacts were made by etching the CdTe cap near the contact area and evaporating a 400 $\AA$ thick layer of gold. Hall mobility and resistivity measurements were made in cloverleaf patterned samples over the temperature range from 10 to 300K. The magnetic field strength was varied from 0.5 to 6.0 kG in the course of this study. The value of E_g corresponding to an absorption coefficient of $\alpha = 500$ cm^{-1} was measured in these samples at room temperature, by Fourier Transform Infrared Spectrometry. This

value was used[13] to determine the Cd-fraction x.

All the layers grown in this reactor, without any intentional doping, were weakly n-type (in the low 10^{15} cm^{-3} range). This may be due to residual impurities in the chemicals or to donor-like defects associated with layers grown on GaAs with a CdTe buffer layer. Typical low temperature mobility values obtained were 4×10^4 cm^2/Vs for layers with a composition of $x \sim 0.28$, and 1×10^5 cm^2/Vs for layers with $x \sim 0.23$. The mobility values quoted above are reasonable for layers of these compositions.

Figure 1 shows the Hall coefficient (R_H) as a function of inverse temperature for TMIn doped layers with $x = 0.28$ and $x = 0.23$. The Hall coefficient shows classical n-type extrinsic behavior over the entire 300 to 10K temperature regime. The Hall coefficient was independent of the magnetic field strength, and the carrier concentration was estimated to be 5×10^{16} cm^{-3} for the layer with $x = 0.28$ and 3×10^{16} cm^{-3} for the layer with $x = 0.23$. Figure 2 shows the mobility as a function of inverse temperature for these layers. The low temperature mobility values of 3.3×10^4 and 7.3×10^4 cm^2/Vs for cadmium compositions of 28% and 23% respectively, are consistent with the corresponding carrier concentration values.

Since the carrier concentration in these doped layers was at least two orders of magnitude higher than in the undoped layers, it was taken to be the donor concentration due to indium. However, this is based on the assumption that the incorporation of indium does not significantly change the concentration of the native defects. Figure 3 shows the variation of the measured carrier concentration with the TMIn partial pressure, for layers with $x = 0.23$. Here, the donor concentration is seen to vary linearly with the partial pressure of TMIn up to $\sim 4 \times 10^{18}$ cm^{-3}, and appears to saturate at $\sim 5 \times 10^{18}$ cm^{-3} for higher TMIn partial pressures.

The linear dependence of the donor concentration on the dopant flux, combined with the high values for mobility, implies an electrical activation of almost 100% for

the indium incorporated in the layers, until a doping level of 4×10^{18} cm^{-3} is reached. A similar dependence of the donor concentration, with 100% electrical activation, was observed in layers grown by molecular beam epitaxy (MBE) up to a 10^{18} cm^{-3} In concentration[14]. At higher values of the dopant flux, however, it is possible that indium gets increasingly incorporated in electrically inactive form as In_2Te_3, as has been reported for In doping of bulk HgCdTe in the melt[15].

The carrier concentration dependence of the 10K electron mobility is shown in Fig. 4 for layers with $x = 0.28$ and $x = 0.23$. In addition to the higher ionized impurity scattering, disorder scattering for any given Cd fraction is also expected to increase with carrier concentration due to its direct dependence on the electron energy[16]. Also shown in this figure are the mobility values reported[14] for the In doped MBE grown samples with $x = 0.2$ to 0.24. An electrical activation of 100% was reported in those samples. It can be seen that the mobility values in our layers agree very closely with those of the MBE samples.

As we have noted earlier, the wave number corresponding to an absorption coefficient $\alpha = 500$ cm^{-1} was measured in these samples at room temperature, and the optical energy gap E_g determined from its value. E_g remained constant, at ~ 200 meV, for doping concentrations up to 1×10^{17} cm^{-3}. However, E_g increased to 350 meV for an electron concentration of 3×10^{18} cm^{-3}. This change in E_g can be interpreted as an increase in x from 0.23 to 0.3. Similar shifts in the composition were reported[11] during growth at 420°C by the interdiffused multilayer process, where a change in x from 0.27 to 0.4 was observed when the TMIn partial pressure was increased from 10^{-6} atm to 1.3×10^{-5} atm. It is possible that x changes with doping concentration due to relative changes in the effective growth rates of the HgTe and CdTe components of these layers. Additionally, the increase in E_g can be accounted for by the Burstein-Moss shift with doping concentration that has been observed in bulk HgCdTe[17]. Further work is

presently being undertaken to resolve this issue.

In conclusion, we have shown that indium doped n-type HgCdTe layers can be grown with carrier concentrations as high as 5×10^{18} cm^{-3} by the alloy growth technique, using TMIn as the dopant source. A linear variation of the donor concentration with TMIn partial pressure was obtained until 3×10^{18} cm^{-3}. This fact, together with high mobility values, suggests a high electrical activation of indium. A saturation in the incorporation of indium has been observed at higher TMIn concentrations. Low temperature mobility values of 3.3×10^4 $cm^2/Vsec$ and 7.3×10^4 $cm^2/Vsec$ were obtained in $\sim 5 \times 10^{16}$ doped layers with $x = 0.28$ and $x = 0.23$ respectively. The optical bandgap of these layers was found to remain unchanged until an electron concentration of 10^{17} cm^{-3} was attained, corresponding to a TMIn partial pressure of 1.5×10^{-6} atm. At higher values of TMIn partial pressure, this bandgap was found to increase. This increase can be due to an increase in Cd fraction, or to a Burstein-Moss shift of the band-edge with doping.

ACKNOWLEDGEMENT

The authors would like to thank J. Barthel for technical assistance on this program and P. Magilligan for manuscript preparation. Partial funding for this program, from the Raytheon Corporation, is hereby acknowledged. This work was sponsored by the Defense Advanced Research Projects Agency (Contract No. N-00014-85-K-0151), administered through the Office of Naval Research, Arlington, VA. This support is greatly appreciated.

LIST OF REFERENCES

1. S.J. Irvine and J.B. Mullin, J. Cryst. Growth, 55, 107 (1981).
2. S.K. Ghandhi and I.B. Bhat, Appl. Phys. Lett., 44, 779 (1984).
3. W.E. Hoke, P.J. Lemonias and R. Taczewski, Appl. Phys. Lett., 45, 1092 (1984).
4. S.K. Ghandhi, I.B. Bhat and H. Fardi, Appl. Phys. Lett., 52, 392 (1988).
5. J. Thompson, P. Mackett, L.M. Smith, D.J. Cole-Hamilton and D.V. Shenai-Khatkhate, J. Cryst. Growth, 86, 233 (1988).
6. H.R. Vydyanath and F.A. Kroger, J. Electron. Mater., 11, 111 (1982).
7. H. Wiedemeier, A.E. Uzpurvis and D. Wang, J. Cryst. Growth, 65, 474 (1983).
8. P. Capper, J. Cryst. Growth, 57, 280 (1982).
9. M.H. Kalisher, J. Cryst. Growth, 70, 365 (1984).
10. M. Brown and A.F.W. Willoughby, J. Cryst. Growth, 59, 27 (1982).
11. J.S. Whiteley, P. Koppel, V.L. Conger and R.E. Owens, J. Vac. Sci. Technol., A6(4), 2804 (1988).
12. S.K. Ghandhi, I.B. Bhat and N.R. Taskar, J. Appl. Phys., 59, 2253 (1986).
13. G.L. Hansen, J.L. Schmit and T.L. Casselman, J. Appl. Phys., 53, 7099 (1982).
14. M. Boukerche, J. Reno, I.K. Sou, C. Hsu and J.P. Faurie, Appl. Phys. Lett., 48, 1733 (1986).
15. H.R. Vydyanath, J. Electrochem. Soc., 128, 2619 (1981).
16. F.J. Bartoli, J.R. Meyer, C.A. Hoffman and R.E. Allen, Phys. Rev. (B), 27, 2248 (1983).
17. Q. Dingrong, T. Wenguo, S. Jie, C. Junhao and Z. Guozhen, Solid State Commun., 56, 813 (1985).

LIST OF FIGURES

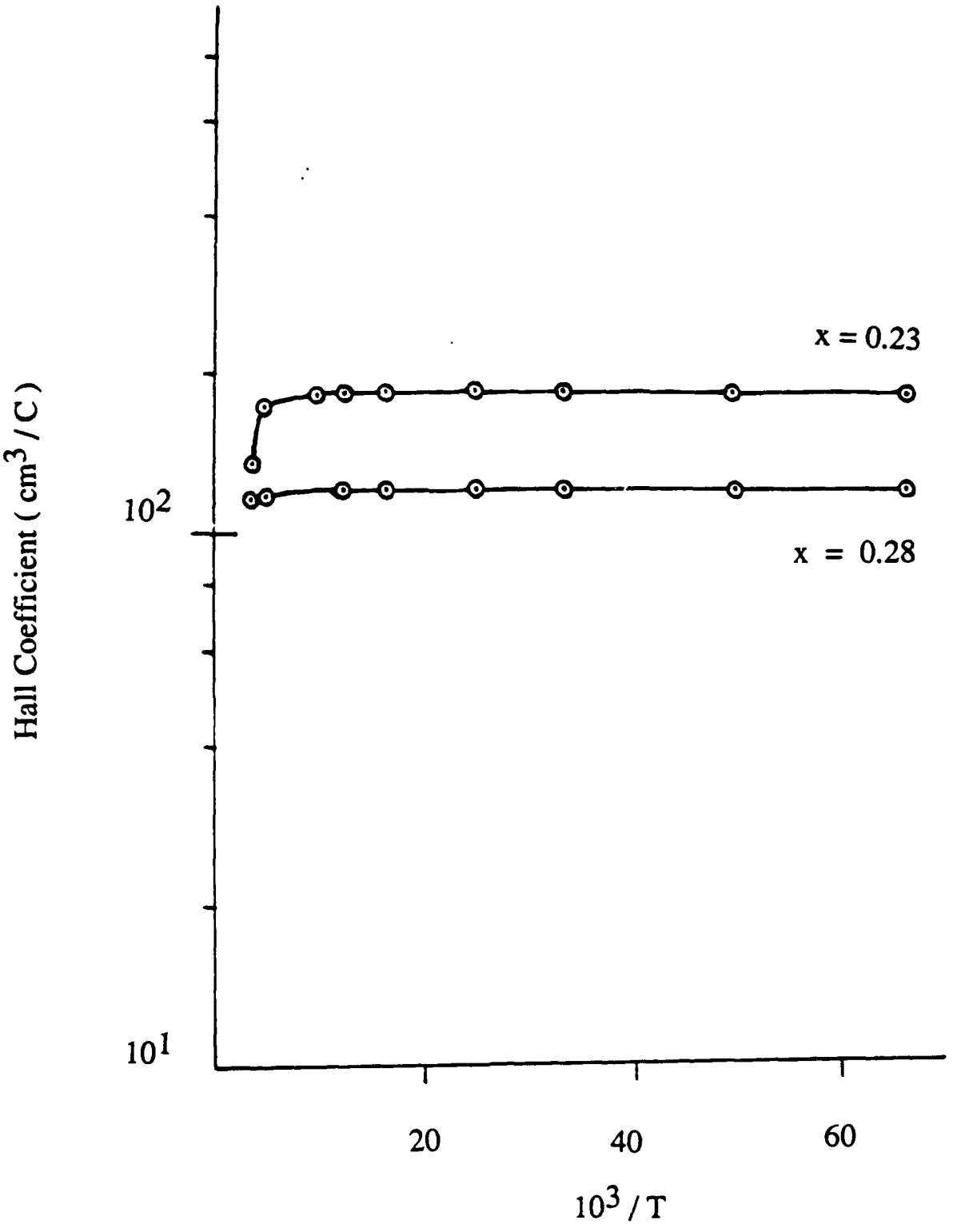
Hall Coefficient (cm3 / C)
10^2
10^1
x = 0.23
x = 0.28
20
40
60
10^3 / T

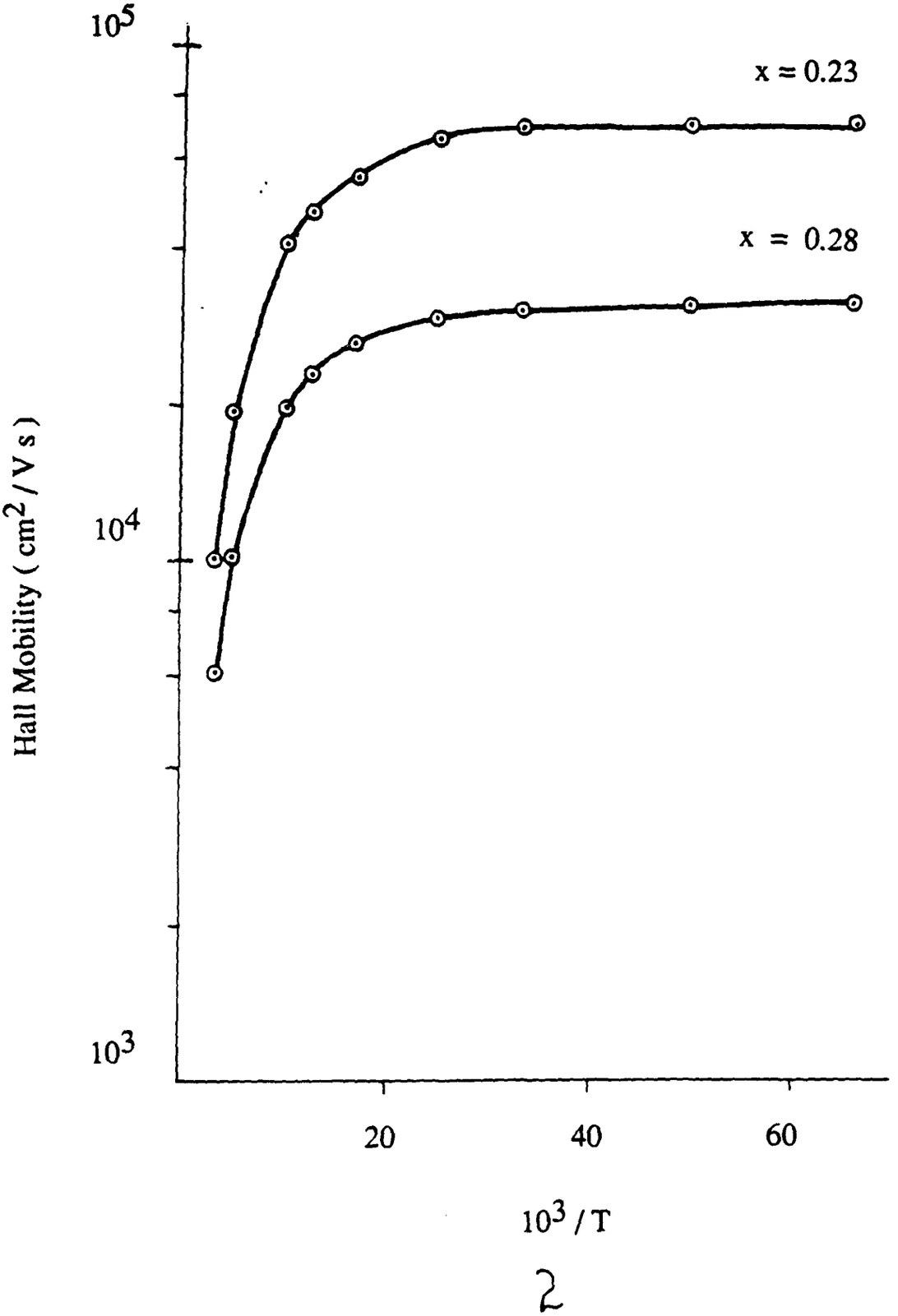

2

SKG.

SKG

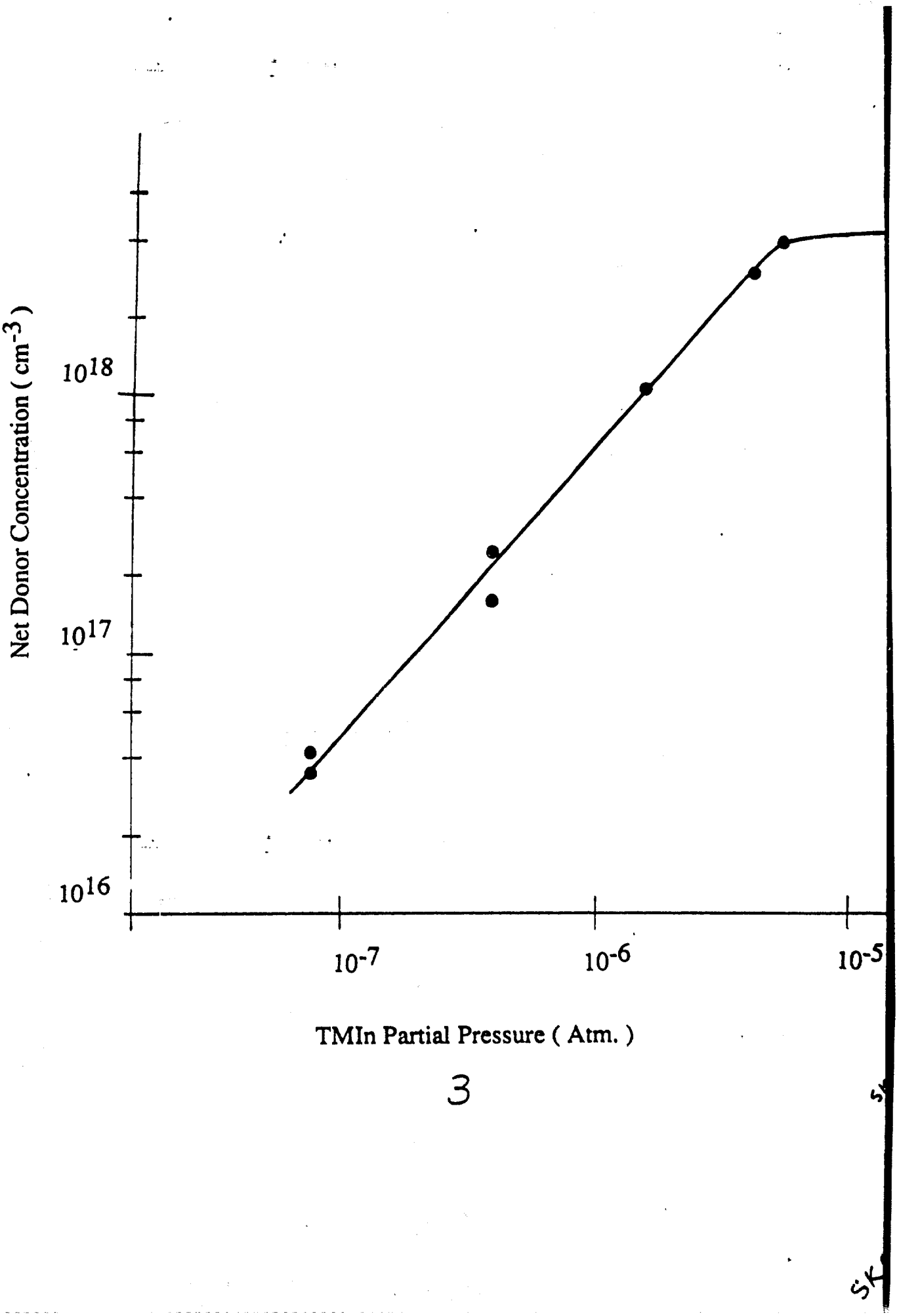
Net Donor Concentration (cm^{-3})
10^{18}
10^{17}
10^{16}
10^{-7}
10^{-6}
10^{-5}
TMIn Partial Pressure (Atm.)

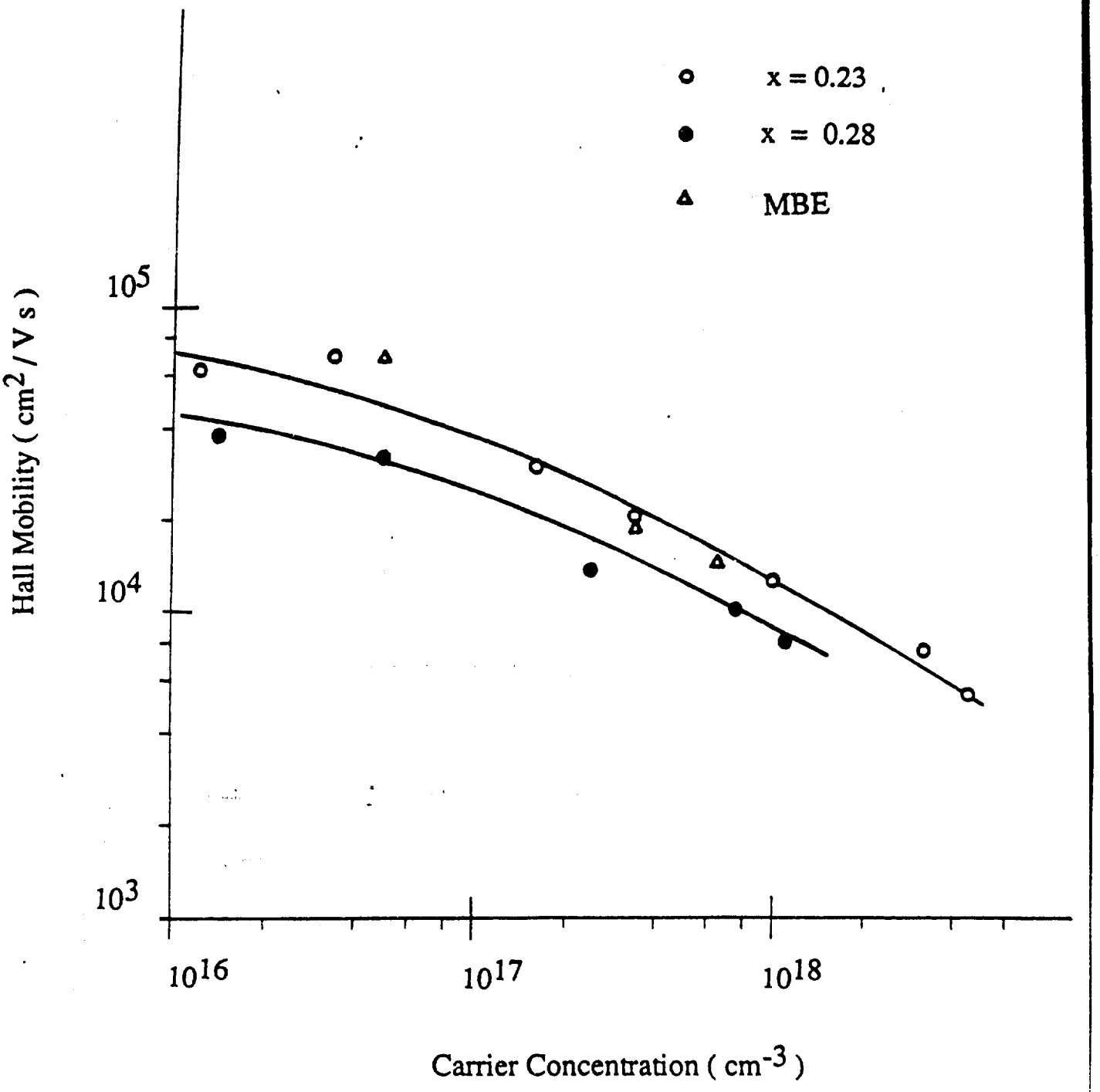
x = 0.23
x = 0.28
MBE
Hall Mobility (cm^2 / V s)
10^5
10^4
10^3
10^{16}
10^{17}
10^{18}
Carrier Concentration (cm^{-3})

SKC

SKC

ANNEALING AND ELECTRICAL PROPERTIES OF $Hg_{1-x}Cd_xTe$ GROWN BY OMVPE

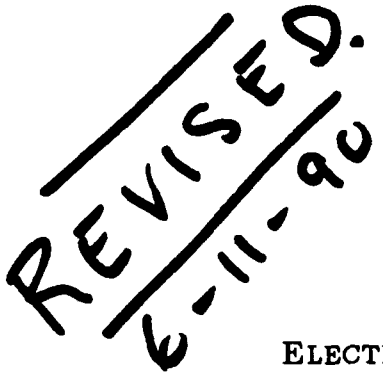

K.K. PARAT

N.R. TASKAR

I.B. BHAT

S.K. GHANDHI

ELECTRICAL, COMPUTER AND SYSTEMS ENGINEERING DEPARTMENT

RENSSELAER POLYTECHNIC INSTITUTE

TROY, NEW YORK 12180

Point of Contact:

S.K. Ghandhi

(518) 276-6085

FAX: (518) 276-6261

For submission to Journal of Crystal Growth

SK-89.24

February 16, 1990

ABSTRACT

The annealing behavior of $Hg_{1-x}Cd_xTe$ layers, grown by the conventional Organometallic Vapor Phase Epitaxy (OMVPE), is reported. Some of the as grown layers, which are p-type with a concentration around $4 \times 10^{16}/cm^3$ of Group II vacancies, become light p-type with carrier concentrations around $1 \times 10^{15}/cm^3$ after Hg saturated annealings at temperatures in the range of 200-230°C. These conditions are typically expected to result in complete annealing and n-type conversion of the layer. These layers can be converted to n-type with a carrier concentration of approximately $5 \times 10^{14}/cm^3$ by a higher temperature anneal at 290°C, followed by a low temperature anneal at 220°C.

Hall effect measurements were made under variable temperature as well as variable magnetic field conditions. Bulk carrier concentrations and mobilities were evaluated by considering the effect of the surface inversion/accumulation layer on the Hall data. It is proposed that p-type conduction in the partially annealed layers is due to the persistence of Group II vacancies in the $Hg_{1-x}Cd_xTe$ layers, which are not completely annihilated during the low temperature anneal. Conversion to n-type is probably due to residual donor impurities in the as grown $Hg_{1-x}Cd_xTe$ layer.

INTRODUCTION

$Hg_{1-x}Cd_xTe$ is a defect semiconductor in which native defects are electrically active [1-2]. Group II vacancy is the most common defect here, usually present in the range of 10^{16}-$10^{17}/cm^3$, and results from the Te excess condition used in the growth of $Hg_{1-x}Cd_xTe$, at typical growth temperatures. These are shallow acceptors so that the as grown layers are heavily p-type. Annealing of these layers at temperatures below 350°C under Hg overpressure reduces the vacancy concentration $[V_{II}]$ to a value lower than the background donor concentration, thus converting the layers to n-type [1-10].

During annealing, Hg from the vapor diffuses into the $Hg_{1-x}Cd_xTe$ crystal, possibly via an interstitial mechanism [3-4]. Subsequently, the Hg interstitials become substitutional by moving into vacant Group II sites. Thus, $[V_{II}]$ is a function of the annealing temperature as well as the concentration of Hg interstitials, $[I_{Hg}]$, which are present in the lattice at the annealing temperature. In turn, $[I_{Hg}]$ is a function of the annealing temperature as well as the Hg overpressure. $[V_{II}]$ can thus be controlled in $Hg_{1-x}Cd_xTe$, by controlling the annealing temperature as well as the Hg overpressure. Values of $[V_{II}]$ as a function of these annealing parameters are available in the literature [1, 2, 6] for different values of x. An effective diffusion coefficient of Hg into $Hg_{1-x}Cd_xTe$, relevant to the annealing process, has been given in [3, 4]. However, most of the annealing results reported in the literature have been on bulk materials.

The annealing characteristics of $Hg_{1-x}Cd_xTe$ layers, grown by epitaxial techniques such as liquid phase epitaxy (LPE) and organometallic vapor phase epitaxy (OMVPE), are less understood [7-10]. As grown layers are typically p-type due to the low Hg vapor pressures used during the growth of OMVPE layers, and the higher temperatures employed in the growth of LPE layers. The reduction of Hg vacancies thus requires a low temperature Hg saturated anneal. In the case of LPE, some authors have noted that complete annealing of layers with alloy compositions greater than 0.20 was not possi-

ble [8]. With OMVPE layers, extremely long anneal times (21 days) have been used to completely anneal a 10 μm layer of $Hg_{1-x}Cd_xTe$ [9]. Additionally, higher temperature anneals have been used for completely annealing these layers [7]. All of this work has focused on fully annealed layers; however, it is necessary to investigate the behavior of partially annealed layers in order to gain an understanding of their annealing behavior.

In this paper we report the annealing characteristic of $Hg_{1-x}Cd_xTe$ layers grown by conventional OMVPE, which stay p-type despite Hg saturated annealings in the temperature range of 200-230°C for durations up to 24 hours. These layers are, however, converted to n-type by using a two-step anneal with a high temperature step at 290°C followed by a low temperature step at 220°C. Electrical properties of partially as well as fully annealed layers are presented. The Hall data were analyzed as a function of temperature as well as magnetic-field (B field) in order to extract the bulk carrier concentrations and mobilities [11-13]. Light p-type layers were also characterized by Hall effect measurements, following surface passivation using an anodic sulfide [14, 15]. A possible reason for such an anomalous annealing behavior of these layers is also proposed.

EXPERIMENTAL

$Hg_{1-x}Cd_xTe$ layers used in this study were grown at 370°C in a vertical reactor by the simultaneous pyrolysis of dimethylcadmium (DMCd), diisopropyltellurium (DIPTe), and elemental Hg [16] in hydrogen. (100) CdTe was used as the substrate. All the work reported here is for layers with alloy compositions (x) in the range of 0.20 to 0.24 and thicknesses in the range of 6 to 12 μm.

The $Hg_{1-x}Cd_xTe$ layers were capped with a 0.5-1.0 μm thick layer of undoped CdTe which was grown in the same reactor run. This cap serves two purposes; first, it prevents any unintentional or partial [17] annealing of the $Hg_{1-x}Cd_xTe$ layers during cool-down (in a hydrogen ambient) after the layer growth. Second, it inhibits the formation of an inversion layer on the $Hg_{1-x}Cd_xTe$ surface, which can affect the Hall char-

acteristics of as grown p-type layers. Cap layers were removed, together with 0.5 μm of the HgCdTe, just prior to the annealing by means of a short etch consisting of 1% Br in methanol.

The epilayer thickness was determined from the interference fringes in the sub-bandgap regime of the IR transmittance curve, using a Fourier Transform Infrared Spectrometer (FTIR). The bandgap of the layer was taken to be the energy at which the absorption coefficient of the material is 500 cm^{-1}. Next, the alloy composition x was determined from the bandgap using the expression for E_g given in [18]. The value of x, determined in this fashion, gave good agreement between the intrinsic carrier concentration calculated at room temperature from the expression in [19], and the corresponding value measured from the Hall effect.

After cap removal, samples were rinsed in methanol, dried with nitrogen, and loaded in a quartz ampoule with mercury of 99.99999% purity. The ampoule was evacuated to 10^{-7} Torr using a turbo-molecular pump equipped with a liquid nitrogen trap, and sealed using an oxy-hydrogen flame. All annealings were carried out with the sample kept 2°C warmer than the Hg reservoir, to avoid Hg from condensing on them. This prevented any surface deterioration during the anneal and sample surfaces showed no sign of damage. The annealed samples were characterized without any further surface treatment. For some samples which exhibited anomalous p-type behavior, the surface was passivated by anodic sulfidization [14] and Hall data were taken once again.

Van der Pauw [20] patterns were delineated by etching in 1% Br-methanol. Evaporated gold was used for making contacts to the layers. Hall measurements were carried out as a function of temperature from 300 to 20 K. In some cases, measurements were made as a function of B field, with the B field varying from 0.5 to 6 kGauss. The Hall analysis was based on a two-layer model, to include the effects of both bulk and surface carriers. The computer simulation was fitted to the experimental data, thus allowing the

separation of bulk and surface parameters. The details of this analysis are provided in the Appendix.

RESULTS

As Grown Layers:

Figure 1 shows the Hall coefficient (R_H) and the conductivity (σ) for a 6.7 μm thick as grown $Hg_{1-x}Cd_xTe$ layer with a 0.5 μm thick undoped CdTe cap layer and an alloy composition of 0.228. The mobility of the sample as a function of 1000/T is shown in Fig. 2. The data were taken at a magnetic field of 2.1 kG. The solid curve shown here is a computer simulation which gives a least square fit to the experimental data. The best fit corresponded to (N_A-N_D) of 3.61 $\times$ $10^{16}/cm^3$, a hole ionization energy of 6.2 meV, and a low temperature hole mobility (μ_{po}) of 840 cm^2/V-s. It was not necessary to consider the presence of any inversion layer in order to obtain this fit.

The theoretical model for simulating the R_H and σ curve [10] assumes that the mobilities remain constant at low temperatures. This is certainly an approximation in the case of hole mobility, which is known to decrease at temperature below 30 to 40 K [19]. This shortcoming of the model is apparent in Fig. 2 where, at very low temperatures, the theoretical plot for the hole mobility stays constant but its experimental value starts to dip.

The usefulness of the CdTe cap layer is seen in the classical p-type behavior exhibited by this sample. There is no detectable sign of the presence of any inversion layer electrons and the simulated curve is for zero inversion layer carrier concentration. The curves shown here are typical of all the as grown layers.

Partially Annealed Layers:

Figures 3 and 4 show the R_H and σ versus 1000/T of a sample annealed at 230°C for 9 hours, taken at 2.1 kG. This sample had an x value of 0.208 and a thickness of 12

μm. From Ref. 4, this combination of temperature and time is expected to be sufficient for annealing a bulk $Hg_{1-x}Cd_xTe$ layer up to a depth of 15 μm. In the present case, though a significant reduction in hole concentration is observed, the n-type conversion of the epilayer is not achieved. The R_H and σ curves were fitted assuming a p-type epilayer with n-type surface inversion. Parameters providing the best fit (represented by the solid curves) are N_A of $1.65 \times 10^{15}/cm^3$, N_D of $4 \times 10^{15}/cm^3$, E_A of 7 meV and a low temperature hole mobility (μ_{po}) of 1620 cm^2/V-s for the bulk layer. The inversion layer carrier concentration was $2.2 \times 10^{11}/cm^2$, with a low temperature surface electron mobility (μ_{so}) of 7000 cm^2/V-s. Note that the theoretical fit to the experimental data points is not very good in the region where R_H begins to fall with decreasing temperature. This is due to some degree of nonuniformity in the hole concentration through the layer (see later).

The fact that this was indeed a p-type layer with surface inversion was verified by sulfidizing the sample in an anodic bath [14]. This anodic sulfide is expected to have a low concentration of fixed positive charges in it, and hence should reduce the inversion layer concentration at the surface [15]. Figures 5 and 6 are plots of R_H and σ for the same sample after passivation with the anodic sulfide. The computer simulations are shown *for the same bulk parameters* as those used in Figs. 3 and 4. However, the surface carrier concentration was reduced to $1.3 \times 10^9/cm^2$ and the inversion layer mobility increased to 33,000 cm^2/V-s. This increase in surface mobility is expected, since passivation tends to reduce surface scattering.

The theoretical fit to the experimental data points in the region of R_H sign-reversal is rather poor here. The reason for this is probably as follows: in this region of the curve, R_H is still determined by the thermal electrons in the sample, whose concentration is given by n_i^2/p, where p is approximately equal to the net acceptor concentration (N_A-N_D). Consequently, variation in (N_A-N_D) with depth in the layer would cause this

region of the R_H curve to stretch out. Due to the nature of annealing, where the in-diffusion of Hg is from the top surface, there would always be a higher concentration of diffusing Hg species near the surface than deeper inside. Hence, there is a gradient in the vacancy concentration in the sample, with the material closer to the surface having less vacancies than the material near the epi-substrate interface. As a result of this gradient in the vacancy concentration, the quantity n_i^2/p varies with depth, and causes the R_H to stretch out in this region of the curve. At sufficiently low temperatures, however, the magnitude of R_H is solely dictated by the bulk holes and the surface inversion layer, and the fit begins to improve. In summary, the theoretical model used here assumes uniform acceptor concentration across the layer, so that the experimental R_H curve of a layer with nonuniform acceptor concentration cannot be fitted very well in the region of R_H sign reversal. However, in the remaining regions, the two curves closely match.

A variation in vacancy concentration of this kind will affect the R_H of the layer more strongly than its conductivity. This is because the electron contribution to the layer conductivity in this region (at temperatures below the point where the R_H is past its peak value) is much less than that due to the holes. As seen from Fig 6, the conductivity of the sample can indeed be fitted with better accuracy. Due to the nonuniform vacancy concentration across the sample depth, the vacancy concentrations quoted here should be inferred as the average over the sample thickness.

Results on a few partially annealed layers are presented in Table 1. In all cases, these annealing conditions should have been sufficient for complete conversion of the layer to n-type [4], but are found to be insufficient for these layers. The bulk parameters were extracted by curve-fitting the R_H and σ versus 1/T data. The fact that the samples were p-type was confirmed in a few cases by sulfidizing and remeasuring the Hall effect. In all the cases, the R_H showed distinct stretch out in the region between its peak and the point of sign reversal, indicating a variation in the Hg vacancy concentration

with depth. Data on an unannealed sample is also presented for comparison purposes.

Fully Annealed Layers:

Figure 7 shows R_H and σ versus 1000/T for a sample annealed at 290°C for 15 hours, followed by a second anneal at 220°C for 13 hours. Figure 8 shows μ versus 1000/T for this sample. The layer was 8.2 μm thick, with $x = 0.205$. The data were taken at 1.1 kG. It is seen from the shape of the R_H curve, as well as the high mobility value, that this is an n-type layer. However, it is possible that the measured electron concentration and mobility are different from the actual bulk electron concentration and mobility, due to the presence of surface electrons. The measurement of R_H as a function of B field allows the effect of these carriers to be separated (see Appendix).

The R_H of this layer, measured at a fixed temperature of 30 K and as a function of B-field, is shown in Fig. 9. The variation in R_H with B-field was fitted to a two carrier model, assuming both bulk and surface electrons. Using this approach, these electron concentrations were calculated to be 5.4 $\times 10^{14}/cm^3$ and 2.4 $\times 10^{11}/cm^2$ respectively, with respective mobilities of 334,000 cm^2/V-sec and 27,500 cm^2/V-sec at 30 K. As the intrinsic carrier concentration in the layer at 30 K is negligible, this bulk electron concentration is, in fact, the net donor concentration in the layer. The temperature dependence of R_H, σ and μ_H, simulated using these values of bulk and surface carrier concentrations and mobilities, are shown by the solid curves in Figs. 7 and 8. The following parameters were used for generating the theoretical curves: (N_D-N_A) of 5.4 $\times 10^{14}/cm^3$, N_s of 2.4 $\times 10^{11}/cm^2$, a low temperature bulk electron mobility (μ_{no}) of 380,000 cm^2/V-sec and a surface electron mobility (μ_{so}) of 30,000 cm^2/V-sec.

Table 2 lists the results of Hall data on this and several other annealed samples, which show complete conversion to n-type. The free electron concentrations and mobilities quoted here were extracted from the σ and the B-field dependence of the R_H at 30 K. Sample numbers 1 to 4 in this table were annealed at 220°C following the initial

high temperature anneal. At 220°C, the equilibrium concentration of vacancies is expected to be in the low $10^{13}/cm^3$ range [6]. Hence, compensation due to the vacancies is expected to be negligible in these layers, so that the net shallow donor concentration N_D approximates the free electron concentration (N_D-N_A). These residual donor impurities are probably associated with process related issues such as chemical contamination from the system and bubblers, as well as the inherent defects in $Hg_{1-x}Cd_xTe$ due to lattice and thermal expansion coefficient mismatch between the epilayer and the substrate. The number of such donor impurities is seen to be in the range of 3-6 $\times 10^{14}$/cc in these layers.

Sample number 5 in this table shows the result for annealing at 290°C for 14 hours. The second step of low temperature anneal was intentionally omitted here in order to check the suitability of a single high temperature process for annealing the $Hg_{1-x}Cd_xTe$ layers. The free electron concentration measured on this sample is only 1.0 $\times 10^{14}/cm^3$ as opposed to 3-6 $\times 10^{14}/cm^3$ observed in the other samples in the same table. This is probably due to the fact that, at 290°C, the equilibrium concentration of Group II vacancies is in the low $10^{14}/cm^3$ range [6], which is comparable to the residual donor concentration in the layer. This would cause the layer to be compensated, resulting in a reduced free electron concentration. Thus, although the free electron concentration in this sample is only 1.0 $\times 10^{14}/cm^3$, the actual donor concentration is probably in the 3-6 $\times 10^{14}/cm^3$ range as is the case with the other samples. Hence, it is necessary for samples to undergo a final low temperature anneal if we wish to maintain a low $[V_{Hg}]$ in the layers.

DISCUSSION

The conversion of p-type layers to n-type after annealing is due to the reduction of Group II vacancies to the iow 10^{13} to $10^{14}/cm^3$ range, at which point residual donor impurities become dominant [1-10]. Following this line of reasoning, it can be argued that

the persistence of p-type conduction in partially annealed layers is due to the fact that the residual impurities involved here are p-type. However, similar samples were converted to n-type by choosing different annealing conditions. Hence, we conclude that p-type behavior is due to the Group II vacancies themselves, which have not been reduced to their lowest possible concentration, or perhaps due to some other native defects which anneal out only at higher temperatures.

The reason for the anomalous annealing characteristics of these layers is not quite clear at the present time. The slower diffusion rate of Hg in epitaxial $Hg_{1-x}Cd_xTe$ has been suggested as one possibility [7] for the observed difference. If this were the case, an epitaxial layer would indeed take a longer time to anneal completely as compared to a bulk layer of the same thickness. However, if the time is insufficient for the complete annealing of the whole layer, the region closer to the surface will get fully annealed and convert to n-type, whereas the region deeper inside will be unannealed and remain heavily p-type [3, 4, 22]. In such a case of partial annealing the diffusion rate of the Hg determines the thickness of the fully annealed region as well as the width of the transition region between the fully annealed and the unannealed region. A smaller diffusion coefficient would give rise to a thinner n-type region and a sharper transition between the fully annealed n-region and the unannealed p-region [3].

The Hall analysis on the partially annealed samples described here shows that the layers are p-type throughout. We do observe an n-type surface inversion layer (see Fig. 3), but this can be almost completely eliminated by anodic surface passivation which consumes less than 0.1 μm of the original layer (see Fig. 5). In addition, the *average* vacancy concentration in the partially annealed layers is down to 1-5% of the initial value (see Table 1). Such a large reduction in the net vacancy concentration requires that almost the entire layer is getting annealed. This suggests that the difference in the annealing behavior of these layers could not be due to a lower diffusion coefficient of Hg.

We now consider the role of Te precipitates in the annealing process. Annealing of bulk grown layers shows that the in-diffusion of Hg annihilates the Te precipitates in the surface region; with time, the precipitate free region gradually extends into the bulk. It is this region which is fully annealed and converted to n-type [22, 23]. In case of epitaxial layers such as the ones examined here, the total epi-layer thickness itself is of the order of the spacing between the precipitates. In such a case, the model of a precipitate free zone gradually moving into the layer might not hold. Instead, we propose that the in-diffusing Hg will annihilate the Te precipitates as well as reduce the Hg vacancy concentration in the region between the precipitates. However, due to the presence of excess Te in the lattice, the Hg vacancy concentration may not go all the way down to the value typical of saturated mercury conditions. As a result, the layer still stays p-type, but with a much reduced hole concentration.

A higher temperature anneal would increase the rate of annihilation of Te precipitates as a result of the enhanced rate of Hg in-diffusion, as well as the higher rate of reaction between Hg and Te. It is also possible that, at higher temperatures, lattice sites necessary to accommodate the newly formed HgTe are created more easily. Once the Te precipitates are fully annihilated at a higher temperature, a subsequent lower temperature anneal brings the Hg vacancy concentration further down, and the layer is eventually converted to n-type.

The concentration of Te precipitates depends on the growth conditions and the post growth cool down process [22, 24]. Hence, it might be possible to alter the reactor conditions and thus be able to grow $Hg_{1-x}Cd_xTe$ layers which can be annealed fully using a single low temperature anneal. This approach to $Hg_{1-x}Cd_xTe$ epitaxy is currently under investigation.

CONCLUSIONS

The annealing results on some OMVPE grown layers were presented. A typical low

temperature ($\sim$ 220°C) anneal, under Hg saturated conditions does not achieve conversion to n-type as is expected [3, 4], but resulted in p-type layers with hole concentrations around $1 \times 10^{15}/cm^3$ range. However, by a two-step annealing process, we have shown that the vacancy concentration can be reduced to the point that the conductivity is determined by residual donors in the layer. For $Hg_{1-x}Cd_xTe$ layers with x in the 0.2-0.24 range, and thickness around 8 μm, conversion to n-type could be achieved by annealing at 290°C for 14 hours followed by a 14 hour anneal at 220°C. The residual donor concentration of $5 \times 10^{14}/cm^3$, accompanied by high mobility, is an indication of the purity of these samples. The influence of surface layer on the Hall effect of both p-type as well as n-type epilayers was described, and the Hall data was analyzed, taking this into consideration. A tentative model for such an annealing behavior was also proposed.

ACKNOWLEDGEMENT

The authors would like to thank J. Barthel for technical assistance on this program and P. Magilligan for manuscript preparation. We would like to thank C.J. Johnson and S. McDevitt of II-VI Inc. for providing the CdTe substrates on which this study was performed. Partial funding for this program, from the Raytheon Corporation, is hereby acknowledged. This work was sponsored by the Defense Advanced Research Projects Agency (contract No. N-00014-85-K-0151), administered through the Office of Naval Research, Arlington, VA. This support is greatly appreciated.

REFERENCES

1. H.R. Vydyanath, J. Electrochem. Soc., 128, (1981) 2609.
2. J.L. Schmit and E.L. Stelzer, J. Electron. Mater., 7, (1978) 65.
3. V.V. Bogoboyashchii, A.I. Elizarov, V.I. Ivanov-Omskii, V.R. Petrenko, V.A. Petryakov, Sov. Phys.-Semicond. (USA), 19, (1985) 505.
4. C.L. Jones, M.J.T. Quelch, P. Capper, and J.J. Gosney, J. Appl. Phys., 53, (1982) 9080.
5. H.F. Schaake, J. Electron. Mater., 14, (1985) 513.
6. H.R. Vydyanath and C.H. Hiner, J. Appl. Phys., 65, (1989) 3080.
7. P. Capper, B.C. Easton, P.A.C. Whiffin, and C.D. Maxey, J. Crystal Growth, 79, (1986) 508.
8. K. Nagahama, R. Ohkata, K. Nishitani, and T. Murotani, J. Electron. Mater., 13, (1984) 67.
9. M.J. Hyliands, J. Thompson, M.J. Bevan, K.T. Woodhouse, and V. Vincent, J.Vac. Sci. Technol., A4, 27 (1986).
10. B. Pelliciari, G.L. Destefanis and L. DiCioccio, J. Vac. Sci. Tech., 7A, (1989) 314.
11. L.F. Lou and W.H. Frye, J. Appl. Phys., 56, (1984) 2253.
12. A. Zemel, A. Sher and D. Eger, J. Appl. Phys., 62, (1987) 1861.
13. K.K. Parat, N.R. Taskar, I.B. Bhat, S.K. Ghandhi, J. Crys. Growth (submitted).
14. Y. Nemirovsky, L. Burstein, and I. Kidron, J. Appl. Phys., 58, (1985) 366.
15. M.C. Chen, Appl. Phys. Lett., 51, (1987) 1836.
16. S.K. Ghandhi, I.B. Bhat, and H. Fardi, Appl. Phys. Lett., 52, (1988) 392.
17. S.J.C. Irvine, J.S. Gough, J. Riess, M.J. Gibbs, A. Royle, C.A. Taylor, G.T. Brown, A.M. Keir and J.B. Mullin, J. Vac. Sci. Tech., 7A, (1989) 285.
18. G.L. Hansen, J.L. Schmit, and T.N. Casselman, J. Appl. Phys., 53, (1982) 7099.

19. G.L. Hansen and J.L. Schmit, J. Appl. Phys., 53, (1983) 1639.

20. L.J. van der Pauw, Philips Research Reports, 13, (1958) 1.

21. W. Scott, E.L. Stelzer, and R.J. Hager, J. Appl. Phys., 47, (1976) 1408.

22. H.F. Schaake, J.H. Tregilgas, J.D. Beck, M.A. Kinch, and B.E. Gnade, J. Vac. Sci. Tech., 3A, (1985) 143.

23. J.H. Tregilgas, J. Vac. Sci. Tech., 21 (1982) 208.

24. D.J. Williams and A.W. Vere, J. Vac. Sci. Tech., 4A (1986) 2184.

25. M.C. Chen, J. Appl. Phys., 65 (1989) 1571.

LIST OF FIGURES

LIST OF TABLES

TABLE 1

Sample	x	Thickness (μm)	Annealing Conditions	$(N_A - N_D)$ (/cm^3)
1.	0.228	6.7	unannealed	3.61×10^{16}
2.	0.219	6.3	205°C/24 hr.	6.5×10^{14}
3.	0.208	12.0	230°C/9 hr.	1.25×10^{15}
4.	0.204	11.4	230°C/24 hr.	0.7×10^{14}
5.	0.232	13.0	240°C/12 hr.	5.0×10^{14}

TABLE 2

Sample	x	Thickness (μm)	Annealing Conditions	$(N_D - N_A)$ (cm^{-3})	$\mu_n(30K)$ (cm^2/V-s)
1.	0.205	8.2	290°C/15 hr. +220°C/13 hr.	5.4×10^{14}	334,000
2.	0.220	5.8	290°C/15 hr. +220°C/13 hr.	6.2×10^{14}	210,000
3.	0.226	5.8	290°C/15 hr. +220°C/13 hr.	3.3×10^{14}	120,000
4.	0.226	5.8	290°C/14 hr. +220°C/12 hr.	3.5×10^{14}	190,000
5.	0.224	4.5	290°C/14 hr.	1.0×10^{14}	110,000

APPENDIX

The temperature dependence of R_H and σ was treated in terms of a three carrier model [11]. The three types of carriers were: bulk holes, bulk electrons and surface electrons. It was assumed that surface and bulk layers are in electrical communication. A uniform bulk doping was assumed. In such a case the Hall coefficient of the total layer is given by:

$$R_H = \frac{1}{B}\frac{\sigma_{xy}}{\sigma_{xx}^2 + \sigma_{xy}^2} \tag{A- 1}$$

where

$$\sigma_{xx} = q\left(\frac{n\mu_n}{1+\mu_n^2B^2} + \frac{p\mu_p}{1+\mu_p^2B^2} + \frac{n_s\mu_s}{1+\mu_s^2B^2}\right) \tag{A- 2}$$

and

$$\sigma_{xy} = qB\left(\frac{-n\mu_n^2}{1+\mu_n^2B^2} + \frac{p\mu_p^2}{1+\mu_p^2B^2} - \frac{n_s\mu_s^2}{1+\mu_s^2B^2}\right) \tag{A-3}$$

Here, n and p represent the bulk electron and hole concentrations, and n_s represents the average concentration (sheet concentration, N_s, divided by the epilayer thickness) of the surface electrons. μ_n, μ_p, and μ_s represent the corresponding mobilities. The effect of light holes is ignored in these calculations.

In the case of p-type layers, the bulk hole concentration was calculated by solving for p from the following charge balance relation:

$$p = n_i^2/p - N_D + N_A/\{1 + 4(p/N_v)exp(E_A/kT)\} \tag{A-4}$$

where $N_v = 2 \times 10^{15}T^{3/2}/\text{cm}^3$. Here N_A is the acceptor concentration and N_D is the donor concentration. N_v is the effective density of states at the valence band edge. The

acceptors were taken to be singly ionized with an ionization energy of E_A [11, 25]. The bulk electron concentration was obtained using the relation:

$$n = n_i^2/p \tag{A-5}$$

The surface electron concentration was assumed to be independent of the temperature.

In p-type layers, the hole mobility was assumed to be limited by lattice scattering (with a $T^{-1.9}$ dependence), and low temperature alloy/ionized impurity scattering, which was assumed to be temperature independent [11]. This is a simple empirical model for the electron and hole mobility, which agrees well with the experimental results (see Figs. 2 and 8). The bulk electron mobility was calculated by multiplying the hole mobility by the inverse of the effective mass ratio. For the surface electrons, an additional, temperature independent, surface scattering limited mobility was also included. These relations are summarized below:

$$\mu_p = 1/[1/\{\mu_{300}(300/T)^{1.9}\} + 1/\mu_{po}] \tag{A-6}$$

$$\mu_n = (m_h^*/m_e^*)\mu_p \tag{A-7}$$

$$\mu_s = 1/(1/\mu_n + 1/\mu_{s0}) \tag{A-8}$$

Here, μ_{300} is the lattice scattering limited mobility of holes at 300K, and μ_{po} is the asymptotic value of the hole mobility in the low temperature limit, in the absence of lattice scattering. Similarly, μ_{s0} is the mobility of the surface electrons in the low temperature limit. In practice, the hole mobility does not increase monotonically with decreasing temperature; instead it peaks around 40-20K [21]. However, for simplicity, the above model for mobility was assumed. For analyzing the Hall data, the composition and thickness of the layer were measured using an FTIR. Then, the values N_A, N_D, E_A, N_S, μ_0, and μ_S were varied and optimized till a reasonable fit to the experimental R_H

and σ is obtained. In the case of p-type layers, the fit was more sensitive to the value of (N_A-N_D) rather than their individual values. As a result, N_D was chosen to be around 5×10^{14}/cc, which was the typical donor concentration in the fully annealed layers. N_A was optimized using this value of N_D.

In the case of n-type layers, the net donor concentration can be determined by measuring the electron concentration in the layer at low temperatures, since the donors do not undergo thermal freeze-out. However, the presence of surface electrons can lead to an overestimation of the actual bulk donor concentration, unless care is taken to account for them. The actual bulk and surface electron concentration and mobility in these n-type layers were determined by analyzing the variation in the R_H of the layer with B-field, which is a very convenient technique [13]. For an n-type layer having a surface electron layer, the Hall coefficient is given by [13]:

$$R_H = -\frac{1}{q} \cdot \frac{(n\mu_n^2 + n_s\mu_s^2) + \mu_n^2\mu_s^2B^2(n+n_s)}{(n\mu_n + n_s\mu_s)^2 + \mu_n^2\mu_sB^2(n+n_s)^2} \qquad \text{(A-9)}$$

and the conductivity σ is given by:

$$\sigma = q(n\mu_n + n_s\mu_s) \qquad \text{(A-10)}$$

At a fixed temperature, R_H was measured at different values of B-field and the various bulk and surface parameters were evaluated [13] from this data.

The variable B-field approach can be used for analyzing the p-type layers as well [12, 15]. However, due to the low mobility of the bulk holes, very high B-fields are required for successfully analyzing light p-type layers having surface inversion layers. In addition, due to the freeze-out of holes, the actual acceptor concentration and the acceptor activation energy can be evaluated only by analyzing the temperature dependence of the hole concentration. As a result p-type layers were exclusively analyzed by studying the temperature dependence of the R_H and σ.

For the sake of completeness, the temperature dependence of R_H, σ and μ of the n-type layers were also simulated using the two layer model. Here the concentration of the bulk electrons is given by the expression:

$$n = \frac{(N_D - N_A) + \{(N_D - N_A)^2 + 4n_i^2\}^{1/2}}{2} \qquad \text{(A-11)}$$

As in the case of p-type samples, the bulk electron mobility is once again assumed to be determined by lattice scattering, and alloy/ionized impurity scattering. Here in addition to the $T^{-1.9}$ dependence of the lattice scattering, the variation in the electron effective mass with temperature also contributes to the temperature dependence of the electron mobility, and was included in the simulation. Thus, the bulk electron mobility μ_n as a function of temperature was assumed to be of the form:

$$\mu_n = 1/[1/\{\mu_{300}(m_e^*(300)/m_e^*(T))(300/T)^{1.9}\} + 1/\mu_{no}] \qquad \text{(A-12)}$$

where μ_{300} is the lattice scattering limited mobility of electrons at 300K, and μ_{no} is the asymptotic value of the electron mobility in the low temperature limit in the absence of lattice scattering. The bulk hole mobility and the surface electron mobility were calculated using Eqs. (A-7) and (A-8). The thickness of the layer and the composition were determined using the FTIR. The values of (N_D-N_A), N_s, μ_{no} and μ_{so} can then be adjusted to make the theoretical R_H and σ curves fit the experimental data points. However, the temperature dependence of R_H and σ of n-type layers are not very sensitive to the individual bulk and surface parameters. On the other hand, the B-field dependence of R_H is very sensitive to these values. Hence, the bulk and surface parameters were extracted using the variable B-field technique; these values were used to simulate the temperature dependence of R_H, μ and σ in order to show that the simulation does indeed match the data.

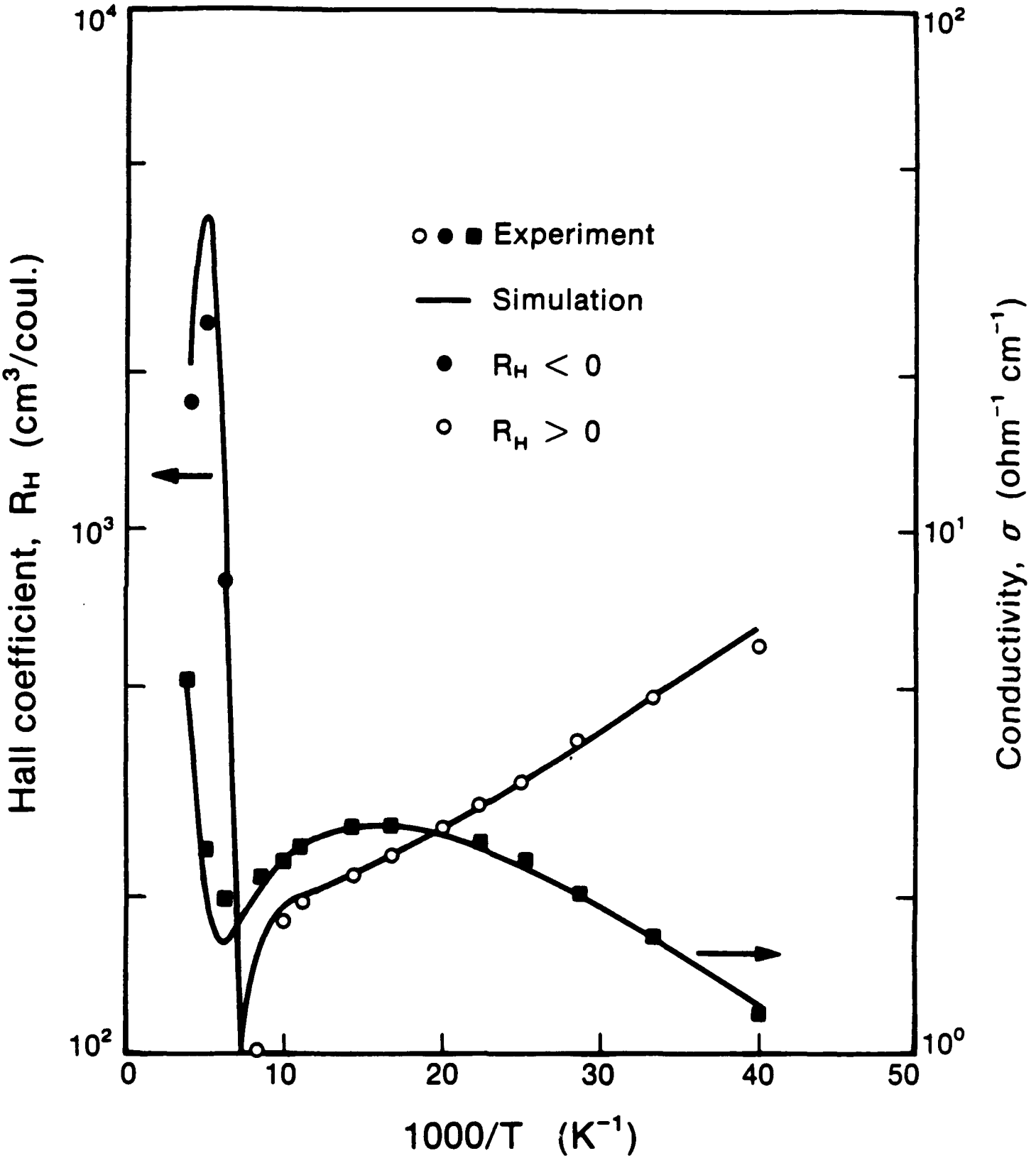
Experiment
Simulation
$R_H < 0$
$R_H > 0$
Hall coefficient, R_H (cm^3/coul.)
Conductivity, σ (ohm^{-1} cm^{-1})
1000/T (K^{-1})
10^4
10^3
10^2
10^2
10^1
10^0
0
10
20
30
40
50

KKP

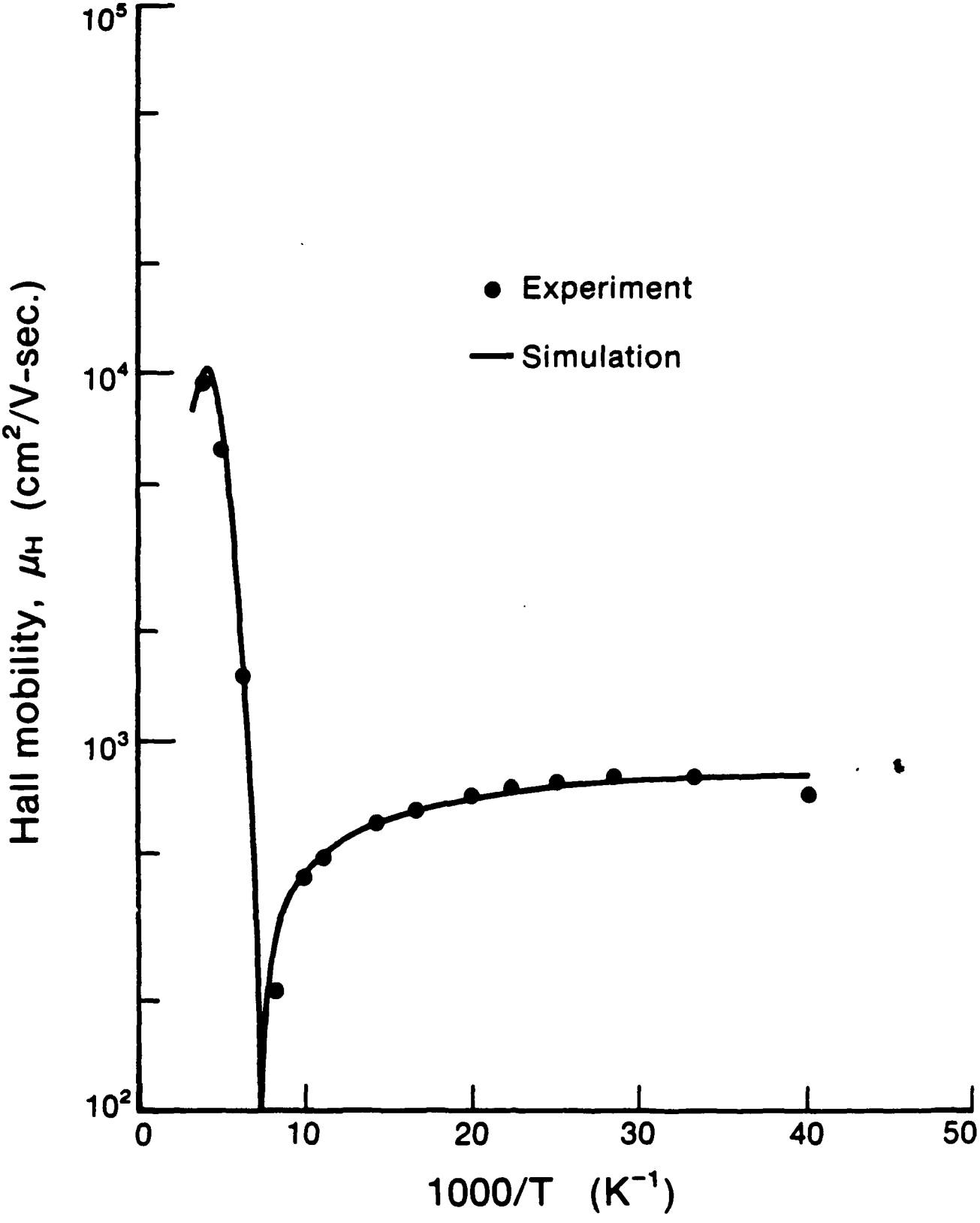
Hall mobility, μ_H (cm^2/V-sec.)
10^5
10^4
10^3
10^2
Experiment
Simulation
0
10
20
30
40
50
1000/T (K^{-1})

KKP

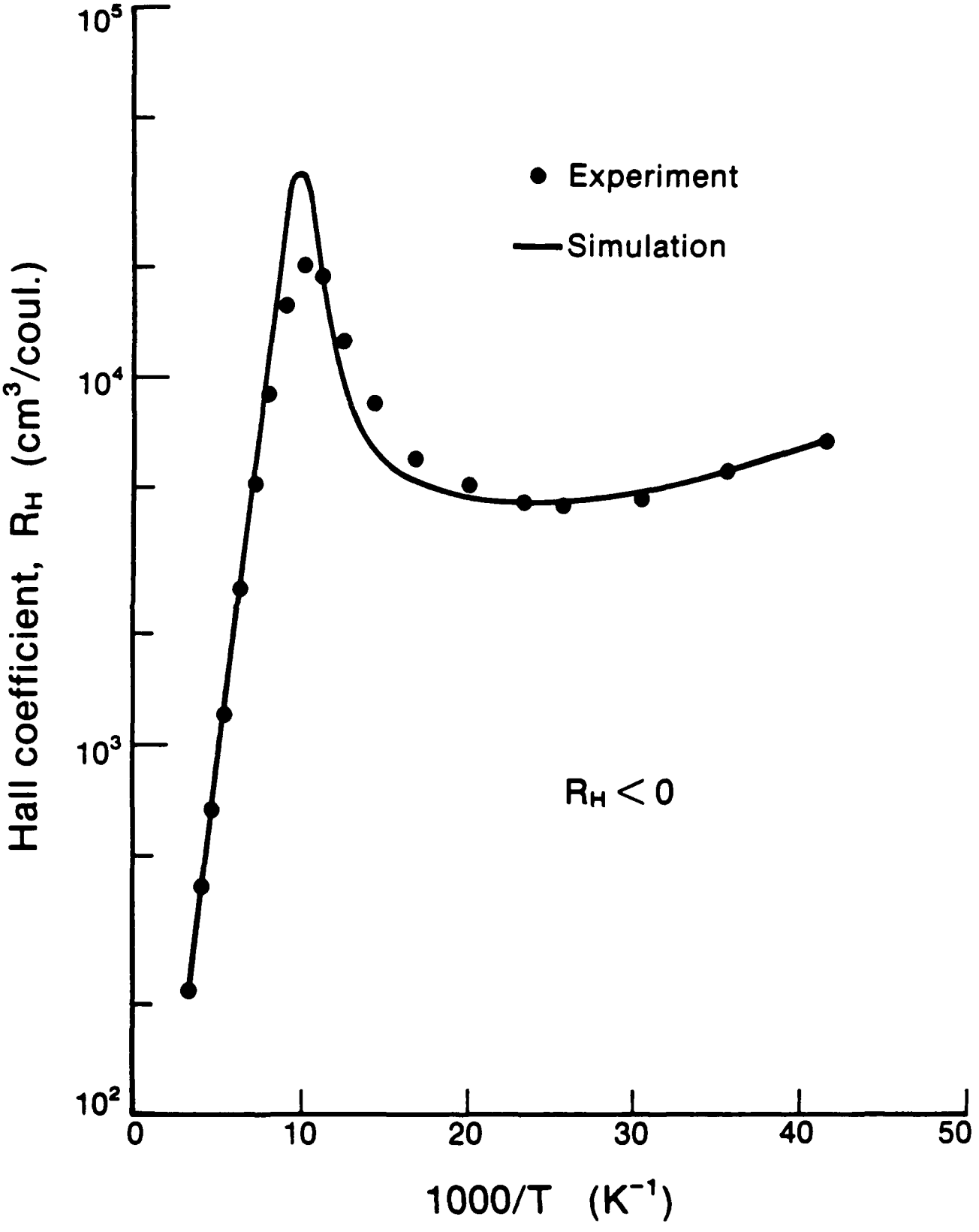
Hall coefficient, R_H (cm^3/coul.)
10^5
10^4
10^3
10^2
Experiment
Simulation
$R_H < 0$
0
10
20
30
40
50
1000/T (K^{-1})

KKP

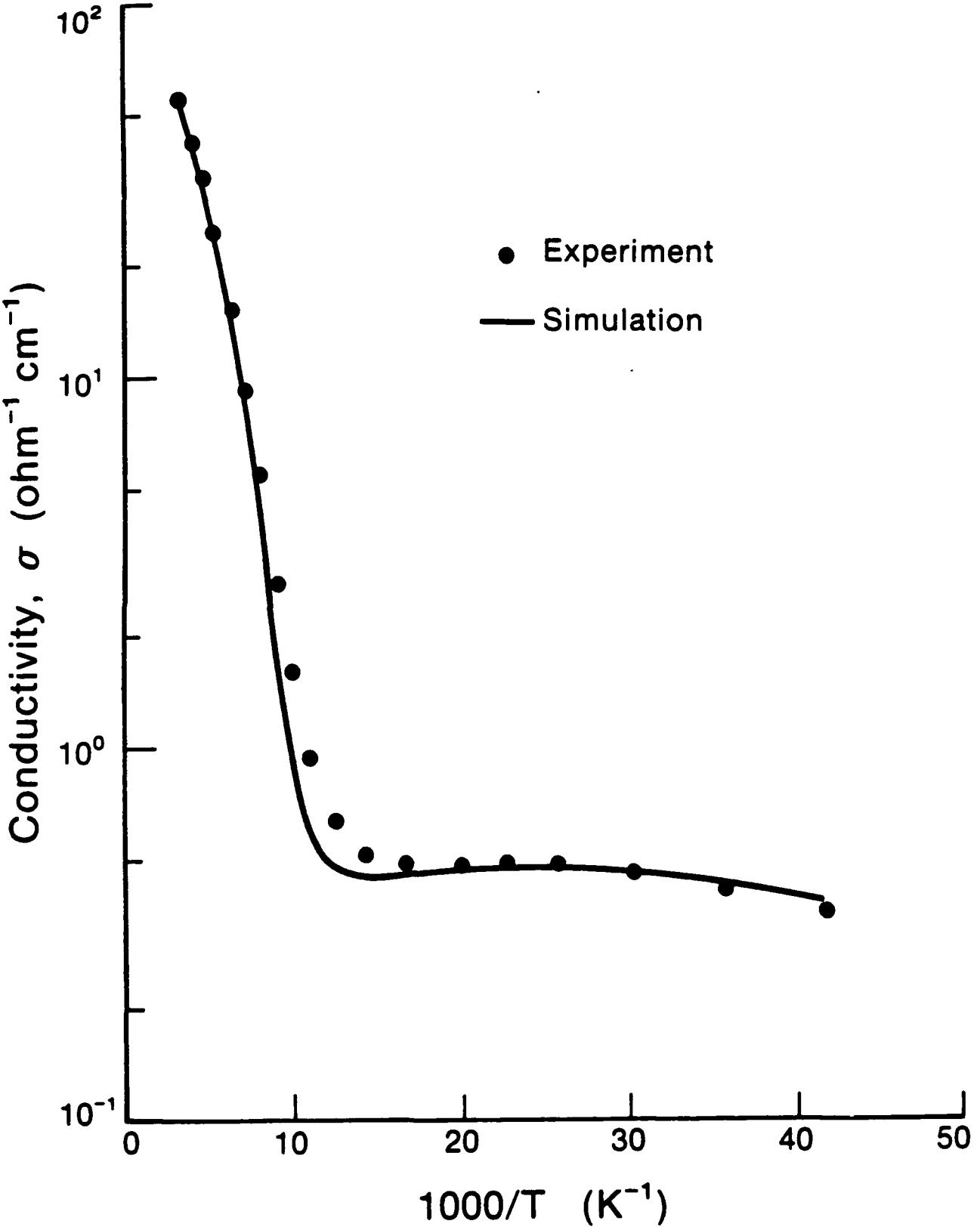
Conductivity, σ (ohm⁻¹ cm⁻¹)
10²
10¹
10⁰
10⁻¹
Experiment
Simulation
0
10
20
30
40
50
1000/T (K⁻¹)

KKP

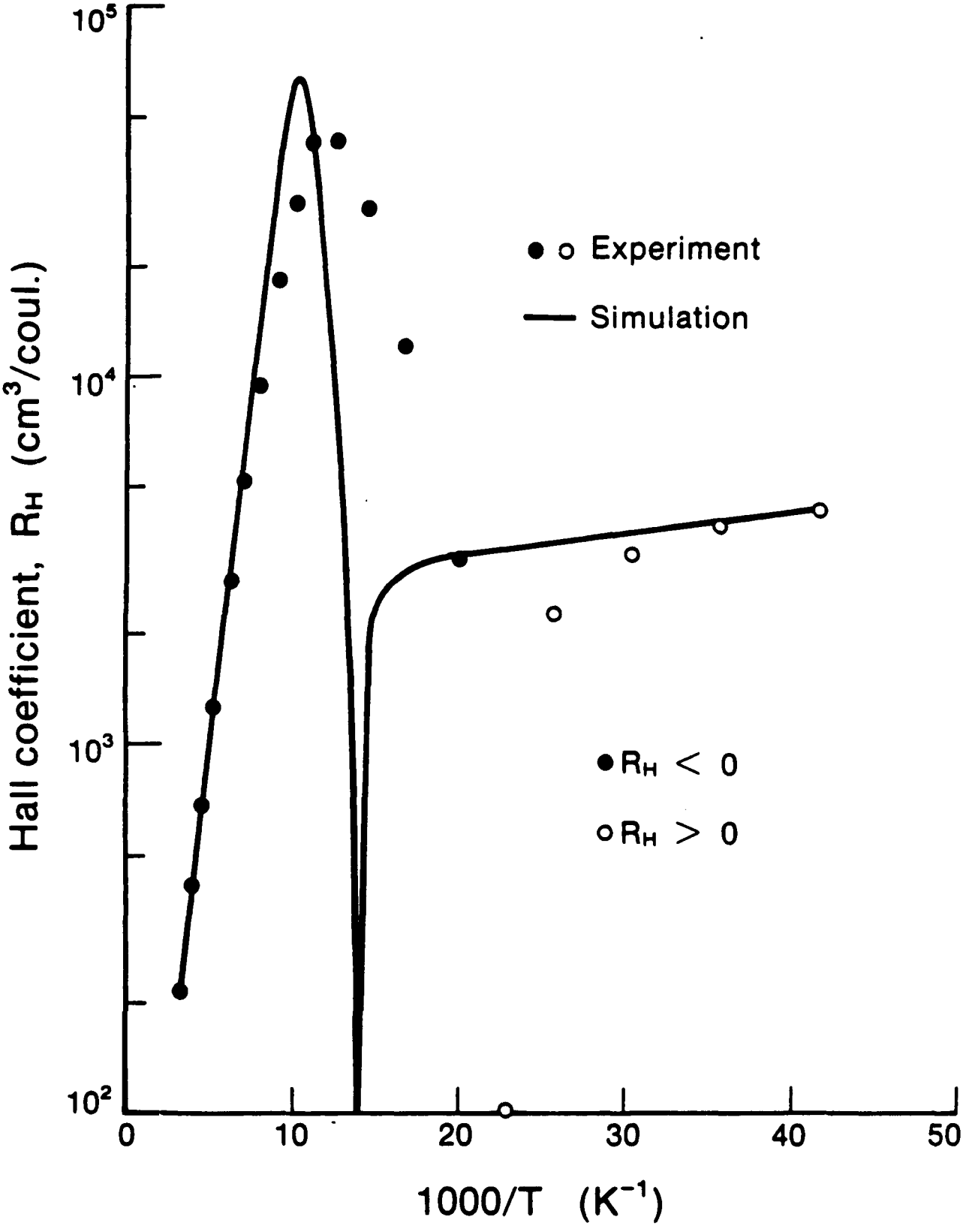
Hall coefficient, R_H (cm^3/coul.)
10^5
10^4
10^3
10^2
0
10
20
30
40
50
1000/T (K^{-1})
Experiment
Simulation
$R_H < 0$
$R_H > 0$

KKP
a-1

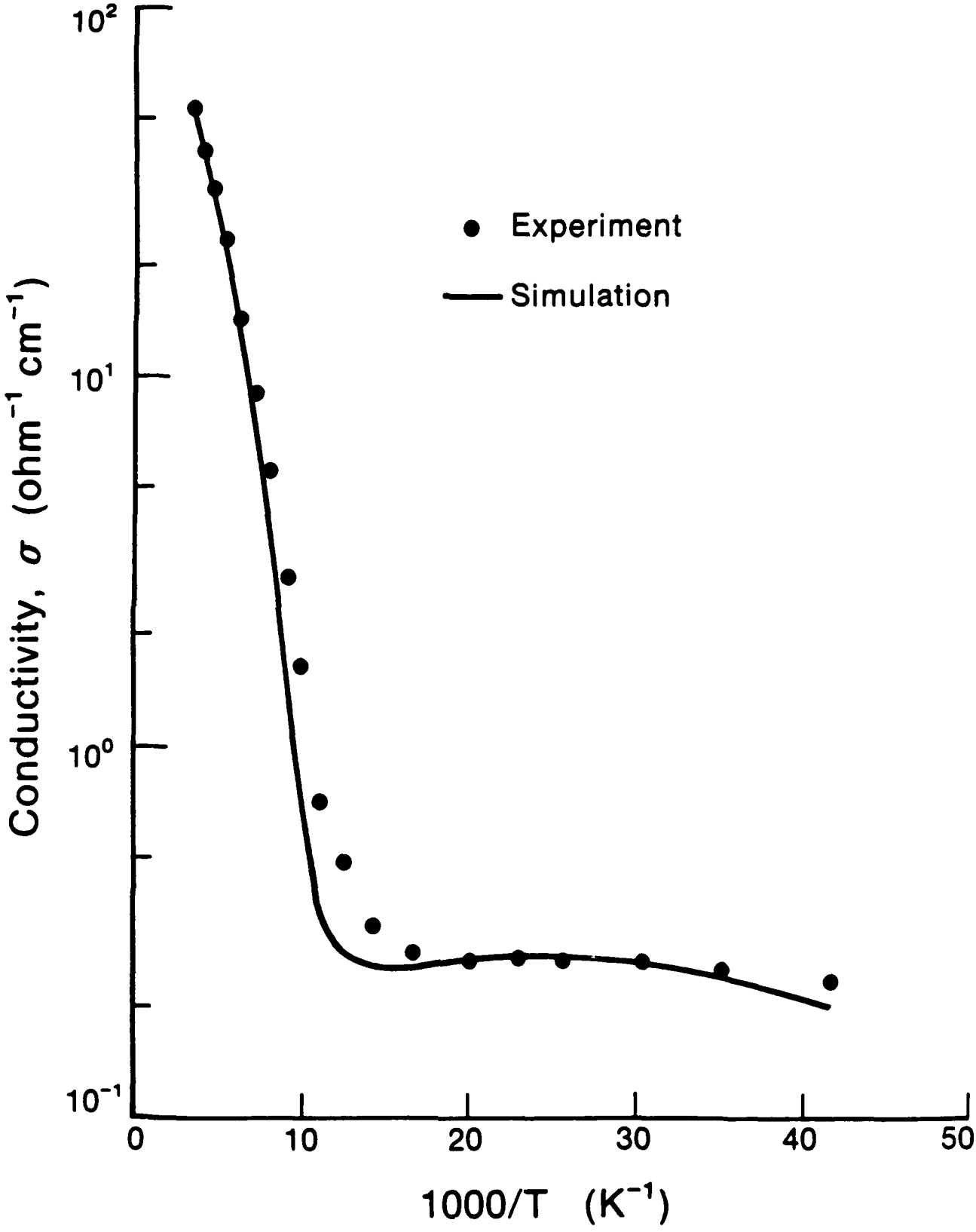
Experiment
Simulation
Conductivity, σ (ohm⁻¹ cm⁻¹)
10²
10¹
10⁰
10⁻¹
0
10
20
30
40
50
1000/T (K⁻¹)

KKP

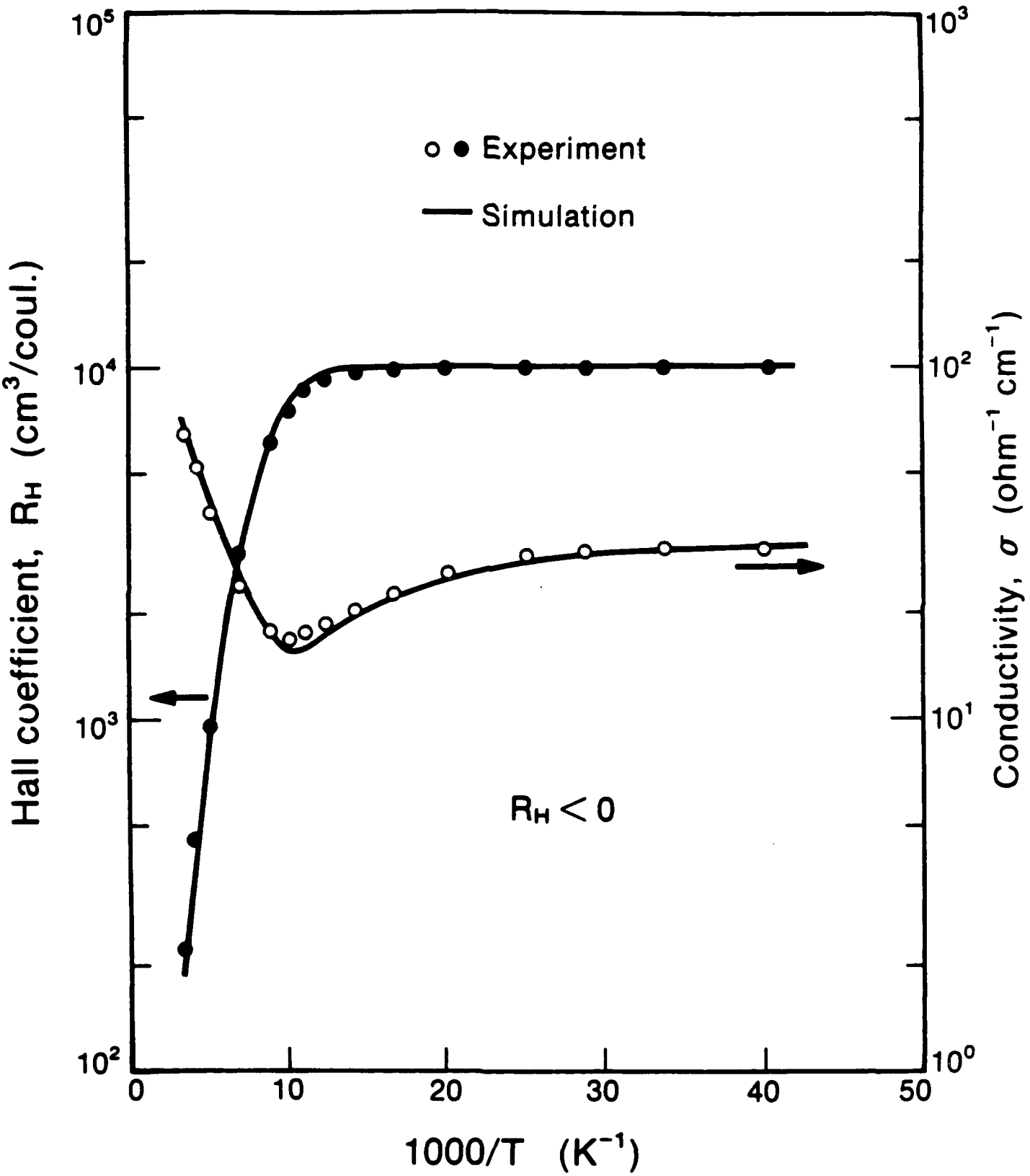
Experiment
Simulation
$R_H < 0$
Hall coefficient, R_H (cm^3/coul.)
Conductivity, σ (ohm^{-1} cm^{-1})
1000/T (K^{-1})
10^5
10^4
10^3
10^2
10^3
10^2
10^1
10^0
0
10
20
30
40
50

KKP

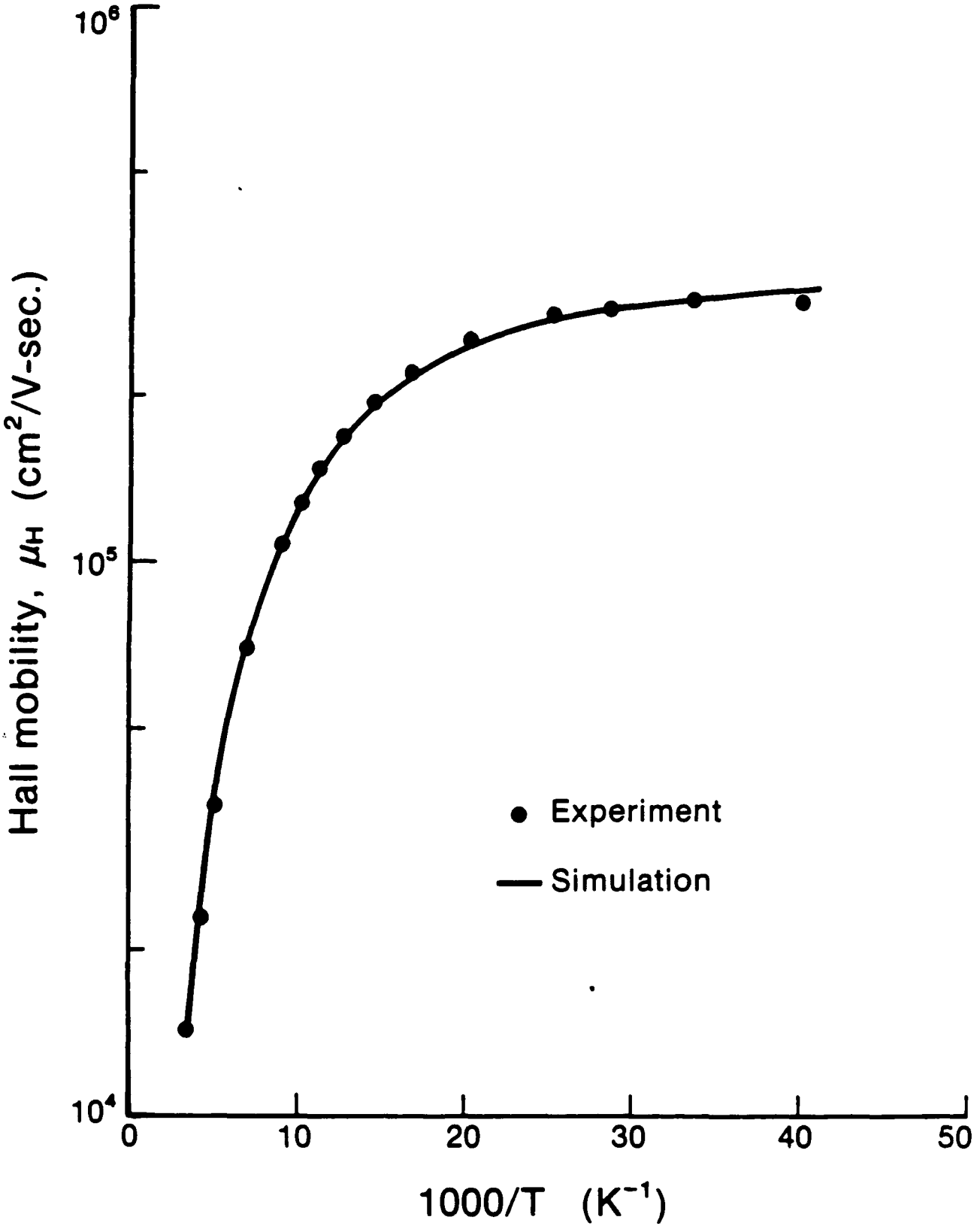
Hall mobility, μ_H (cm^2/V-sec.)
10^6
10^5
10^4
0
10
20
30
40
50
1000/T (K^{-1})
Experiment
Simulation

KKP

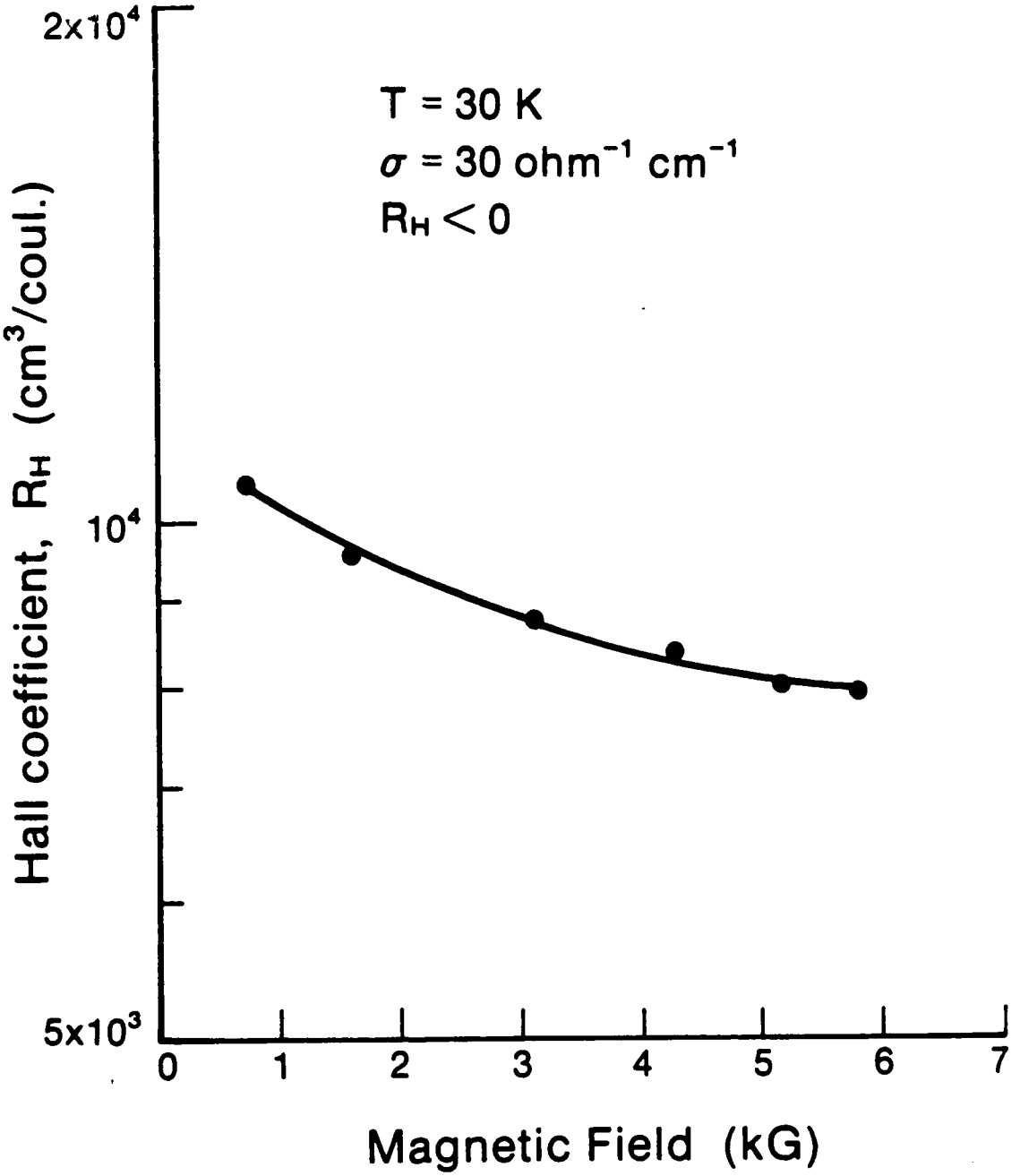
2x10⁴
10⁴
5x10³
T = 30 K
σ = 30 ohm⁻¹ cm⁻¹
R_H < 0
Hall coefficient, R_H (cm³/coul.)
0
1
2
3
4
5
6
7
Magnetic Field (kG)

D

THE INFLUENCE OF ACCUMULATION LAYERS ON THE HALL-EFFECT IN n-TYPE $Hg_{1-x}Cd_xTe$

K.K. PARAT

N.R. TASKAR

I.B. BHAT

S.K. GHANDHI

ELECTRICAL, COMPUTER AND SYSTEMS ENGINEERING DEPARTMENT

RENSSELAER POLYTECHNIC INSTITUTE

TROY, NEW YORK 12180

Submitted to Journal of Crystal Growth

Point of Contact:

S.K. Ghandhi

(518) 276-6085

FAX: (518) 276-6261

SK-89.35

July 21, 1989

ABSTRACT

The presence of an electron accumulation layer on the surface of n-type $Hg_{1-x}Cd_xTe$ causes the measured Hall mobility and carrier concentration to be significantly different from the actual bulk values. This discrepancy is not readily apparent in the temperature dependence of the Hall coefficient, R_H, as is the case with p-type layers. However, it is observed in the magnetic-field dependence of the R_H. The B-field dependence of R_H is analyzed to extract the actual concentration and mobility of the bulk and surface carriers in $Hg_{1-x}Cd_xTe$ layers grown by organometallic vapor phase epitaxy. The bulk parameters thus calculated were verified by passivating the surface of these layers using an anodic sulfide to reduce the concentration of surface electrons.

The presence of a surface inversion layer on lightly doped p-type $Hg_{1-x}Cd_xTe$ is readily apparent, since it gives rise to anomalous behavior in the Hall Coefficient (R_H) vs. Temperature data. This behavior, which has been analyzed in great detail [1-4], is a consequence of the fact that these inversion layer electrons, induced by the fixed positive charges in the native oxide of $Hg_{1-x}Cd_xTe$, have surface mobilities which are a factor of 10 to 20 times higher than those of the bulk holes. Their concentrations lie in the range of 3×10^{11} to $1 \times 10^{12}/cm^2$, depending on the nature of the surface, and its treatments.

In the case of n-type $Hg_{1-x}Cd_xTe$, the presence of an electron accumulation layer at the surface causes the effective Hall mobility to be lower than the bulk electron mobility, and the carrier concentration to be higher than the bulk carrier concentration. Moreover, the presence of this layer results in the measured carrier concentration and mobility becoming functions of the magnetic field at which the Hall measurement is done. Although these are undesirable effects from the point of characterizing the actual bulk layer, they are often overlooked since the R_H vs. T characteristic is very similar to that of an n-type $Hg_{1-x}Cd_xTe$ layer which does not have an accumulation layer.

Due to the large surface to bulk ratio, these surface effects are severe in the case of epitaxial layers. Surface effects, which have normally been neglected in the case of bulk layers, cannot be neglected here. Similar surface and interface effects have also been observed in the case of epitaxial InAs and polycrystalline InSb layers [5-6].

In this paper, we evaluate, for the first time, the effect of a surface accumulation layer of electrons on lightly doped n-type epitaxial $Hg_{1-x}Cd_xTe$ layers. The B-field dependence of the Hall coefficient is analyzed to extract the true concentration and mobility of the bulk carriers. These layers were subsequently passivated using anodic sulfide [4, 7]. Here, the measured Hall mobility and carrier concentration approach the bulk values, due to the lower concentration of surface electrons in these layers. This demonstrates the suitability of anodic sulfidization for passivation of $Hg_{1-x}Cd_xTe$, and at the

same time establishes the usefulness of the variable B-field technique on n-type layers..

Experimental data on one specific sample was chosen among others for the purpose of demonstration. This $Hg_{1-x}Cd_xTe$ layer was grown on a (100) CdTe substrate with a cadmium fraction of 0.217, by the simultaneous pyrolysis of mercury, dimethylcadmium and diisopropyltellurium [8]. After the growth, the layer was annealed under Hg saturated conditions to reduce the Hg vacancies and thus convert it to n-type. The van der Pauw [9] technique was used for Hall effect measurements from 300 K down to 10 K, and as a function of B-field from 0.5 KG to 6.0 KG.

Figure 1 shows the Hall coefficient R_H, and the Hall mobility μ_H, as a function of reciprocal temperature for a 7.2 μm thick layer. A magnetic field strength of 1.6 KG was used for this measurement. The measured carrier concentration was $8.0 \times 10^{14}/cm^3$ and the mobility at 30K was 188,000 cm^2/V-sec. In the case of p-type $Hg_{1-x}Cd_xTe$, the presence of surface electrons would make the temperature dependence of R_H and μ_H drastically different from that of a classical p-type layer [2]. Here, however, R_H as well as the μ_H show a monotonic variation with temperature, of the form which is observed for n-type layers, where surface effects are absent.

The presence of the surface electrons becomes evident when the R_H is measured at different B-fields. Figure 2 shows the R_H of this sample measured as a function of B-field at a fixed temperature of 30K. This temperature was chosen because the measured mobility (Fig. 1) reaches its maximum around this value. Moreover, as the sample is fully extrinsic at this temperature, only electrons are expected to be present in the bulk of the layer. If there were no additional surface or interface electrons with mobilities different from those of the bulk electrons, R_H would be independent of the B-field, and be equal to $1/qn$, where n is the concentration of electrons in the layer. Here we have assumed that the Hall constant r_H is unity, and that it does not vary with the B-field. It is possible that r_H, which is usually greater than unity at low B-fields and approaches

unity at higher B-fields, contribute to the variation of R_H with the B-field [11]. Theoretical calculations show that this variation would be less than 10% for HgTe and less than 3% for CdTe [12]. Additionally, in more heavily doped n-type layers grown in our laboratory, where surface effects are negligible compared to the bulk, we find that R_H remains constant with the B-field. Thus, the variation in R_H seen here, which is about 40% as the B-field is increased from 0 to 6 KG, cannot be due to the variation in r_H. This variation can, however, be explained by including the presence of the surface electrons in addition to the bulk electrons in the Hall analysis.

For a layer containing bulk as well as surface electrons, R_H and σ are given by the following expressions [see Appendix]:

$$R_H = -\frac{1}{q}\frac{(n\mu^2 + n_s\mu_s^2) + \mu^2\mu_s^2B^2(n+n_s)}{(n\mu + n_s\mu_s)^2 + \mu^2\mu_s^2B^2(n+n_s)^2} \tag{1}$$

$$\sigma = q(n\mu_n + n_s\mu_s) \tag{2}$$

Here, n is the bulk electron concentration and n_s is the average concentration (total sheet carrier concentration, divided by the total thickness of the $Hg_{1-x}Cd_xTe$ layer) of the surface electrons. μ_n and μ_s are the corresponding mobilities.

From the measured values of R_H and σ, the values of n, n_s, μ and μ_s were calculated. Here the low mobility electrons were assumed to be surface electrons. By multiplying the average volume concentration n_s of the surface electrons by the total thickness of $Hg_{1-x}Cd_xTe$ layer, the actual sheet concentration N_s of the surface electrons was determined.

The bulk carrier concentration in the above sample was calculated to be 5.0 $\times$ $10^{14}/cm^3$ with a mobility of 269,000 cm^2/V-sec at 30 K. The surface carrier concentration was calculated to be 5.2 $\times$ $10^{11}/cm^2$ with a mobility of 25,000 cm^2/V-sec at 30 K. These values can be contrasted with the composite values (n = 8.0 $\times$ $10^{14}/cm^3$ and μ

= 188,000 cm^2/V-sec) obtained directly from Fig. 1, i.e., values which assume a single homogeneous layer. The solid curve drawn in Fig. 2 is the theoretical curve for R_H as a function of B-field for the above values of surface and bulk parameters.

To verify that the bulk parameters extracted by this technique are indeed the true values, and that the B-field dependence of the R_H was indeed caused by the effect of surface electrons, the layer was passivated using anodic sulfide and the Hall measurements were repeated. This treatment should reduce the surface electron concentration, while leaving the bulk parameters (n, μ_n) intact. Before sulfidization the sample was given a 30 seconds etch in 1% Br in methanol. Sulfidization was carried out in a non-aqueous solution of sodium sulfide in ethylene glycol [7]. After growing about 400$\AA$ of native anodic sulfide, the layer was capped with 2500$\AA$ of evaporated ZnS, to provide additional protection to the surface passivation during long term storage. The layer thickness was now 6.4 μm because of etching and native sulfide growth.

The R_H of the passivated sample, as measured at 30K, as a function of B-field is shown in Fig. 3. The sample still exhibits some variation in R_H with B-field. Its extent, however, is much less than in the case of the unpassivated sample and the value of R_H is also quite higher than in the previous case. The variation in R_H with the B-field was again fitted using the two carrier model, with a bulk carrier concentration of $5.0 \times 10^{14}/cm^3$ and a mobility of 269,000 cm^2/V-sec, along with a surface carrier concentration of $1.1 \times 10^{11}/cm^2$ with a mobility of 28,000 cm^2/V-sec. Note that the bulk carrier parameters (n, μ_n) are the same as before; however, the surface carrier concentration is now a factor of 4-5 lower due to the sulfidization. The Hall coefficient and mobility of the passivated sample are shown in Fig. 4 measured at a B-field of 1.6 KG as in the previous case. Compared to the situation before passivation, the increase in the measured R_H and mobility is quite apparent. Assuming a homogeneous layer, the composite values of concentration and the mobility at 30 K, as obtained from this measure-

ment were $5.7 \times 10^{14}/cm^3$ and 243,000 cm^2/V-sec. These values are much closer to the bulk values calculated using the variable B-field technique, than the ones measured prior to passivation. However, the presence of this light surface accumulation layer still causes the measured values of carrier concentration and mobility to differ from the correct bulk values.

In the case of an n-type layer with surface electrons, composite values of carrier concentration and mobility approximate the bulk values at low B-fields. In the zero B-field limit, R_H is given by $C_1 = \frac{-1}{q} \times \left[\frac{(n\mu_n^2+n_s\mu_s^2)}{(n\mu_n+n_s\mu_s)^2}\right]$. As the B-field is increased, these measured values deviate increasingly from the bulk values and R_H asymptotically approaches $C_2/C_3 = (-1/q(n+n_s))$. The transition in R_H from the higher value of C_1 to the lower value of C_2/C_3 results in a variation in R_H with B-field. If the concentration of the surface electrons is very low compared to that of the bulk electrons, then a Hall measurement using a very low B-field can give carrier concentration and mobility values which are close to the actual bulk values. This is the case with the passivated layer. Here, a measurement at 0.5 KG gives a composite carrier concentration of $5.3 \times 10^{14}/cm^3$ and a mobility of 264,000, which are comparable to the bulk values ($n = 5.0 \times 10^{14}/cm^3$, μ_H = 269,000). In samples where the surface layer concentration is not low, the R_H and μ_H measured at low B-fields can still be considerably different from the bulk values. Such is the case with the unpassivated layer, where the composite value of carrier concentration and mobility measured at 0.5 KG are $6.6 \times 10^{14}/cm^2$ and 228,000 cm^2/V-sec, far from the actual bulk values. Hence, especially in the case of light n-type epilayers which are not passivated, a single Hall effect measurement at one magnetic field can lead to erroneous results.

The results reported here were for the case of one particular sample with a bulk doping of $5 \times 10^{14}/cm^3$. However, surface effects have been routinely observed in all n-type layers which have not been passivated. Their effect is more pronounced in layers

with low doping, and less so in layers with heavier doping. Due to the high mobility of the bulk electrons, even a B-field as low as 1.0 KG is high enough ($\mu B > 1.0$) to cause the Hall-effect measurement to be a high field measurement.

One important consequence of this high electron mobility is that it becomes possible to carry out a variable B-field analysis of the type described above using relatively low B-field strengths (0-5 KG), as most of the variation in R_H occurs within this range. This is in contrast to the situation with p-type layers, where separation of the surface electrons from the bulk holes require much larger B-field strengths, in the 5 to 20 KG range [3, 4].

In conclusion, we have shown, for the first time, that the presence of a surface accumulation layer of electrons on n-type layers of $Hg_{1-x}Cd_xTe$ results in a composite carrier concentration and mobility, which are significantly different from the true bulk concentration and mobility. Further, we have shown that the true bulk carrier concentration and mobility can be determined in these situations by measurement of R_H as a function of the B-field, in the 0-5 KG range. The results obtained by this technique were verified by passivating $Hg_{1-x}Cd_xTe$ layers using anodic sulfide, which reduces the concentration of surface electrons, and thus reduces the surface effects.

ACKNOWLEDGEMENT

The authors would like to thank J. Barthel for technical assistance on this program and P. Magilligan for manuscript preparation. CdTe substrate material was kindly supplied by C.J. Johnson and S. McDevitt of II-VI, Inc., Saxonburg, PA. Partial funding for this program, from the Raytheon Corporation, is hereby acknowledged. This work was sponsored by the Defense Advanced Research Projects Agency (Contract No. N-00014-85-K-0151), administered through the Office of Naval Research, Arlington, VA. This support is greatly appreciated.

APPENDIX

The expression for the Hall coefficient R_H and σ used n the Hall analysis is derived here [10]. Consider a uniformly doped n-type layer of thickness d, with a bulk electron concentration of n (cm^{-3}), at the surface of which there is an accumulation layer which has a sheet electron concentration of N_s (cm^{-2}). The bulk and surface electrons have mobilities of μ and μ_s respectively. The sheet conductance of this layer is given by:

$$\sigma_{SHEET} = q(nd\mu + N_s\mu_s)$$

The average conductivity of the layer can then be written as:

$$\sigma = \sigma_{SHEET}/d = q\{n\mu + (N_s/d)\mu_s\}$$

By replacing (N_s/d) by n_s, the average volume concentration of the surface electrons, σ, can be rewritten as:

$$\sigma = q(n\mu + n_s\mu_s)$$

The Hall coefficient R_H of this layer is:

$$R_H = \frac{1}{B}\frac{\sigma_{xy}}{\sigma_{xx}^2 + \sigma_{xy}^2}$$

where σ_{xx} and σ_{xy} are:

$$\sigma_{xx} = q\frac{n\mu}{1+\mu^2B^2} + q\frac{(N_s/d)\mu}{1+\mu_s^2B^2}$$

and

$$\sigma_{xy} = -q\frac{n\mu^2B}{1+\mu^2B^2} - q\frac{(N_s/d)\mu_s^2B}{1+\mu_s^2B^2}$$

Substituting these in the expression for R_H, and replacing (N_s/d) by n_s, the following expression for R_H is obtained:

$$R_H = \frac{1}{q} \frac{(n\mu^2 + n_s\mu_s^2) + \mu^2\mu_s^2 B^2(n + n_s)}{(n\mu + n_s\mu_s)^2 + \mu^2\mu_s^2 B^2(n + n_s)^2} \quad (1)$$

As noted earlier, n_s here is the average concentration of the surface electrons, which is the total sheet concentration N_s divided by the thickness of the $Hg_{1-x}Cd_xTe$ layer. The actual volume concentration of the surface electrons is determined by the Debye length near the surface, and varies exponentially with depth. However, Hall effect measurements primarily determine the sheet conductivity and the sheet carrier concentrations in the layer; the conductivity and volume concentrations of carriers in the layer are subsequently obtained by dividing these values by the thickness of the total layer. Thus, it is the average concentration of the different types of carriers in the layer which are important in the Hall measurement, and not their local concentrations. An important assumption made here is that the layer is uniform in the lateral direction, and all the surface electrons can be characterized by a single mobility.

In the case of the bulk electrons as well, it is their net sheet concentration which is obtained by Hall effect measurements. However, since we know the total thickness of the $Hg_{1-x}Cd_xTe$ layer (by FTIR reflectance measurements), and we assume that the bulk electron concentration is uniform through the $Hg_{1-x}Cd_xTe$ layer, we are able to quote their actual volume concentration.

REFERENCES

1. W. Scott, E. L. Stelzer, and R. J. Hager, J. Appl. Phys. 47, (1976) 1408.
2. L. F. Lou and W. H. Frye, J. Appl. Phys. 56, (1984) 2253.
3. A. Zemel, A. Sher and D. Eger, J.Appl. Phys. 62, (1987) 1861.
4. M. C. Chen, Appl. Phys. Lett., 51, (1987) 1836.
5. H. H. Wieder, Appl. Phys. Lett. 25, (1974) 206.
6. A. Zemel and J. R. Sites, Thin Solid Films 41, (1977) 297.
7. Y. Nemirovsky, L. Burstein, and I. Kidron, J. Appl. Phys. 58, (1985) 366.
8. S. K. Ghandhi, I. B. Bhat, and H. Fardi, Appl. Phys. Lett. 52, (1988) 392.
9. L. J. van der Pauw, Philips Research Reports 13, (1958) 1.
10. A. Nedoluha, and K.M.Koch, Z. Phys. 132, (1952) 608.

FIGURES

Fig. 1. Hall coefficient and Hall mobility vs. $1000/T$ for an n-type $Hg_{1-x}Cd_xTe$ layer. $x = 0.217$, layer thickness = 7.3 μm. B-field = 1.6 KG.

Fig. 2. Hall coefficient vs. B-field for the sample of Fig. 1 at 30K. The solid curve is the theoretical fit to the experimental data for two carrier conduction.

Fig. 3. Hall coefficient vs. B-field for the sample in Fig. 2 at 30K after surface passivation. The solid curve is the theoretical fit to the experimental data for two carrier conduction.

Fig. 4. Hall coefficient and Hall mobility vs. $1000/T$ for the sample in Fig. 1 after surface passivation. $x = 0.217$, layer thickness = 6.4 μm. B-field = 1.6 KG.

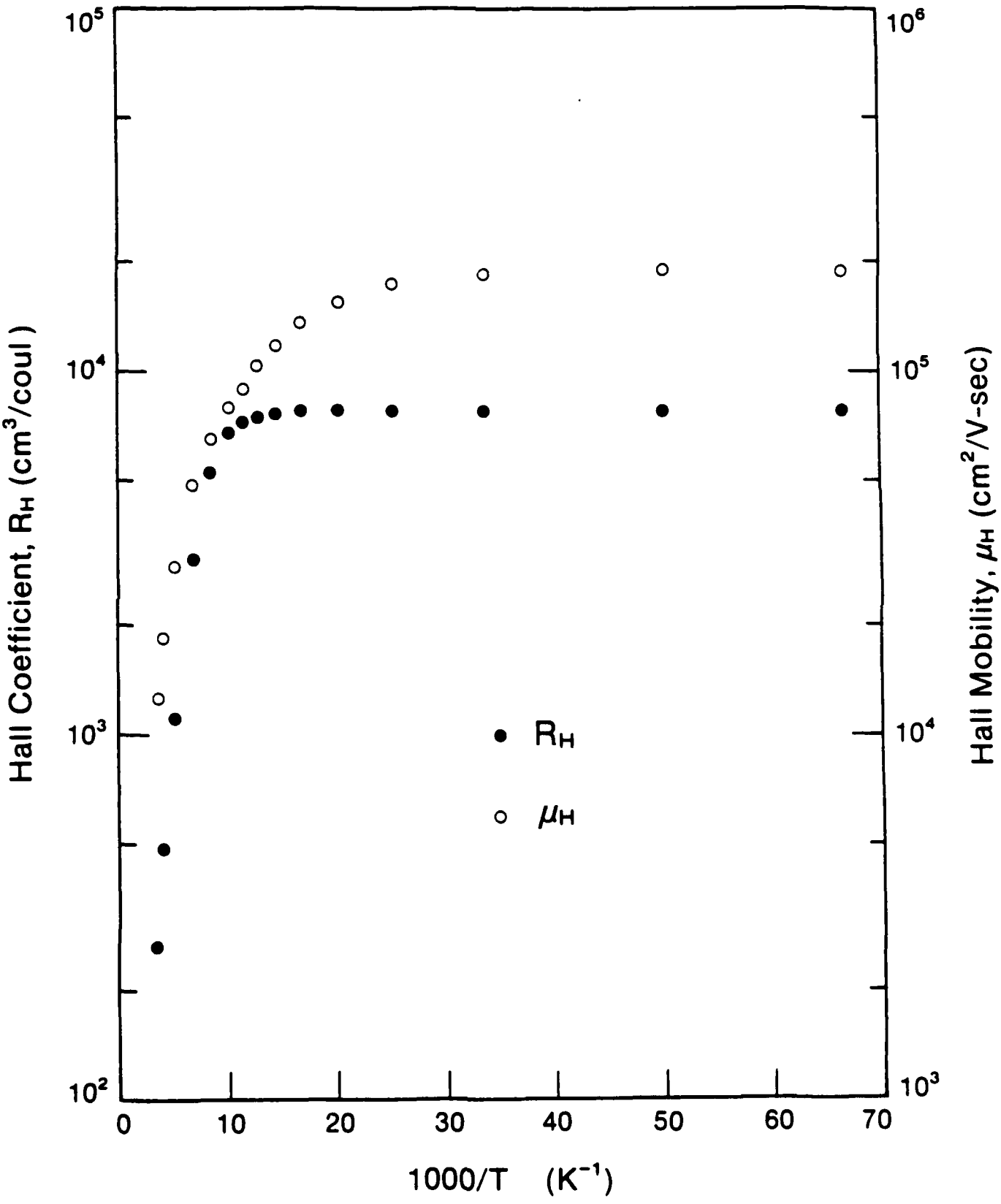
10^5
10^4
10^3
10^2
10^6
10^5
10^4
10^3
0
10
20
30
40
50
60
70
Hall Coefficient, R_H (cm^3/coul)
Hall Mobility, μ_H (cm^2/V-sec)
1000/T (K^{-1})
R_H
μ_H

1

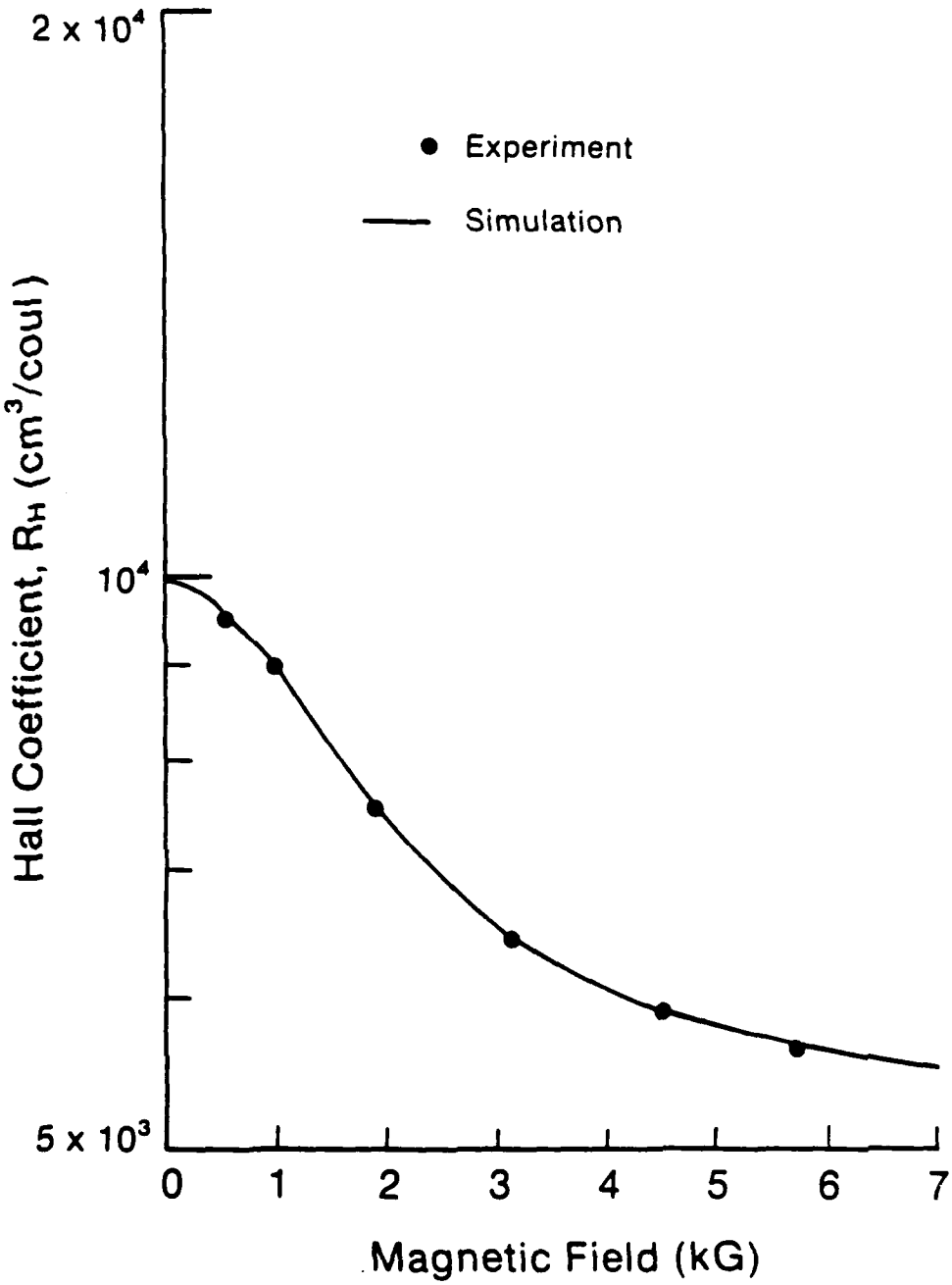
2 x 10⁴
10⁴
5 x 10³
Hall Coefficient, R_H (cm³/coul)
Experiment
Simulation
0
1
2
3
4
5
6
7
Magnetic Field (kG)

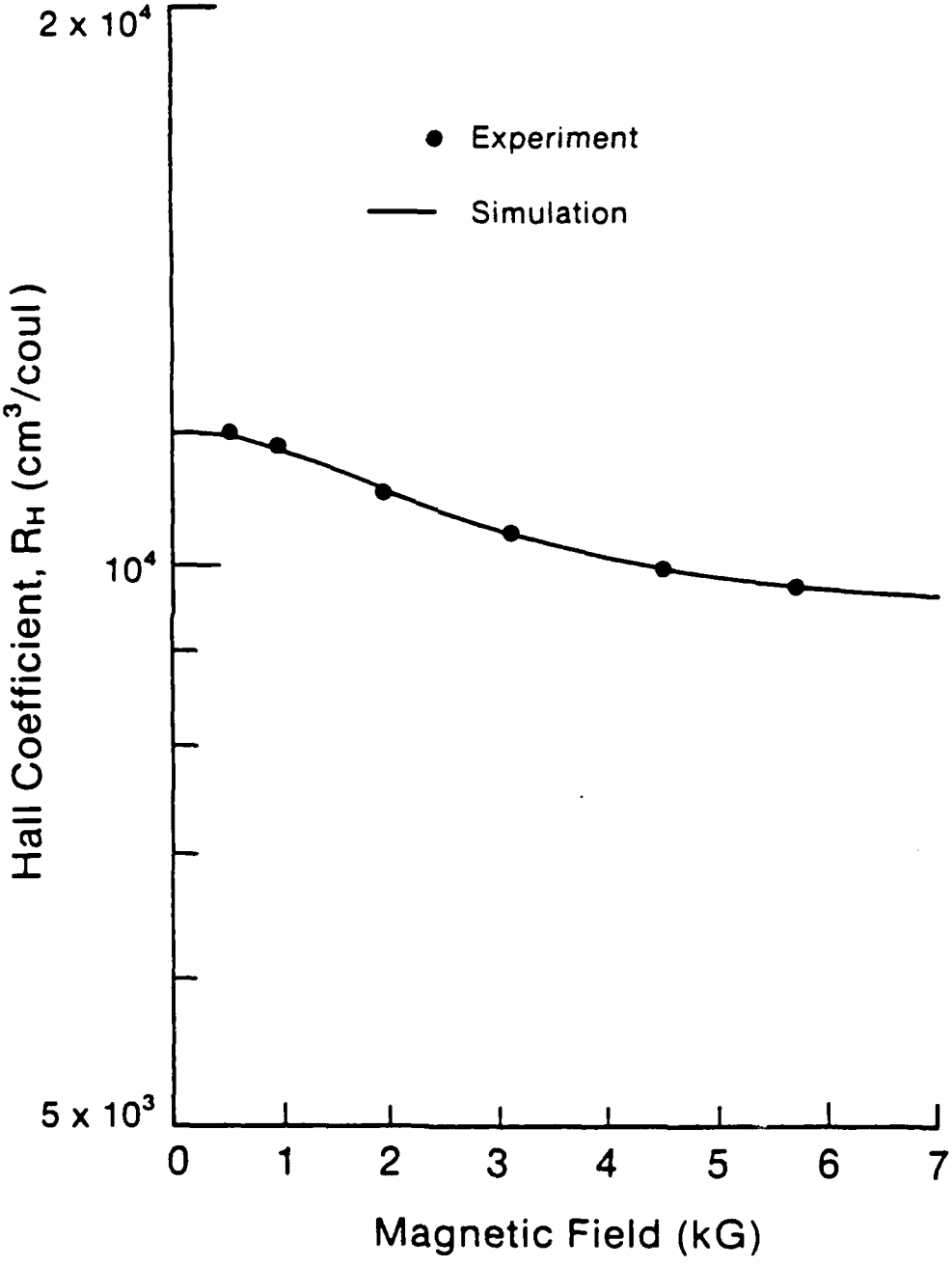
2 x 10⁴
10⁴
5 x 10³
Hall Coefficient, R_H (cm³/coul)
Experiment
Simulation
0
1
2
3
4
5
6
7
Magnetic Field (kG)

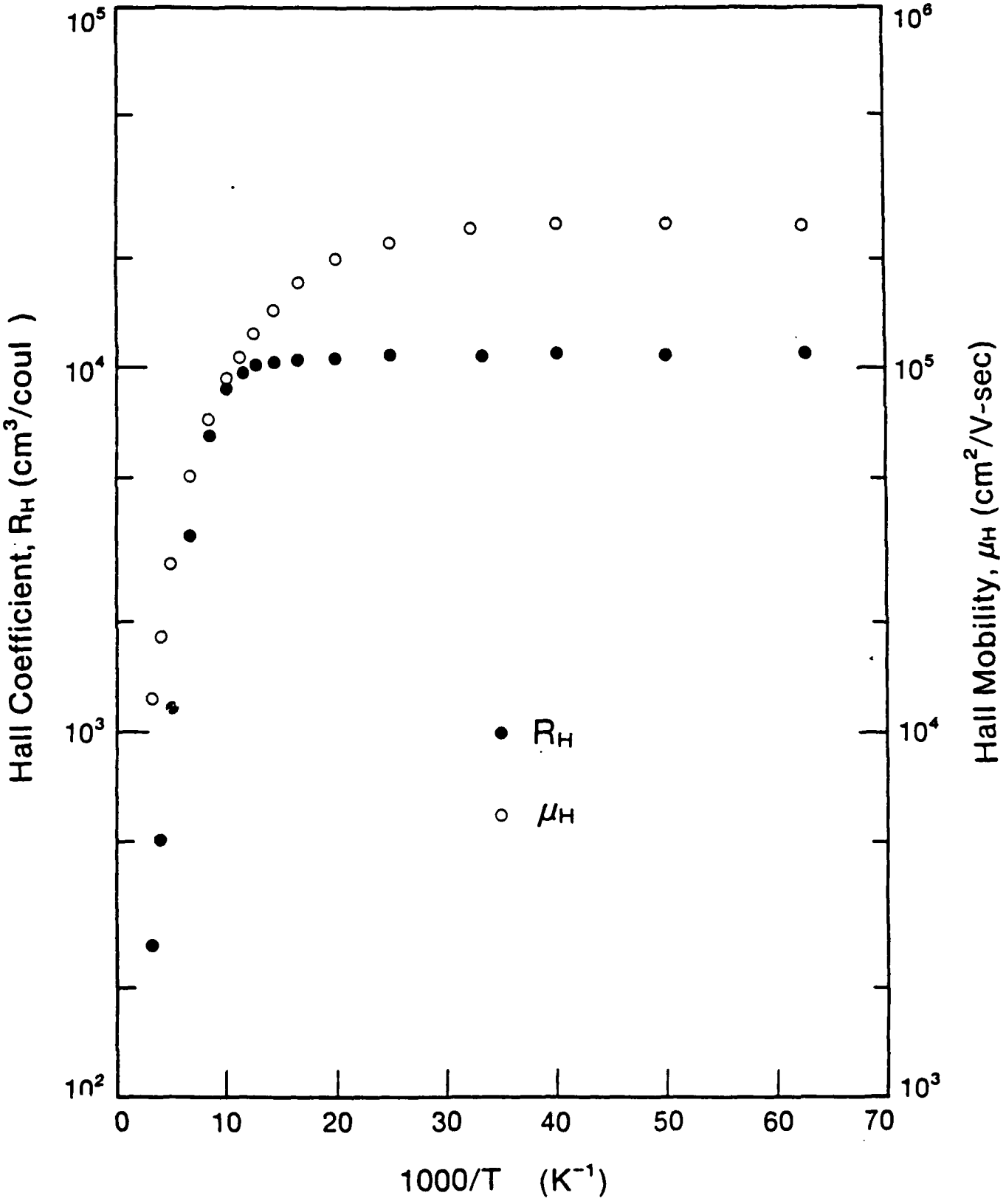
Hall Coefficient; R_H (cm^3/coul)
Hall Mobility, μ_H (cm^2/V-sec)
10^5
10^4
10^3
10^2
10^6
10^5
10^4
10^3
R_H
μ_H
0
10
20
30
40
50
60
70
1000/T (K^{-1})

4

FIG 4